P-CYCLE BASED PROTECTION IN WDM MESH NETWORKS

Honghui Li

A thesis

in

The Department

of

Computer Science & Software Engineering

Presented in Partial Fulfillment of the Requirements

For the Degree of Doctor of Philosophy

Concordia University

Montréal, Québec, Canada

September 2012

CONCORDIA UNIVERSITY

SCHOOL OF GRADUATE STUDIES

This is to certify that the thesis prepared

By: **Honghui Li**

Entitled: ***p*-Cycle Based Protection in WDM mesh Networks**

and submitted in partial fulfillment of the requirements for the degree of

DOCTOR OF PHILOSOPHY (Computer Science)

complies with the regulations of the University and meets the accepted standards with respect to originality and quality.

Signed by the final examining committee:

__________________________________ Chair
Dr. M.R. Soleymani

__________________________________ External Examiner
Dr. A. Shami

__________________________________ External to Program
Dr. A. Agarwal

__________________________________ Examiner
Dr. C. Lam

__________________________________ Examiner
Dr. J. Opatrny

__________________________________ Thesis Supervisor
Dr. B. Jaumard

Approved by __________________________________
Dr. V. Haarslev, Graduate Program Director

October 19, 2012

____
Dr. Robin A.L. Drew, Dean
Faculty of Engineering and Computer Science

Abstract

p-Cycle Based Protection in WDM Mesh Networks

Honghui Li, Ph.D.

Concordia University, 2012

WDM techniques enable single fiber to carry huge amount of data. However, optical WDM networks are prone to failures, and therefore survivability is a very important requirement in the design of optical networks. In the context of network survivability, p-cycle based schemes attracted extensive research interests as they well balance the recovery speed and the capacity efficiency. Towards the design of p-cycle based survivable WDM mesh networks, some issues still need to be addressed. The conventional p-cycle design models and solution methods suffers from scalability issues. Besides, most studies on the design of p-cycle based schemes only cope with single link failures without any concern about single node failures. Moreover, loop backs may exist in the recovery paths along p-cycles, which lead to unnecessary stretching of the recovery path lengths.

This thesis investigates the scalable and efficient design of segment p-cycles against single link failures. The optimization models and their solutions rely on large-scale optimization techniques, namely, Column Generation (CG) modeling and solution, where segment p-cycle candidates are dynamically generated during the optimization process. To ensure full node protection in the context of link p-cycles, we propose an efficient protection scheme, called node p-cycles, and develop a scalable optimization design model. It is shown that, depending on the network topology, node p-cycles sometimes outperform path p-cycles in

terms of capacity efficiency. Also, an enhanced segment p-cycle scheme is proposed, entitled segment Np-cycles, for full link and node protection. Again, the CG-based optimization models are developed for the design of segment Np-cycles. Two objectives are considered, minimizing the spare capacity usage and minimizing the CAPEX cost. It is shown that segment Np-cycles can ensure full node protection with marginal extra cost in comparison with segment p-cycles for link protection. Segment Np-cycles provide faster recovery speed than path p-cycles although they are slightly more costly than path p-cycles. Furthermore, we propose the shortcut p-cycle scheme, i.e., p-cycles free of loop backs for full node and link protection, in addition to shortcuts in the protection paths. A CG-based optimization model for the design of shortcut p-cycles is formulated as well. It is shown that, for full node protection, shortcut p-cycles have advantages over path p-cycles with respect to capacity efficiency and recovery speed. We have studied a whole sequence of protection schemes from link p-cycles to path p-cycles, and concluded that the best compromise is the segment Np-cycle scheme for full node protection with respect to capacity efficiency and recovery time. Therefore, this thesis offers to network operators several interesting alternatives to path p-cycles in the design of survivable WDM mesh networks against any single link/node failures.

Acknowledgments

First and foremost, I would like to express my sincere and earnest gratitude to my supervisor Dr. Brigitte Jaumard. As Concordia University Research Chair (Tier 1) on the Optimization of Communication Networks, she is recognized as one of the principle pioneers of optical networking optimization. She leaded me to the graceful world of operation research and optical networks. She guided me throughout my thesis with her knowledge and infinite patience. I appreciate the time she put into the discussion on my thesis work and her numerious helpful suggestions and encouragement during the past five years.

Besides, I am grateful to all members of my thesis committee for their prompt evaluation and comments. I also would like to thank my office mates for the delightful work environment they have provided me with.

Last but not least, I am indebted to my dear parents who support me with the unconditional encouragement and love. I also owe my deepest gratitude to thank my husband and my daughter for their understanding and patience during the past few years. This thesis would not have been possible without their support and encouragement.

Contents

List of Figures

List of Tables

List of Acronyms

APS Automatic Protection Switching

BLSR Bi-directional Line Switched Ring

CAPEX CAPital EXpenditure

CG Column Generation

DBLP Dedicated-Backup Link Protection

DBPP Dedicated-Backup Path Protection

DCF Dispersion Compensating Fiber

DGE Dynamic Gain Equalizer

EXC Electrical Cross connect

ELH Extended Long Haul

FIPP Failure-Independent Path-Protecting

GMPLS Generalized Multi-Protocol Label Switching

GRWA Grooming and Routing Wavelength Assignment

ILP Integer Linear Program

LH Long Haul

LP Linear Program

MILP Mixed Integer Linear Program

OADM Optical Add Drop Multiplexer

OC Optical Carrier

OLA Optical Line Amplifier

OXC Optical Cross connect

PWCE Protected Working Capacity Envelope

PXT Pre-cross-connected Trails

RWA	Routing Wavelength Assignment
SBLP	Shared-Backup Link Protection
SBPP	Shared Backup Path Protection
SDH	Synchronous Digital Hierarchy
SHR	Self-Healing Ring
SONET	Synchronous Optical Network
SRLG	Shared Risk Link Group
ULH	Ultra Long Haul
WDM	Wavelength Division Multiplexing

List of Publications

Journals

1. Brigitte Jaumard and Honghui Li and Caroline Rocha, "Design of Efficient Node p-Cycles in WDM Mesh Networks," *Optical Switching and Networking* (under review).

2. Honghui Li and Brigitte Jaumard, "Minimum CAPEX Design of Segment p-Cycles with Full Node Protection," *Journal of Lightwave Technology* (under review).

3. Brigitte Jaumard and Honghui Li and Caroline Rocha, "Shortcut p-Cycles: Free of Loop Back for Full Node Protection," *Computer Networks* (under review).

4. Brigitte Jaumard and Honghui Li, " A Survey on p-Cycle Based Scheme Design and Solution Methods for WDM Mesh Networks," *IEEE Communications Surveys and Tutorials* (under review).

Conference proceedings

1. Brigitte Jaumard and Honghui Li, "Minimum CAPEX Design of Segment p-Cycles with Full Node Protection", in *Proc. 16th Working Conference on Optical Network Design and Modelling (ONDM)*, Colchester, UK, Apr. 2012.

2. Brigitte Jaumard and Honghui Li, "Segment p-Cycle Design with Full Node Protection in WDM Mesh Networks, " in *Proc. 18th IEEE Workshop on Local Metropolitan Area Networks (LANMAN)*, Chapel Hill, NC, USA, Oct. 2011.

3. Brigitte Jaumard and Honghui Li, "Design of p-Cycles for Full Node Protection in WDM Mesh Networks", in *Proc., IEEE International Conference on Communications (ICC)*, Kyoto, Japan, May 2011.

4. Brigitte Jaumard and Honghui Li and Samir Sebbah, "Design of Path-segment-protecting p-Cycles in Survivable WDM Mesh Networks", in *Proc. 14th International Telecommunications Network Strategy and Planning Symposium (NETWORKS)*, Warsaw, Poland, Sep. 2010.

5. Brigitte Jaumard and Honghui Li and Samir Sebbah, "Design of Multi-granularity Directed Segment p-Cycles", in *Proc. IEEE Sarnoff Symposium*, Princeton, NJ, USA, Apr. 2010.

Chapter 1

Introduction

1.1 Overview

With the current wavelength-division multiplexing (WDM) technology, a single fiber can carry hundreds of non-overlapping wavelength channels, each of which is with a bandwidth of up to 100Gb/s, for parallel data transmission [SS12]. Thus, WDM mesh networks may carry huge amounts of traffic. Therefore, a single outage in a WDM optical network can have catastrophic and far reaching consequences.

Fiber cuts occur frequently. It is reported in [Lem] that the 2006 Hengchun earthquake off Taiwan damaged several submarine communications cables. Internet services in many Asian countries were disrupted, and the foreign exchange market were seriously affected. In August 2009, nine undersea fiber cables had been damaged due to the Hualien earthquake off Taiwan and Typhoon Markot. The phone and Internet services were disrupted from China to the United States and Europe [Xin]. In spite of significant efforts made at physical protection of cables, FCC (Federal Communications Commission) statistics show that metro networks suffer 13 cuts per 1000 miles of fiber and long haul 3 cuts per 1000 miles every year

[Gro04a]. The estimation from Gartner Group is that through 2004, large U.S. enterprises have lost more than $500 million [HP99] in potential revenue due to network failures affecting crucial business functions.

Node failures may also happen. Entire central offices can fail due to the disasters, such as fires and flooding. Node failures are much less frequent than link failures. However, a node failure may result in widespread disruption. For example, Hurricane Katrina in 2005 caused the obliteration, flooding, and power outages at central offices [RSS09]. Hence, providing resilience to failure is very essential in WDM optical networks.

As a part of the service level agreement (SLA) between a carrier and its customers which leases a lightpath, the carrier commits the connection with certain availability, e.g., 99.999%, which implies that the network downtime is equal to or less than 5 minutes per year. *Availability* is the asymptotic probability that a system will be found in the operating state at a random time in the future. To achieve a high availability, survivability, capability of continuous service delivery in the event of failures must be carefully taken into account when designing optical networks.

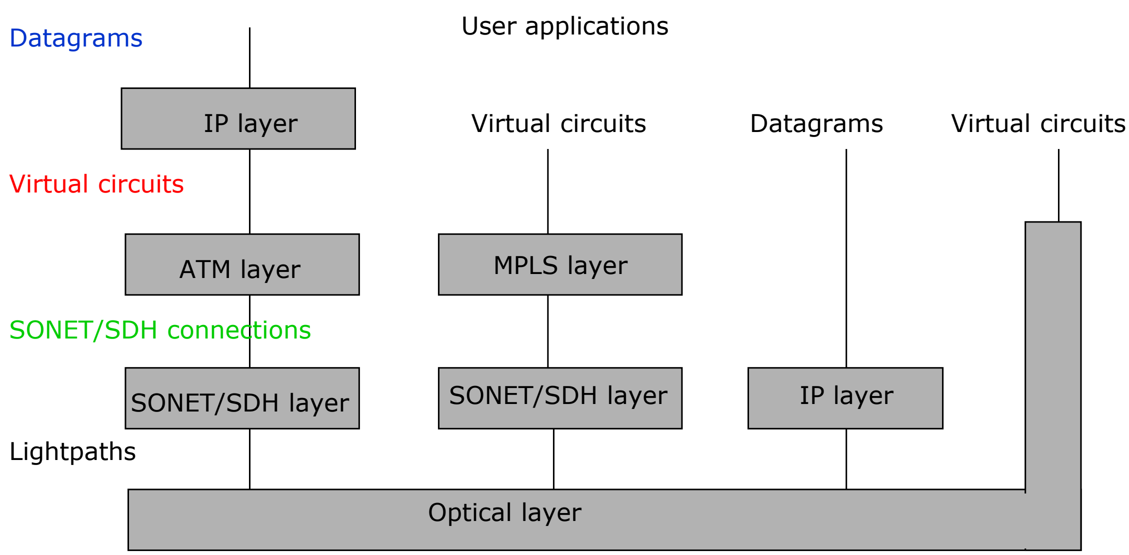

Figure 1.1: Layered network architecture in WDM optical networks [RSS09]

In WDM optical networks, the utilization of optical switches and all-optical network elements introduce a new network layer, called the optical layer or WDM layer to the protocol hierarchy. The optical layer provides services to other client layers. The optical layer provides services to various types of client layers, as illustrated in Figure 1.1. The client layers include, for example, IP (Internet Protocol), SONET/SDH (synchronous optical network / synchronous digital hierarchy) as well as other possible protocols.

Regarding the client layers over the optical layer, each one may incorporate protection and restoration functions. However, the optical layer need to provide its own protection mechanisms. The reasons are as follows [RSS09].

- SONET networks include extensive protection functions, while other layers, e.g., IP layer, do not hold the same degree of protection.
- Significant cost savings can be obtained by utilizing the optical layer protection in comparisons with the other client layer protection.
- The optical layer can cope with some faults more efficiently than the client layers. A fiber cut leads to the failure of all lightpaths on it. Without protection at the optical layer, each channel must be recovered separately by their related client layers. Also, a large number of alarms flood in the network management system. On the contrary, if recovered at the optical layer, fewer lightpaths need to be rerouted individually. As a result, the recovery process is simpler and faster.

Two different mechanisms enable WDM mesh network survivability. One is restoration, with which, protection paths are calculated on the fly in the event of failure occurrence. The other is protection, with which, backup paths are calculated and spare capacities along the backup paths are reserved before a single failure occurs. Disrupted traffic is switched to the backup paths in case of failure. Protection outperforms restoration in terms of recovery time as well as guaranteed survivability. Restoration cannot provide 100% guaranteed survivability since restoration path may not be found upon failure due to resources limitation. Therefore, we only deal with protection in this thesis.

To design survivable WDM networks, two protection metrics, the failure recovery time and the capacity efficiency, are very important. Various protection approaches have been proposed which try to balance between these two metrics. In SONET rings, Bidirectional Line Switch Ring (BLSR) protection is favored due to its simplicity and fast recovery speed. Upon a single failure, only the end nodes of the failed link take a real-time action to switch automatically the disrupted traffic to the backup paths. However, with BLSR, the ratio of spare capacity over working capacity may be over 200% [SG00a].

In WDM mesh networks, several shared protection approaches have been proposed, which outperform the rings in terms of capacity efficiency. However, the capacity efficiency is achieved at the expense of a recovery speed than with the rings. With the mesh-based shared protection, spare capacities are shared among different working paths, and thus the switches along those paths cannot be cross-connected ahead of a failure. Signaling is needed to cross-connect switches along backup paths in case of failure.

p-Cycles (short for pre-configured protection cycle) proposed by Grover and Stamatelakis [GS98] well integrate the advantages of SONET rings and the mesh based shared protection. p-Cycles hold the ring-like recovery speed with mesh-like capacity efficiency. Upon a single link failure, with p-cycles, only the end nodes of the failed link perform real-time switching and reroute the affected traffic automatically to the protection paths along p-cycles. In this way, p-cycles can achieve a ring-like recovery speed. p-Cycles can protect on-cycle and straddling links. For each straddling link, one unit p-cycle can offer two units of protection paths. Thereby, p-cycles can achieve mesh-like capacity efficiency. Due to this unique characteristics, p-cycles have attracted extensive research interests, such as in [GS98, SGA02, HS07, GO09, EM09, WYH10a, OG11] in the design of survivable WDM networks. Later, p-cycles have been extended to path-segment p-cycles [SG03] and FIPP (short for Failure-Independent Path-Protecting) p-cycles [KG05]). Among these p-cycle based schemes, segment p-cycles offer the best compromise between link p-cycles and the FIPP p-cycles in terms of capacity efficiency and recovery delay.

Single failures are the predominant form of failures in optical networks [RSM03]. A single failure refers to the failure scenario that one failure is repaired before another failure occurs in the network. It has been widely acknowledged that when a failure occurs, we have the time to repair it before another failure occurs [ZM04]. Only single failure scenarios are investigated in this thesis although multiple, near-simultaneous failures are also possible in real-world networks.

1.2 Problem Statements and Motivations

In general, this thesis investigates the design of survivable WDM mesh networks based on the p-cycle based schemes and their enhancements such that the protection cost is minimized against any single failures. The protection cost is evaluated as either spare capacity usage or spare CAPital EXpenditure (CAPEX) cost.

Toward design of p-cycle based survivable networks, several issues exist and need to be tackled. One is related to the scalability issue. In the convention design of, say, segment p-cycles in [SG03], the design problem is formulated as an integer linear programming (ILP) model. To solve the ILP model, the pre-requisite is to offline enumerate all candidate segment p-cycles. The number of candidate p-cycles increases exponentially with the network size increase. For large network instances, if all candidate p-cycles are pre-enumerated, this leads to an intractable ILP model; if only a subset of candidates is enumerated, the solution quality may be significantly affected, see, e.g., [JRBG07].

Most work on the p-cycle design protects traffic against single link failures, such as in [GS00,SGA02,LT04,KSG05,LHP$^+$06,RJ08,WYH10a,RJ12]. Although single link failures are the dominant failure scenario in optical networks, the failure of a single node can occur, even though not so often, due to a disaster, such as flooding or fire tearing down a whole node. A single node failure is equivalent to the failure of all adjacent fiber links and all connections going across this node. The consequences of a single node failure are therefore catastrophic.

Overwhelming majorities of studies on the design of p-cycle based schemes have focused on minimizing the spare capacity usage [GS00,SGA02,KSG05,RJ08,EM09,RJ12]. Although it is certainly a decisive design criterion, once optical fibers have been deployed, the CAPEX cost becomes significant in order to set up p-cycle structures.

Large p-cycles are preferred in many situations in order to achieve high capacity efficiency [GS98]. As a result, the protection paths based on such p-cycles travel many fiber links and nodes. No doubts, the recovered signals carried on the protection paths will revisit some nodes and links in the working paths. Such revisit leads to the formation of loop backs, and accordingly, the recovered path becomes unnecessarily large. The long recovery path length slows down the optical recovery speed, and also causes optical signal degradation en route. Moreover, the probability of survival from dual link failures will be reduced as well.

To address these issues, specifically, the following problems are investigated in this thesis.

- Given a network topology and working segment set, design segment p-cycles to protect the working segment set from any single link failure. The objective is to minimize the spare capacity usage of segment p-cycles. Two network costs will be investigated: the bandwidth usage and the node equipment (e.g., transponders) cost. In order to deal with the scalability issue in the conventional design, the optimization models need to be formulated and solved using column generation (CG) techniques.

- Enhance the classical link p-cycle scheme to ensure protection against any single link / node failure in WDM networks. For the design of such p-cycle enhancements, an efficient and scalable optimization model is developed given the network topology and the routed connection requests. The objective is to minimize the spare capacity usage such that WDM mesh networks can survive any single link / node failure.

- The classical segment p-cycles cannot ensure 100% node protection against a single failure. We therefore propose an efficient segment p-cycle enhancement for full node protection, and evaluate such an enhancement with respect to both capacity efficiency and CAPEX cost. For this, we again study the design under two objectives, i.e., spare capacity usage and CAPEX cost, such that the given working segment set can be protected against any single link / node failure.

- Propose a p-cycle scheme in WDM mesh networks which offers 100% guaranteed protection against any single link or node failures. Such a p-cycle scheme should provide recovery paths, which are free of loop backs so that it can make full use of spare capacity. In order to design and evaluate such scheme, we plan to develop a scalable optimization model. Given the network topology and the routed connection requests, the objective is to minimize spare capacity usage such that a WDM network can survive from any single link / node failure.

1.3 Thesis Contributions

This thesis has made the following contributions:

- A scalable and efficient design method is proposed for segment p-cycles in WDM mesh networks based on a large scale optimization tool, namely column generation techniques (CG). In contrast with the conventional p-cycle designs, the CG based optimization approach dynamically generates segment p-cycles with their protection capabilities during the optimization process. Computational results show that our design method of segment p-cycles is much more capacity efficient and scalable than the conventional design in [SG03].

- Multi-granularity segment p-cycles are proposed to protect working segments carried with different granularities, such as OC-48, OC-192 and so on. An ILP-based design approach is developed for WDM multi-granularity segment p-cycles. The objective is to minimize the nodal equipment (e.g., transponder) cost in order to provide 100% single link failure protection. Based on CG techniques, the p-cycle candidates are generated dynamically as needed during the optimization process. Thereby, it avoids a costly time and space that a priori enumeration of all candidate p-cycles. Numerical results show that the protection design corresponding to the nodal cost optimization is more effective than the one for optimization of link spare capacity.

- Node p-cycles are proposed with 100% guranteed protection against a single node failure. A scalable optimization model, which relies on a CG formulation, is formulated in order to design node p-cycles. Computational results show that node p-cycles offering node and link protection only require slightly more spare capacity than link p-cycles, while requiring sometimes less, sometimes more spare capacity than FIPP

p-cycles, depending on the network topology. In comparison with the work of Grover and Onguetou (2009), results show that the proposed node p-cycle scheme clearly outperforms their design in terms of capacity efficiency.

- An efficient protection approach, called segment Np-cycles, is proposed based on segment p-cycles. Np-cycles ensure 100% protection against any single link / node failure (endpoints of requests are excluded). An optimization model is developed for the design of Np-cycles based on the CG techniques. The objective is to minimize the spare capacity usage against any single link / node failure. The use of the CG techniques eliminates the need to explicitly enumerate all segment Np-cycle configurations, but instead leads to a process where only improving configurations are generated. Numerical results demonstrate that segment Np-cycles are comparable, sometimes even more efficient, than path p-cycles with respect to their capacity requirement. In addition, in order to ensure 100% node protection, they only require a marginal extra spare capacity than the regular segment p-cycles.

- A scalable CAPEX optimization model is presented for the optimal design of segment Np-cycles. We compare the best trade-off between regular segment p-cycles and the proposed Np-cycles. Also, we develop formulas for the calculation of the recovery time for each of the three p-cycle protection schemes. Numerical results show that protection against single node failures can be ensured with very marginal extra CAPEX and spare capacity, throughout an adaptation of segment p-cycles. This suggests that segment Np-cycles constitute an attractive protection scheme for protection against single node or link failures. In contrast with path p-cycles, segment Np-cycles hold faster average recovery speed, and are more capacity efficiency in sparse networks although segment Np-cycles may have a higher CAPEX cost.

- We propose a protection scheme, called shortcut p-cycles for 100% guranteed protection of links and nodes against any single failure in WDM mesh networks. As in p-cycle based schemes, shortcut p-cycles are a pre-cross connected shared protection scheme. In contrast with the classical link- and segment-protecting p-cycles, shortcut p-cycles provide the recovered paths free of loop backs. Shortcut p-cycles differ from FIPP p-cycles by reducing the recovery time, as they have no requirement that the related cycles must pass through the two end nodes of the protected working paths. To design shortcut p-cycles, we develop a scalable optimization model based on CG techniques. Numerical results show that shortcut p-cycles are more capacity efficient that node p-cycles and path p-cycles for full node protection. The performance advantage is achieved at the price of a higher calculation complexity.

- We then synthetize the design problems of original and enhanced p-cycle schemes according to protection units (i.e., links, segments or paths), protected failure scenarios, traffic patterns (i.e., static traffic or dynamic traffic) as well as the objectives. We survey and categorize the associated design and solution methods in the literature. We also provide a first quantitative comparison of the classical (resp. enhance) p-cycle based schemes for protection against single link (resp. single link /node) failures. The numerical results are obtained both for the minimum spare capacity design and the minimum CAPEX design. It is shown that, under the design of minimization of spare bandwidth, segment p-cycle (resp. segment Np-cycle) outperforms the other schemes for recovery from link (resp. link/node) failure. As far as the CAPEX cost is concerned, path p-cycle have an advantage over the others.

The optimization models presented in this thesis have been implemented in C++. The ILP models have been solved using the CPLEX 11.0.1 MIP solver. For the CG models, their linear (restricted master problems) and ILP (pricing problems) programs solved by CPLEX 11.0.1 solver [IBM11]. The proposed column generation based algorithms have been implemented in C++ as well.

1.4 Thesis Organization

The thesis is organized as follows. Chapter 2 reviews the background on survivable WDM mesh networks and the p-cycle based schemes. Also, most related work in the literature is reviewed. In Chapter 3, multi-granularity segment p-cycles are proposed for protection of traffic carried with the different granularities. Optimization models are presented for the designs of classical segment p-cycles and multi-granularity segment p-cycles, subject to single link failures. Chapter 4 propose node p-cycles for full node and link protection. A scalable optimization model is formulated for the node p-cycle design against any single link / node failures. Chapter 5 proposes segment Np-cycles and presents two optimization models, which differ by their protection cost. A formula is also developed for estimation of the failure recovery time, for segment p-cycles, Np-cycles and path p-cycles. Chapter 6 presents the proposed shortcut p-cycle scheme, and develops a scalable optimization model for the design of shortcut p-cycles. Chapter 7 presents a thorough comparison of whole continuum of p-cycle based schemes. We conduct a first exhaustive quantitative comparisons of classical p-cycle based schemes against any single link failures, and enhanced p-cycle schemes against any single node/link failures. In Chapter 8, the conclusions of this thesis are drawn, and the future research directions are suggested.

Chapter 2

Background on Optical Network Survivability and Related Work

In WDM optical networks, the optical layer provides lightpaths to other client layers. A *lightpath* represents a circuit-switch end-to-end optical channel traversing multiple intermediate links and nodes. In the absence of wavelength converters, a lightpath must occupy the same wavelength on all the fiber links through which it traverses; this requirement is known as the *wavelength-continuity constraint* [ZJM00].

Some of the terminology is clarified as follows, which is used in this thesis. The path carrying connections from their source to their destination in the normal operation situation is referred to as the *primary path* or the *working path*. The alternative path that is used after a failure occurs is referred to as the *backup path* or the *protection path*. The network capacity that is allocated for the backup paths is referred to as the spare capacity.

Optical networks may suffer different kinds of failures. Link and node failures are commonly considered situations. Link failures are usually caused by fiber cuts, which are rather common; node failures occur because of equipment failure at network nodes. Besides these two cases, a channel failure is also possible due to the failure of a transponder on that wavelength. Regarding the failure scenarios, there may exist single failures and dual link failures. Single failure scenario refers to the scenario where one failure is assumed to be recovered before another failure happens in the network. Most related studies cope with the single failure scenario as it is prevalent in optical networks, and it happens much more often than dual or multiple failures [Gro04a].

The recovery mechanisms proposed to ensure survivability of optical mesh networks can be classified into two categories: protection and restoration mechanisms [RSM03]. Restoration approaches are briefly recalled in Section 2.1. General protection approaches are introduced in Section 2.2, and the p-cycle based schemes are illustrated in Section 2.3.

2.1 Restoration

With the restoration schemes, the backup paths are computed in real time rather than precomputed and pre-reserved ahead of any failure. When a primary path fails, a search is launched for a backup path which does not use the failed components. If such a backup path is found, it is assembled on the fly based on reconfigurable Optical Cross-Connects (OXCs). Then, the disrupted traffic is recovered and carried on the backup path.

Several restoration schemes have been proposed based on the OXC functionality, the traffic demand, and the network control [RM99]. Based on the rerouting strategies, restoration schemes are classified into path-based and linked-based schemes [RM99, RSM03].

The link-based restoration reroutes the disrupted traffic around a failed link. One failed link leads to several disrupted working paths. Upon a link failure occurrence, the two end nodes of the failed link take responsibility of searching dynamically the backup paths around the failed link. If such backup paths are found, the end nodes switch the disrupted working paths onto the backup paths. Otherwise, the disrupted connections are dropped if no path is available.

With the path-based restoration, the source and the destination nodes reroutes the affected working paths in the presence of a failure. The end nodes of the disrupted primary paths take responsibility to discover an end-to-end backup path. If no backup path can be found for a failed connection, then the connection is dropped.

2.2 Protection

Protection denotes the recovery approach, with which the backup paths are precomputed and required network resources are either pre-reserved or pre-cross-connected before a single failure occurs. Protection is superior to restoration for WDM mesh network survivability. Protection provides faster failure recovery speed than restoration as with protection, the backup paths are pre-planned and available ahead of any failure. Moreover, protection can provide guaranteed survivability from single failures. In addition, protection schemes have simpler and faster control protocols, and allow for transparent service recovery to the clients [GR00].

According to the network topology, the protection approaches can be classified into two categories, the ring-based and the mesh-based approaches.

2.2.1 Protection in SONET

In SONET rings, the protection classification is shown in Figure 2.1. The SONET protection approaches can be classified as Automatic Protection Switching (APS), Self-Healing Ring (SHR) and dual homing. APS is a link based protection approach, which can be classified into three categories: 1+1 APS, 1:1 APS and 1:N APS in terms of the backup

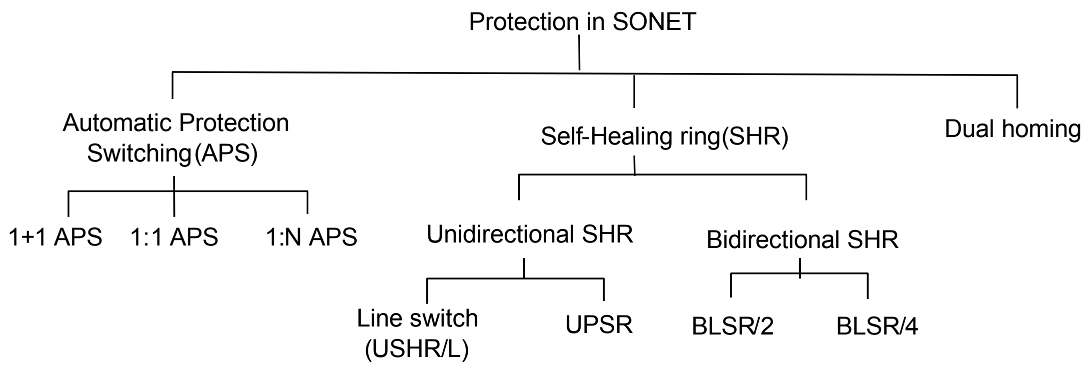

Figure 2.1: Protection in SONET [ZS00]

resource assignment strategy. SHR is employed to protect the networks with the cyclic topologies. SHR can protect node and link against failures, whereas, APS can only restore link failure(s). The backbone networks generally consist of multiple SONET rings. To protect the interconnection nodes of these rings against failures, dual homing is exploited. This scheme makes use of two hub nodes to interconnect two rings. Traffic across rings is duplicated in the two hub nodes [ZS00].

2.2.2 Protection in Optical Mesh Networks

In WDM mesh networks, the classification of the protection approaches is shown in Figure 2.2. In terms of the protection unit, the mesh-based protection can be classified into link based, segment based and path based approaches, each of which can be further classified as dedicated or shared protection. With the dedicated protection approaches, backup paths are all pre-cross-connected before a failure occurs as each backup path is dedicated for protection of a single working path. With the shared protection, the backup network resources are shared among multiple working paths. According to the cross-connection of the switches on the backup paths, the shared protection approaches can be further classified into two categories, the pre-planned and the pre-cross-connected one. With the pre-planned protection, along the backup path, the capacity and the wavelength channels are reserved but the OXC/OADM switches en route are not cross-connected ahead of a failure occurrence. In contrast with the pre-planned protection, under the pre-cross connected protection, the switches along the backup paths are pre-cross connected before a failure occurs.

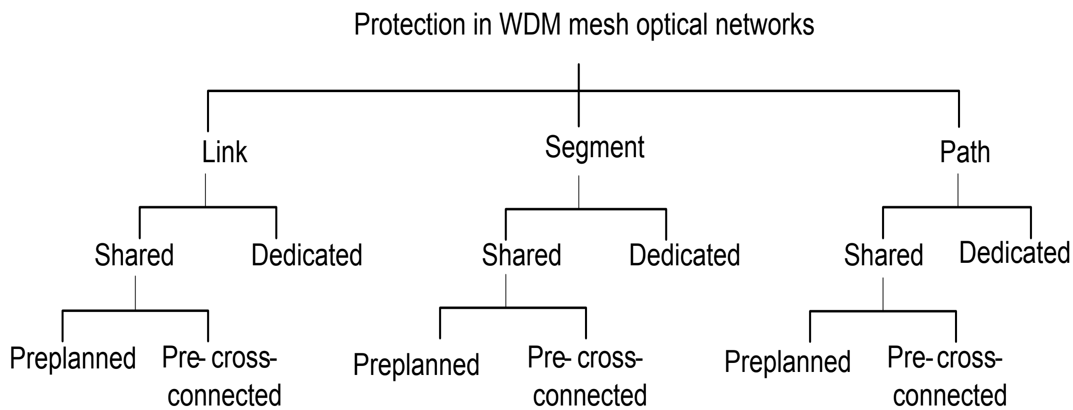

Figure 2.2: Protection in optical mesh networks

Until recently, node protection was only discussed in the context of path protection under the assumption that the protection and the working paths are node disjoint. When researchers deal with a single link-failure protection, unless it is explicitly specified, they do not care about node protection.

Link based protection approaches

The link-based protection approach reserves backup paths for each link in optical networks. In contrast with restoration, backup paths in the link protection approach are pre-planned rather than computed after failure occurrences. Each link may carry many wavelength channels, each of which has a backup path. Backup paths for these wavelength channels may use different routes or wavelengths. When a link fails, the end nodes of the link switch disrupted traffic to the backup paths around the failed link. With a link based protection, node failures cannot be handled. Link protection can be further classified as a dedicated or shared ones, see Figure 2.3.

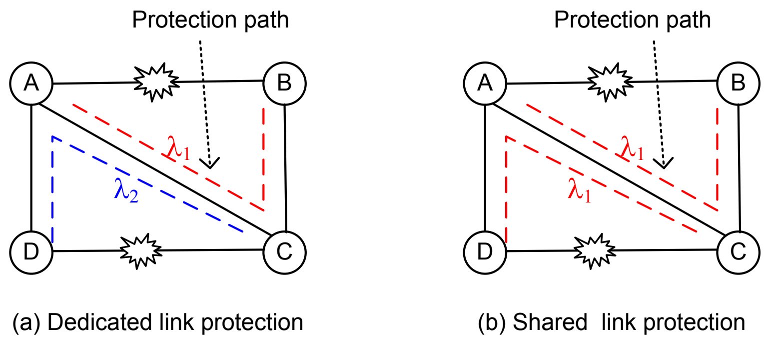

Figure 2.3: Link protection

Dedicated-backup link based protection approaches (DBLP). In dedicated-backup link protection (1+1), a protection channel is dedicated to a working channel. In this way, even if two backup paths overlap, they must be assigned two different wavelengths on the common link, one for each backup path. Figure 2.3(a) shows that backup paths A-C-B and D-A-C protect links A-B and C-D, respectively. The two backup paths have a common link A-C. With DBLP, they must traverse different wavelength channels, say λ_1 and λ_2. In this respect, link protection can survive multiple link failures.

Shared-Backup Link Protection (SBLP). In SBLP, backup paths can share reserved resources, such as wavelength on common links only if the related working channels are routed on different links. SBLP is illustrated in Figure 2.3(b), where, backup paths for links A-B and C-D can share the same wavelength, say λ_1, on link A-C provided that failures do not occur simultaneously on the different working links. Thus, backup channels are shared for protection of different links. Therefore, SBLP is more capacity-efficient compared to DBLP.

However, due to sharing backup resources on the common link, protection paths have to be cross-connected on the fly after a failure occurs; while, in DBLP, along backup paths, spare capacities are pre-connected and switches are pre-configured in case of failure occurrence. Therefore, the recovery speed of the shared link protection is slower than the dedicated one.

Path protection

To improve capacity efficiency, path based protection methods have been explored in WDM mesh optical networks. Path protection denotes end-to-end rerouting of the disrupted working path(s). Upon establishment of each working path, a corresponding link-and-node disjoint backup path is determined, along which spare capacities are reserved and switches are either pre-cross-connected or pre-planned. As in path restoration, the end nodes of a working path switch disrupted traffic over the backup path when any link or intermediate node fails on the working path. In contrast with path restoration, the backup path is computed ahead of failure occurrence in path protection. Note that signaling is required to notify the end nodes of the affected working path(s) upon a failure.

In terms of backup capacity sharing, path protection approaches are classified as Dedicated-Backup Path Protection (DBPP) and Shared-Backup Path Protection (SBPP) [RSM03], as illustrated in Figure 2.4.

Dedicated-Backup Path Protection (DBPP). In DBPP, like DBLP, a backup wavelength on a link is reserved for only one working path. Then, the switches are pre-cross connected ahead of the failure occurrence. Figure 2.4(a) illustrates DBPP. Working paths A-B-C-D and E-F-G-H are protected by backup paths A-J-K-D and E-J-K-H, respectively, which overlap on link J-K. The two backup paths require two wavelengths on the common

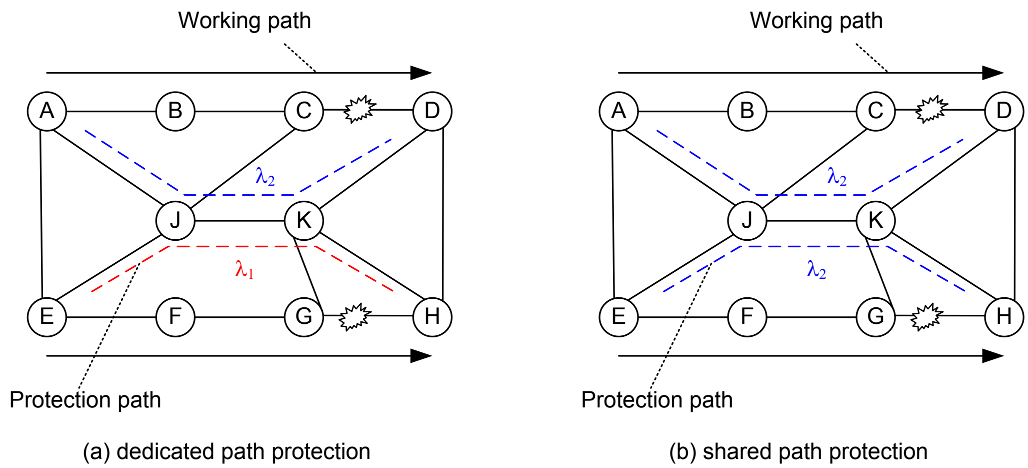

Figure 2.4: Path protection

link J-K. Thus, this method is not capacity efficient due to extra spare capacity required for protection. When there is no failure, spare capacities are either kept idle or carry some low priority, pre-emptible traffic.

Shared-Backup Path Protection (SBPP). With SBPP, a backup wavelength on a link can be used to protect more than one working path. Prerequisite for sharing backup resources is that the physical routes for working paths must be disjoint, and the corresponding backup paths must share one or several links. This protection approach is more capacity efficient than the dedicated one. However, the SBPP recovery speed is slower than DBPP because upon failure happening, SBPP requires signaling and assembles the protection resources on the fly, e.g., switch configuration, although the resources have been reserved in advance. Figure 2.4(b) illustrates SBPP. Backup paths A-J-K-D and E-J-K-H, which protect working path A-B-C-D and E-F-G-H, respectively, are carried on the same wavelength on the common link J-K. Thus one wavelength is saved compared to DBPP.

Segment protection

To balance the recovery time and the capacity efficiency between link and path protection, segment (sub-path) protection is introduced in [XXQ03]. A segment is a subset of consecutive links on a path. In segment protection, working paths are divided into multiple segments upon connection setup. For each working segment, a link/node disjoint protection segment is calculated prior to failure occurrence.

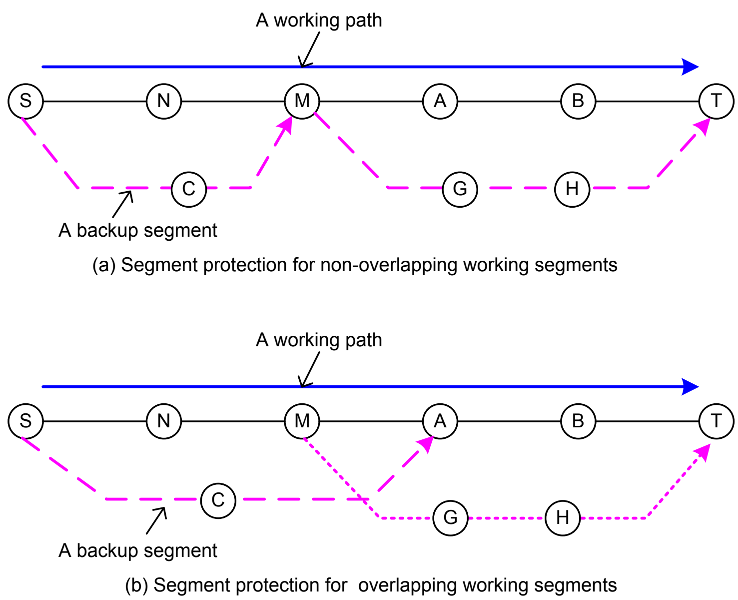

Figure 2.5: Segment protection

Segment protection can be classified into two categories depending on the node protection capability. One approach copes with single link failures. With this approach, a working path is divided into a sequence of non-overlapping segments, and each working segment is protected individually. In case of failure, the end nodes of the affected segment switch disrupted traffic to its protection segment, and other working segments work as usual to carry traffic.

As illustrated in Figure 2.5(a), working path S-T is divided into two non-overlapping segments: one is segment S-N-M protected by backup segment S-C-M; the other is segment

M-A-B-T protected by backup segment M-H-G-T. If a link, say, A-B fails, the traffic carried on the affected segment,M-A-B-T, is switched to the backup segment M-H-G-T, and the other working segment S-N-M carries their traffic as usual.

This kind of segment protection cannot protect against the failure of the segment end node, which is also an intermediate node of a working path, e.g. node M in Figure 2.5(a). For protection of such segment end nodes, another segment protection has been proposed in [XXQ03]. Under this last segment protection, a working path is divided into several overlapping segments. Each working segment is protected individually, as illustrated in Figure 2.5(b). Working path S-T is divided into two overlapping segments: one with segment S-N-M-A protected by backup segment S-C-A, the other with segment M-A-B-T protected by backup segment M-H-G-T.

As in the path or the link based protection, segment based protection can also be categorized as shared and dedicated. For the dedicated schemes, backup resources are reserved only for one segment. However, with the shared protection, backup resources can be shared among pairwise link-and-node disjoint working segments only if their backup segments have common links.

Segment protection, in general, is comparable with or superior to path protection in terms of recovery time and capacity efficiency. Segment protection generally holds faster recovery speed than path protection as it requires shorter failure notification time, which in turn comes from the fact that a segment is shorter than the related path in terms of the number of links. Non-overlapping segment protection generally holds higher backup sharability and thus is more capacity efficient than path protection, since, in terms of probability of being node-and-link disjoint, two working segments hold lower value than two working paths, and then have more chances to share backup resources.

2.3 p-Cycle Based Protection Schemes

2.3.1 Link p-Cycles

In SBLP, the backup resources, such as wavelength channels on the common links, can be shared among the protection paths. Thereby, SBLP holds a high capacity efficiency. However, due to the backup resource sharing, upon a single link failure, the protection paths are assembled on the fly. In SONET rings, such as BLSR, protection paths are preplanned and pre-cross connected. Upon a single failure, only the end nodes of the failed link perform real-time switching to re-route the affected traffic to the related protection paths. Thus, 50ms recovery time can be obtained. It is much faster than SBLP, which requires more than 100 ms [RSM03] to reroute disrupted traffic. However, BLSR is less capacity efficient than SBLP as it requires at least 100% redundant capacity [Gro04a].

p-Cycles (short for pre-configured protection cycles) well balance the capacity efficiency and the recovery speed between SBLP and BLSR. p-Cycles have BLSR ring-like recovery speed and SBLP-like capacity efficiency [GS98]. p-Cycles are fully pre-configured cycles. Upon a single link failure, similar to BLSR, only the two end nodes of the failed link take action and switch automatically the disrupted traffic to the associated protection paths. In this way, p-cycles hold the ring-like recovery speed.

As in SONET rings, a p-cycle can protect on-cycle links. Moreover, a p-cycle can protect straddling links. A straddling link of a p-cycle is such a link that it does not belong to the p-cycle but its two end nodes do. For each straddling link, a p-cycle can offer two protection paths without requiring any extra spare capacity. Therefore, p-cycles can achieve SBLP-like capacity efficiency.

A p-cycle is illustrated in Figure 2.6. A network topology and a unit p-cycle c_1 is

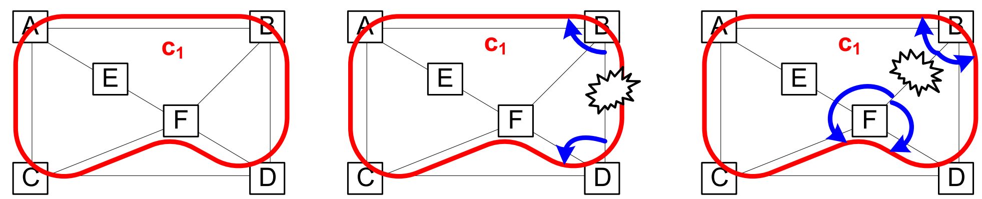

(a) Network topology and link p-cycle

(b) An on-cycle link failure

(c) A straddling link failure

Figure 2.6: p-Cycle protection approach

presented in Figure 2.6(a). Upon an on-cycle link failure, as, e.g., link B-D shown in Figure 2.6(b), the p-cycle provides one unit of protection path B-A-C-F-D along the survival part of this p-cycle, as BLSR does. In case of a straddling link failure, as, e.g., link B-F shown in Figure 2.6(c), this p-cycle offers two units of protection paths B-A-C-F and B-D-F to recover two units of the disrupted traffic.

2.3.2 FIPP p-Cycles

With SBPP, spare capacity can be shared among various protection paths only if the associated working paths are mutually disjoint and the associated protection paths share some links. Thereby, SBPP holds a high capacity efficiency. However, some issues exist when SBPP is used to protect WDM networks. With SBPP, protection paths must be cross-connected on the fly upon failure occurrence due to sharing backup resources. The associated protection paths then cannot be pre-engineered and tested. As a result, their transmission quality cannot be guaranteed for carrying connections properly as even in the design of a 10 Gb/s point-to-point optical link, approximate 20 different DWDM network impairments [Fre02] need to be handled carefully.

In this context, Failure-Independent Path-Protection (FIPP) p-cycles have been proposed. Protection paths along FIPP p-cycles are fully pre-cross connected. Thus, through pre-engineering and pre-testing, the protection paths can be fitted for the delivery of the

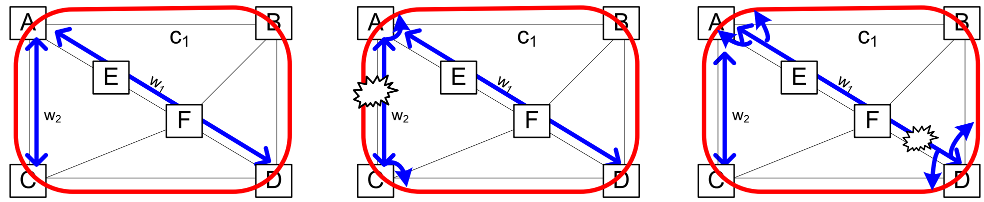

(a) Network instance and FIPP p-cycle (b) On-cycle path failure (c) Straddling path failure

Figure 2.7: FIPP p-Cycle protection approach

disrupted connections. The signal quality of the recovered traffic can thereby be guaranteed.

In case of failure occurrence, only the two end nodes of a failed path perform real-time switching, FIPP p-cycles therefore retain the ring-like recovery speed. FIPP p-cycles can protect on-cycle working paths as well as straddling working paths. With respect to a FIPP p-cycle, a straddling path is such a path that its two end nodes sit on the p-cycle but not any link. For each on-cycle working path, a FIPP p-cycle provides one protection path; for each straddling working path, a FIPP p-cycle can offer two protection paths. Thus, FIPP p-cycles can obtain SBPP-like capacity efficiency.

As in SBPP, the two end nodes of failed working paths switch the disrupted end-to-end connections to associated protection paths in case of any failure. Thereby, the intermediate nodes of working paths can be protected as well. In addition, with end-to-end backup switching, failure localization is also bypassed. FIPP p-cycles are therefore very suitable for protection of WDM networks where the detection of light loss is awkward.

A network instance and a path p-cycle are presented in Figure 7(a). Upon a link failure, as, e.g., link A-C shown in Figure 7(b), the end nodes of the failed working path A-C switch failed connection to protection path A-B-D-C. Upon a straddling path failure, as shown in Figure 7(c), the end nodes of the failed work path A-E-F-D perform end-to-end switching to protection paths A-B-D and A-C-D. Two units of working paths can thereby be recovered.

2.3.3 Flow p-Cycles

Shen and Grover in [SG03] proposed the concept of path-segment-protecting p-cycles (flow p-cycles for short). Therein, a *working segment* is defined by a sequence of contiguous links on a working path (but not necessarily routed on the same wavelength). With this definition, optical signal carried on a working segment does not necessarily keep in optical domain.

In this thesis, we assume that, a working segment is a set of contiguous links of a working path such that the signal carried on the segment keeps in optical domain, and only at its two end nodes, undergoes optical-electrical-optical conversion. This suggests that protection switching is only performed at the end nodes of working segments. Next, we will illustrate flow p-cycles based on this assumptions.

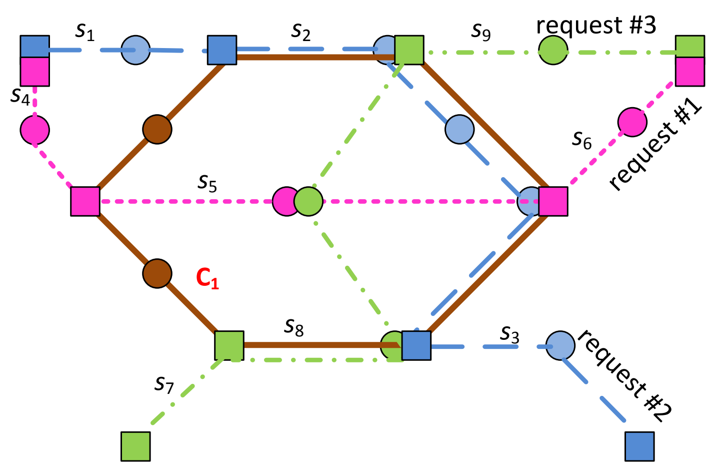

Figure 2.8: Segment p-cycles

An illustration of the various types of protected segments is given in Figure 2.8 where a p-cycle, represented by the brown solid line, protects three working segments belonging to three different requests. Each request is supported by a 3-hop path, where endpoints of the segments are represented by squares, and segment intermediate nodes are represented by circles. For a given segment p-cycle, working segments can be of three types: *(i)* on-cycle segments, as for segment s_2 of request #2 (blue dashed line): all its links and intermediate nodes are protected by its complement part in the p-cycle; *(ii)* straddling segments, as for segment s_5 of request #1 (pink dotted line): all its links and intermediate nodes are protected by the two halves of the p-cycle defined by the endpoints of s_5, meaning that one unit of s_5 is provided two protection units by the p-cycle; *(iii)* hybrid segments, as for segment s_8 of request #3 (green dash-dot line): all its links and intermediate nodes are protected by the p-cycle arc delimited by its two endpoints, which does not contain any link of s_8.

To simplify notations and to improve the readability, in the sequel, we will talk about link, segment, path p-cycles in place of p-cycles, flow p-cycles and FIPP p-cycles.

2.4 Related work

In this section, we attempt to synthetize the design problems of p-cycle schemes according to protection units, protected failure scenarios, traffic patterns as well as the objectives. Table 2.1 summarizes the literature related to the design of p-cycle based survivable WDM mesh networks. We survey the associated design and solution methods. Specifically, overview of the papers on the p-cycle is reviewed next. Following this, we categorize the design problems systematically and survey the associated design and solution methods for link p-cycles, path p-cycles and segment-protecting p-cycles.

Grover and Stamatelakis, and Grover in [GS00, Gro04a] present a good introduction and summary on the early work regarding p-cycle concept, design and networking. The authors in [KAJ09] review the different facets of p-cycles and the associated studies. Also, therein, they review the work on path p-cycles, on the availability-aware p-cycle design and on p-cycles for protecting multi-cast networks.

Table 2.1: References for p-cycle design

Protection Scheme	Problem: Against failures of: Single link	Mult. links	Single link/node	Traffic type: Sta.	Dyn.	Objective: Min. spare band.	Min. total band.	Min. CAPEX	Max. PWCE	Others	Reference
Link p-cycle	✓			✓		✓					[GS98, GS00, SGA02, GS02, ZY02, DHGY03] [Gru03, LT04, ZYL04, KSG05, Sch04, LHP+06] [RJ08, RJB09, WYH10a, OG08a, WYH10b]
	✓			✓			✓				[Mau03, GD02, RA02, Gro04a, ST05, NHP+06] [HS07, AR08, EM09, NHP10, WYH10a, HJ11a]
	✓			✓				✓			[GGC+09, OG11]
	✓			✓						✓	[SSG03, LW06]
	✓				✓	✓					[HFS05, MJ09, JM10, MJ11b]
	✓				✓				✓		[SG05, ZZB05, SJ08a, SJ08c]
	✓				✓					✓	[ZZ05, Sch05a, RTL06, JM10, MJ11b]
		✓		✓		✓					[CG02, SGC04, CG05b, LDZ07, DLZ07, AD09] [SD09, SJ09, Sch03a, WM05, LR06b, MAA06] [KRJA09]
		✓		✓			✓				[CG05a]
		✓		✓						✓	[CG02, Sch03b, CG05b]
			✓	✓		✓					[Sch05b, OG08b, GO09, JL11a]
FIPP p-cycle	✓			✓		✓					[KG05, KGD05, ZZ06, OBG09, JRBG07] [RJB09, RJ12]
	✓			✓			✓				[GBSZ07, BGK08]
	✓			✓				✓			[GGC+09, OG11]
	✓				✓					✓	[HCM07, HCM08, MJ11a]
		✓		✓		✓					[RA09, ELS12, HJ11b, JHD12]
Segment p-cycle	✓			✓		✓					[SG03, JLS10]
	✓				✓		✓				[LR06a]
			✓	✓		✓					[SG03, JL11b]
			✓	✓				✓			[JL12]

2.4.1 Link *p*-Cycle Design

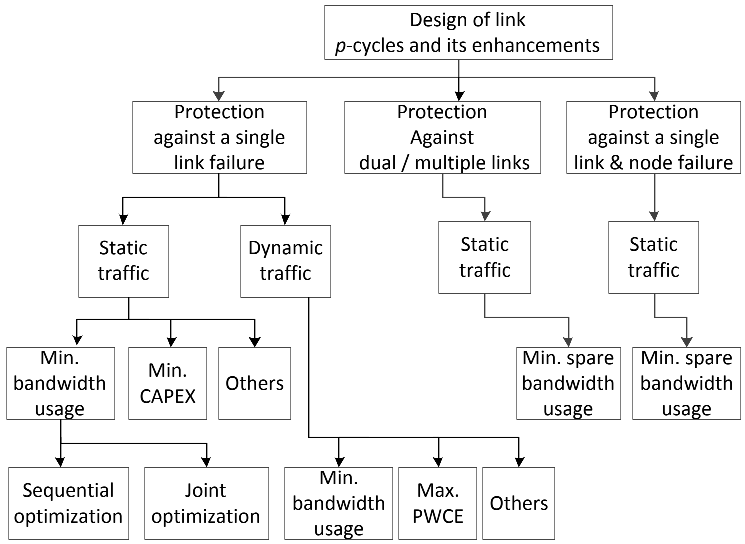

Figure 2.9: Taxonomy of *p*-cycle design

In this section, we survey the literature on the survivable network design based on link *p*-cycles. The classification of these design problems is shown in Figure 2.9. From the viewpoint of protection against the failure scenarios, these designs fall into three recovery scenarios: *(i)* a single link failure, or *(ii)* dual or multiple link failures, or *(iii)* a single link/node failure. The first scenario, i.e., *p*-cycle design against single link failures has been extensively studied. According to the traffic pattern considered, this first scenario can be further studied under two assumptions, static traffic and dynamic traffic. Regarding the other two failure scenarios, all studies in the literature deal with static traffic, and the objective is to minimize spare bandwidth usage.

Static Traffic Protection against Single Link Failures

Given a traffic matrix, design *p*-cycles such that 100% survivability can be guaranteed againsta any single link failure. Most studies on *p*-cycle design are with the objective of minimizing spare bandwidth usage. In this respect, two ways exist to design *p*-cycle networks. One way is the sequential optimization, where the traffic is routed before p-cycle design. The objective is then to minimize spare bandwidth usage of p-cycles. The other way is joint optimization, with which the traffic routing and p-cycle design are determined simultaneously. Accordingly, the objective is to minimize overall capacity usage of working paths and p-cycles.

Sequential Optimization

The sequential p-cycle optimization studies the following problem. Given a network topology and the routed connection requests, design p-cycles such that 100% survivability can be guaranteed against any single link failure. The objective is mainly to minimize the spare bandwidth usage.

Mathematical Model. Let us represent a WDM mesh network by a graph $G = (V, L)$, where V is the set of nodes indexed by v, and L is the set of fiber links indexed by ℓ. Let ω_ℓ be the number of traffic units on link ℓ. For a given working path $p \in P$, let d_p be the number of connection requests carried on it, and let V_p be the set of its intermediate nodes.

To address the optimized design of p-cycles against any single link failure, integer linear programming (ILP) has been extensively exploited. In order to present the ILP model, let us introduce the concept of configurations where a p-cycle configuration c is made of a one unit cycle, and a subset of links protected by this cycle. Formally, a p-cycle configuration c is represented by a vector $(a_\ell^c)_{\ell \in L}$. The vector component $a_\ell^c \in \{2, 1, 0\}$ denotes the number of traffic units on link ℓ which can be protected by p-cycle c. Let COST^c be the spare cost of the p-cycle c.

Variables $z_c \in \mathbb{Z}^+$ denotes the number of copies of unit p-cycle configuration c that are selected in the solution.

Uncapacitated networks. Assuming that there is no capacity limitation on each link of a network, the optimization model can then be formulated as follows [RJ08].

$$\min \quad \sum_{c \in C} \text{COST}_c \, z_c \tag{1}$$

$$\text{subject to:} \qquad \sum_{c \in C} a_\ell^c \, z_c \geq \omega_\ell \qquad \ell \in L \tag{2}$$

Constraints (2) ensure that the overall traffic is protected against any single link failure.

Capacitated networks. Given that a network is capacitated, i.e., each link ℓ is with W_ℓ capacity available. Then, the following set of constraints are also required besides constraints (2) for p-cycle design.

$$\sum_{c \in C} a_\ell^c \, z_c + \omega_\ell \leq W_\ell \qquad \ell \in L \tag{3}$$

Constraints (3) say that, for each link, the working load and p-cycles across it cannot overrun its capacity limitation.

Solution methods. Many studies investigate the efficient and scalable methods for solution of the ILP model.

- Off-line enumeration of all possible p-cycle candidates

Earlier studies in [GS98, GS00, GS02] enumerate all p-cycle candidates in a network. Then, the ILP model selects p-cycles among the candidates. For small networks, this solution method can reach an optimal solution. However, for dense or large networks, there may exist huge number of p-cycle candidates as the number of p-cycles in a network increases exponentially with the network size. The resulting large-scale ILP becomes intractable. Therefore, this exact solution method suffers the scalability issue.

- Off-line enumeration of a subset of p-cycle candidates

In order to deal with the scalability issue, many efforts have been put for pre-selection or generation of a good subset of p-cycle candidates. Then, the ILP model is solved based on this generated candidate set. Thus, the resulting solution methods are scalable. However, there is no tool to evaluate the solution accuracy. Studies in [SGA02,Gru03] set a maximum length limit on p-cycle candidates to reduce the number of p-cycle candidates. Simple (resp. non-simple) p-cycle candidates are enumerated in [SGA02] (resp. [Gru03]). Alternatively, the study in [GD02] proposes two metrics, i.e., the Topological Score (TS) and the Apriori Efficiency (AE) for ranking and pre-selecting a subset of candidate p-cycles. For a p-cycle c, TS is calculated as the number of links which can be protected by c, while AE is the ratio of the potential protected working capacity to the total cost of c. These two metrics can help to reduce the number of p-cycle candidates fed into the ILP model. However, the enumeration is still required of all possible candidate p-cycles in a WDM network.

Zhang and Yang [ZY02] propose the Straddling Link Algorithm (SLA) for generation of a promising candidate p-cycle subset. The SLA main idea is to build one p-cycle for each link in a network such that the link straddles the p-cycle if possible. Liu and Ruan [LT04] propose an algorithm which can generate a good small subset of candidate p-cycles. Therein, the main idea is as follows. One generates two kinds of candidate p-cycles, i.e., high efficient cycles and short cycles individually for each link in a network. Then, one can use the high efficient cycles to protect heavy traffic while using the short cycles for light traffic. For each link, a high efficient cycle is calculated using the proposed Weighted DFS-based Cycle Search (WDCS) algorithm. Two short cycles are built for each link in such a way that one takes the link as on-cycle link, and the other holds the link as a straddling link if such a cycle exists.

SLA and WDCS can enumerate a small set of candidate p-cycles. Based on the p-cycle candidates from SLA, however, the ILP model may not produce good solutions because in such candidates, each p-cycle has no more than one straddling link. On the other hand, the ILP model with the WDCS-enumerated candidates can produce near optimal solution, however, the trade-off exists between the candidate number and the solution quality.

In order to ensure the transmission quality of the protection paths, also to reduce the requirement for the costly regenerators along p-cycles, the work in [KSG05] is the first one which sets limits on the associated protection paths. Therein, an ILP model is proposed, and pre-enumerated candidates are supplied to the ILP for solution. The work in [OG08a] explores the p-cycle design with the requirement different from those in [KSG05]. p-Cycles are designed in such a way that the lightpath length in the recovered state should meet the length limit after a link fails en route. Again, an ILP model is formulated and requires the candidate pre-enumeration.

The papers reviewed above assume the WDM mesh networks with full wavelength conversion capability at each node. However, the papers in [SSG03, LW06] study the design of p-cycle based survivable WDM mesh networks with sparse wavelength conversion capability. Therein, the studies formulate individually the problem as ILP models. The objective of these models is identical, i.e., minimization of the overall cost of spare capacity usage and the required wavelength converters. To solve these ILP models, a subset of p-cycle candidates are enumerated a priori. The differences between [SSG03, LW06] these two studies exist in the assumptions on the network architecture. In [SSG03], no specific limitation exists for network architecture, and two wavelength conversion methods are proposed for

p-cycle deployment. However, in [LW06], the assumption is that the network under consideration holds sparse wavelength converters in a subset of nodes, and the maximum number of converters in such nodes is limited.

It is shown in [SSG03] that, with respect to p-cycles, with only a small increase in spare capacity usage, the total number of wavelength converters required can be greatly reduced. The numerical results in [LW06] show that, in terms of protection cost, the proposed approach significantly outperforms the approach for p-cycle design under the wavelength continuity constraints. Also, in comparison with p-cycle design provided that each node holds wavelength conversion capability, the proposed approach can achieve the identical optimal performance, but requires fewer wavelength conversion sites and fewer wavelength converters.

- Column generation based method

In order to deal with the scalability issue in the conventional design, Rocha and Jaumard in [RJ08, RJB09] propose the scalable solution method based on the CG techniques, where, only promising candidate p-cycles are generated dynamically when needed. With the CG, the p-cycle design is decomposed into the master problem and the pricing problem. The master problem is used to select p-cycles from the candidates which are generated by the pricing problem iteratively in the course of the optimization process. In order to achieve the integer solution, the ILP model is solved using CPLEX MIP solver with the candidates generated during the CG process. Therefore, the design methods in [RJ08, RJB09] are scalable.

- ILP without p-cycle enumeration

Schupke in [Sch04] presents the first ILP model for p-cycle design without requiring any candidate cycle enumeration. The ILP model consists of the constraints for cycle definition, p-cycle selection as well as identification of on-cycle link and straddling links. In this ILP, a cycle is defined as a close path where each node in the network holds either 2 or 0 on-cycle link(s) adjacent to it. With this cycle definition, a candidate p-cycle may include multiple node disjoint cycles. If this is the case, it will make identification of the straddling links difficult. To ensure that a candidate p-cycle only contains one cycle, a flow-based mechanism is proposed. As the ILP model is too complex, a four-step heuristic is proposed for solution of the ILP model.

More recently, Wu *et al.* [WYH10a] develop the ILP models without prerequisite for enumeration of candidate p-cycles. Therein, three ILP models are proposed with the same cycle definition as in [Sch04]. In contrast with the model in [Sch04], the first two models in [WYH10a] allow that a candidate p-cycle contains multiple disjoint cycles. Then, to identify the protected links, a recursion process and a flow conservation approach are adopted respectively. It is shown that the flow conservation approach is more efficient than the recursion process. The third model combines the advantages of Schupke's ILP [Sch04] (easy identification of link protection) and their own models just reviewed (simplification of the cycle generation). Accordingly, the solution process of the third model is much faster than the first two models. To solve these ILP models, the limit is set on the number of cycles which a p-cycle candidate can contain. Therefore, these design methods are heuristic and scalable.

Pure heuristics. The studies in [DHGY03, ZYL04, LHP$^+$06] propose pure heuristics for p-cycle survivable network design without using any ILP model. Doucette *et al.* [DHGY03] propose the first pure heuristic, named as Capacitated Iterative Design Algorithm (CIDA) for p-cycle design. CIDA iteratively selects p-cycles from the candidate p-cycle set until all working capacities are protected. In each iteration, a p-cycle is selected and equipped in the network, then, the unprotected working bandwidth is reduced accordingly. p-Cycle selection depends on the proposed *capacity-weighted efficiency* metric. A p-cycle is selected if it has the highest efficiency. Candidate p-cycles are constructed in two steps. Firstly, SLA [ZY02] is invoked to generate primary cycles. Then, the proposed algorithms, i.e., 'Add', 'Join', 'Expand' or 'Grow', generate larger p-cycles. Among these proposed algorithms, 'Grow' generates the most efficient candidate p-cycles due to the large number of straddling links added to the set of candidate p-cycles.

Zhang *et al.* in [ZYL04] propose an *ER-based unity-p-cycle design algorithm*. This algorithm is quite similar to CIDA [DHGY03] except for enumeration of candidate p-cycles. Therein, directed p-cycles are exploited.

Lo *et al.* [LHP$^+$06] propose an algorithm for p-cycle design in a capacitated WDM network. This algorithm consists of two sequential heuristics: the heuristic p-cycle selection (HPS) and the refine selected cycles (RSC). HPS is exploited first for iterative selection of a cycle from the candidate set based on the cycle efficiency. The cycle candidates are created with an algorithm very similar to SLA [ZY02]. Then, the RSC heuristic is utilized to merge two or more cycles selected by HPS into one cycle such that the required spare capacity is reduced without compromising the number of protected working capacity units.

Joint Optimization

The joint optimized design of the p-cycle based survivable WDM network design is described as follows. Given the network topology and the traffic matrix, route connection requests and built p-cycles for protection against a single link failure simutaneously. The objective is to minimize the overall bandwidth usage of working paths and p-cycles.

Offline candidate enumeration. Grover and Doucette in [GD02] first address this joint optimization problem. Therein, the problem is formulated as an ILP model. To solve the ILP model, the candidate p-cycles are pre-selected from all possible candidates in the network using one of the proposed metrics, i.e., the topological score (TS) and the apriori efficiency (AE).

Mauz [Mau03] proposes an ILP model and a heuristic respectively for this joint optimization problem without and with wavelength continuity constraint. The objective is to minimize the total bandwidth usage for connection provisioning and p-cycle deployment. It is found there, with a single pair of fibers for each link, wavelength conversion can significantly save spare capacity.

Nguyen *et al.* in [NHP10] propose a hierarchical method for the joint optimization of p-cycle network design. In the first step, an ILP model is formulated for selecting the fundamental cycles and the available straddling links. A fundamental cycle refers to a cycle without any straddling link. The available straddling links are the links which can be obtained by merging two or more fundamental cycles. Then, the other ILP model is proposed for translation of the previous ILP solution to p-cycles. In contrast with the previous work, non-simple p-cycles are used for protection.

Schupke *et al.* [SSG03] investigate the joint p-cycle design (in addition to the sequential design) in WDM mesh networks with limited wavelength conversion capability. Therein, two basic strategies are proposed for setting the wavelength converters on p-cycles. The design problem is formulated as an ILP model. The objective is to minimize the overall cost of working paths, p-cycles and wavelength converters. To solve the ILP model, the candidates of working paths and cycles are offline pre-enumerated.

He and Somani in [HS07] compare the capacity efficiency of p-cycles with other shared path protection approaches under the wavelength continuity constraints. For this, the authors propose an ILP for the joint design of p-cycle network. As in the previous work, the working paths and p-cycle candidates are off-line pre-enumerated.

Eshoul and Mouftah in [EM09] also investigate the joint optimization of p-cycle network design under the wavelength continuity constraints. Therein, the problem is formulated as an ILP. To solve the ILP, working path candidates and p-cycle candidates are pre-enumerated. In order to reduce the number of the p-cycle candidates which in turn reduce the complexity of the ILP model, a metric named as Route Sensitive Efficiency (RSE) is introduced. Based on RSE, the p-cycle candidates are ranked and pre-selected before fed into the ILP model.

For the joint optimization of p-cycle design, all studies reviewed so far are heuristic, and the solution accuracy keeps unaware.

Dynamic candidate generation. The study of Rajan and Atamturk [RA02] is the first one that proposes the CG model for the joint optimization of p-cycle design. The candidates are generated dynamically when needed. The master problem takes care of the path and p-cycle selection respectively from the path candidates and p-cycle candidates. The two pricing problem are used respectively to generate path candidates and p-cycle candidates. To generate directed p-cycles, a heuristic is proposed and later an ILP is formulated in [AR08]. A branch-and-cut algorithm is suggested in [AR08] to obtain the integer solution. However, the authors in [AR08] assume that the spare capacity cost can be fractional rather than a multiple of unit capacities. This assumption is unrealistic from the networking point of view. Stidsen and Thomadsen in [ST05] also propose the CG model, which is different with the one in [RA02] by using undirected p-cycles.

Under the wavelength continuity constraints, Hoang and Jaumard in [HJ11a] propose a first scalable CG model for the joint optimization of p-cycle network design. The objective is to minimize the total bandwidth usage for the design of p-cycle based survivable WDM networks. Therein, a new decomposition scheme of the joint optimization problem is suggested. The master problem is used to select working paths and p-cycles from the candidates which are produced by the unique pricing problem. A candidate contains a wavelength, a p-cycle and the protected working paths carried on the wavelength. Also, both simple p-cycles and non-simple p-cycles can be used for protection. Moreover, the authors allow a p-cycle to comprise several node disjoint cycles, thereby the model scalability is greatly improved. The study in [HJ11a] shows clearly that under the wavelength continuity constraints, the total bandwidth requirement is slightly more that without such constraints. The early related work in [SGA02, Mau03] reports the contradictory results. Therein, these work adopts either the sequential designs or the heuristic solution methods.

ILP without candidate enumeration. Wu *et al.* [WYH10a] investigate joint optimization of traffic routing and p-cycle design. They formulate the problem as an ILP model. This is the first model for joint optimization without requirement of p-cycle candidate enumeration. The ILP model consists of the constraints for p-cycle definition and traffic routing and identification of the protected links.

Minimum CAPEX Design

Based on the normalized NOBEL cost model in [GLW$^+$06, HGMS08], the CAPEX of p-cycles was first calculated in [GGC$^+$09, OG11]. There, the authors proposed a node architecture and a protection switching mechanism for p-cycles, and then computed the CAPEX of p-cycles, once they have been designed using a design with minimum spare capacity usage. The equipment for p-cycle deployment is employed with the same network-wide Maximal Transmission Distance (MTD), i.e., optical reach.

Dynamic Protection Provision

The current trend in WDM networks is to dynamically provision survivable connections, i.e., set up survivable working paths for the connection requests when they arrive. Several work on p-cycles copes with dynamic traffic.

Maximize PWCE. Grover [Gro04b] proposes Protected Working Capacity Envelope (PWCE) to support dynamic traffic in p-cycle networks. The PWCE concept is as follows. Given spare capacity budgets in the network, p-cycles are built in such a way that the total protected working capacities (PWCE) are maximized. Then, the incoming requests which are routed over the PWCE will be protected automatically. Thereby, dynamic survivable service provisioning is accomplished.

To design p-cycle-based PWCE, two ILPs are formulated in [SG05] with the objective of maximization of the PWCE against single link failures. These two ILPs vary with the input and the output. The input to the first ILP is the spare capacity budget on each link in the network, while the input to the second one is the network-wide spare capacity budget. The solution of the first ILP is the best combination of p-cycles selected from the candidate cycle set. For the second ILP, the solution comprises the selected p-cycles as well as the spare capacity distribution on each link in the network. Zhang *et. al.* in [ZZB05] also develop an ILP model for the PWCE maximization given spare capacity budget on each link. In contrast with the work in [SG05], directed p-cycles is adopted. These methods suffer the scalability issue as the candidate p-cycles need to be pre-enumerated.

Sebbah and Jaumard in [SJ08a, SJ08c] propose efficient and scalable CG-based solution methods for maximum PWCE design. Based on the CG techniques, the PWCE design problem is decomposed into the master problem and the pricing problem. The master problem is used to select p-cycles which are generated dynamically by the pricing problem. In contrast with the design in [SJ08a], the design in [SJ08c] allows using non-simple p-cycles to build PWCE, and the resulting PWCE size is bigger than that using simple p-cycles in [SJ08a].

Minimize bandwidth usage and others. The work in [ZZ05, Sch05a] investigates the dynamic service provisioning using p-cycles. The objective is to minimize the blocking probability. Zhong and Zhang in [ZZ05] propose pure heuristics without using any ILP model. They extend the *ER-based unity-p-cycle design* heuristic [ZYL04] for p-cycle selection. When a new request arrives, the related RWA (short for routing and wavelength assignment) is solved using the algorithm one prefers. Once the new lightpath sets up successfully, it can be protected either by the existing p-cycles, or new ones, or a combination of them. Three strategies have been suggested, and differ from each other in the ways to release and rebuilt the existing p-cycles. Schupke in [Sch05a] proposes two approaches which are similar to the strategies in [ZZ05].

Ruan *et al.* [RTL06] propose a strategy to deal with dynamic survivable service provisioning based on p-cycles. Therein, the main idea is similar to the one in [ZZ05]. When a new request arrives, its working lightpath is established first without releasing any existing p-cycle. Then, for each link on the working path, one tries to find an existing p-cycle to protect the link. If it is not successful, a new p-cycle is built to protect the link. In contrast with the one in [ZZ05], this strategy takes p-cycles reuse into account when calculating the working lightpath. As a result, the blocking probability is improved significantly in comparison with that in [ZZ05].

Metnani and Jaumard [MJ09, JM10, MJ11b] investigate the p-cycle-based survivable dynamic provisioning within the framework of small-batching provisioning, as in [Gro07]. For this, in [MJ09], the authors propose three strategies for p-cycle setup. In the first strategy, it is forbidden that the established p-cycles are re-configured. In the second one, it is allowed that a small set of p-cycles can be modified. In the last one, all existing p-cycles reset. For each strategy, the mathematical model is developed with the objective of minimization of the spare bandwidth usage such that 100% survivability can be ensured from any single link failure.

In [JM10, MJ11b], in order to study the p-cycle stability, a new mathematical model is formulated, where the objective consists in minimizing the number of optical bypass reconfigurations upon modification/upgrade of the existing p-cycles. To solve these models, the CG based solution method is introduced. With the CG method, the promising p-cycle candidates are generated dynamically when needed using the pricing problem. The experimental results show the high scalability of the mathematical models and the high stability of p-cycle.

Protection against Dual/Multiple Link Failures

Clouqueur and Grover [CG02] present the first work that investigates the design of p-cycle networks with complete or enhanced dual failure recoverability. Therein, three ILP models are proposed. The first one, with the objective of minimizing spare bandwidth usage, is used to select p-cycles such that 100% survivability is guaranteed against any dual link failures. The second one takes care of selecting p-cycles for maximizing the dual failure restorability under the given spare capacity budget. The third one is formulated to deploy p-cycles with minimum spare bandwidth usage such that only the specifically intended services or customers obtain full dual failure restorability.

Schupke [Sch03b] investigates the tradeoff between the number of configured p-cycles and the ability to survive dual fiber duct failures in the network which is designed for surviving from any single link failure. To this end, the ILP model (1) - (2) is modified through replacing the objective function (1) with the new proposed formulas. Based on the solutions obtained, the dual failure restorability is calculated posteriorly. Results show that the number of configured p-cycles has a big impact on the dual failure restorability.

The work in [LDZ07, DLZ07, AD09] studies design of p-cycle networks with a specified minimum dual-failure restorability. The problem is formulated as an ILP model in each work. The difference between the work in [LDZ07] and [DLZ07] consists in the way to calculate the dual failure recovery ratio. The work in [AD09] extends the one in [DLZ07] through the proposed enhance dual failure recovery strategy. With this enhanced strategy, the numerical results show that, the spare bandwidth cost is reduced considerably compared with [DLZ07]. To solve these ILP models, therein, a subset of p-cycle candidates is offline pre-enumerated, and thus the solution quality cannot be guaranteed.

Sebbah and Jaumard [SJ09] propose a scalable optimization solution method for the p-cycle design such that the specific level of dual link failures can be guaranteed. Therein, the design problem is formulate as an ILP. In contrast with all previous related work, based on the CG, very limited number of promising p-cycles are calculated on the fly in the course of optimization process. The author conclude that p-cycles are quite expensive in terms of spare capacity usage in order to design survivable WDM networks against any dual link failures.

The work in [SGC04, MAA06, SD09] investigates, based on reconfigurable p-cycles, the design of survivable networks against dual failures. The assumption is that the second failure occurs after the first one has been recovered by p-cycles. The objective is to minimize spare capacity usage such that 100% guranteed survivability can be ensured against dual link failures. In these work, different strategies have been proposed for p-cycle reconfiguration, and different ILP models have been developed accordingly. The capacity efficiency of the solutions from these designs is ranked as the order shown. To solve these ILP models, the p-cycle canadiates are off-line enumerated with/without length limitation. The tradeoff exists in these designs between the scalability and solution quality.

Wang and Mouftah in [WM05] study the p-cycle network design in order to survive against multiple failures which may occur in larger networks. Liu and Ruan in [LR06b] investigate p-cycle design in the presence of the failure of any shared risk link group (SRLG). A SRLG refers to a set of links which shares the same risk of failure. For this, an ILP model is formulated, and its objective aims at minimizing spare capacity usage such that 100% survivability can be guaranteed against any single SRLG failure. The p-cycle candidates are offline enumerated and supplied to the ILP for p-cycle selection. To avoid enumeration of all possible cycles in a nework, a heuristic has been proposed to generate a basic p-cycle candidate set. Thus, the solution time is comprimised with the spare capacity usage of the ILP solution.

Clouqueur and Grover in [CG05a] present the first work on joint optimization of traffic routing and p-cycle design such that the demands with higher availability requirements can be met besides 100% guaranteed survivability from any single failure. For this, two mathematical models are developed with different demand routing strategies. The objective is identical, i.e., to minimize the total capacity usage of working paths and p-cycles. To solve the ILP models, a subset of candidate routes and candidate p-cycles are pre-enumerated respectively. Therefore, the design method is heuristic and scalable.

The authors in [KRJA09] investigate the p-cycle design such that the unavailability of all end-to-end working paths is kept less than a given upper bound. The objective is to minimize spare capacity usage. This problem is formulated as an ILP model. To solve the ILP model, given routed demands, all possible candidate p-cycles in the network are enumerated and pre-selected. Since only a subset of candidate p-cycles is offline enumerated, the scalability of this design method compromises with the solution accuracy.

Protection against Single Link/Node Failures

A few studies have investigated the link-protecting p-cycle design for full node protection. Stamatelakis and Grover [SG00b] propose node-encircling p-cycles (NEPCs) for node protection. With NEPCs, each node is surrounded by a p-cycle which traverses all the associated adjacent nodes. Thus, the traffic transiting each node can be protected against a single node failure. However, another set of link-protecting p-cycles is also needed to protect against a single link failure.

As NEPCs are too costly for protection against any single link/node failures, Schupke [Sch05b] proposes an Automatic Protection Switching (APS) protocol enhancement to provide the means for node protection using p-cycles. Therein, to design p-cycles against any single link/node failures, an ILP model is develop with the objective of minimization of space capacity usage. Candidate p-cycles, which are supplied to the ILP model, are pre-enumerated in such a way that each candidate is routed through all the nodes on the associated working paths. Under this design, the associated p-cycles may be less capacity efficient due to their limited routing paths.

In order to provide node protection, p-cycles have been generalized to segment p-cycles in [SG03]. Segment p-cycles can protect on-cycle and straddling working segments. Thereby, the intermediate nodes of the working segments can be inherently protected but not the end nodes of the working segments. Kodian and Grover [KG05] proposed path p-cycles to provide end-to-end path protection. Note that flow p-cycles and FIPP p-cycles are usually more capacity efficient than link protection schemes [SG03, KG05]. However, the recovery speed is slower as in any path or segment protection schemes.

Onguetou and Grover [OG08b] proposed a new insight of node protection with overlapping p-cycles providing partial or full protection of all the intermediate nodes of the working paths. The same authors later restrict in [GO09] the segments to be two-hop segments in order to retain the simplicity of p-cycle switching operations. Onguetou and Grover in [OG08b] develop an ILP model for link Np-cycle design with minimum spare capacity usage for protection against any single link/node failure. Therein, a subset of Np-cycle candidates are pre-enumerated for solution of the ILP model. Therefore, this design method is heuristic and scalable.

2.4.2 Path *p*-Cycle Design

Several studies in the literature investigate path p-cycle design. The classification of the path p-cycle designs is shown in Figure 10(a). In general, path p-cycle design problems can be divided into two categories in terms of the protected failure scenarios: (*i*) a single link/node failure and (*ii*) dual/multiple link failures.

Path p-cycle design problems against a single link failure can be further classified into two groups according to the traffic pattern under consideration, i.e., static traffic or dynamic traffic. In each group, the design problems may vary with the objective pursued.

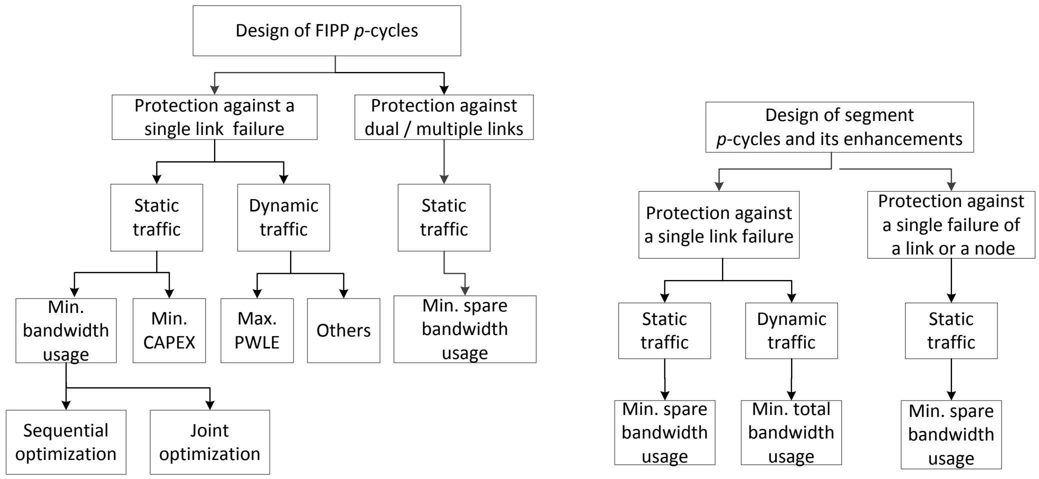

(a) Path p-cycle design (b) Segment p-cycle design

Figure 2.10: Taxonomy of path and segment p-cycle design

Protection against a Single Failure

Sequential Optimization

The following states the sequential optimization of path p-cycle design. Given the network topology and the routed connection request set, design path p-cycles such that 100% survivability can be guaranteed against any single link failure. The objective is to minimize spare capacity usage of path p-cycles.

Mathematical models and solution methods. The first work on path p-cycles design is report in [KG05], where the problem is formulated as an ILP model. To solve the ILP model, a subset of cycles is pre-enumerated in a network. Then, the ILP is solved to determine the best combinations of cycles and the given working paths such that the spare capacity usage is minimized against any single link failure. As there may exist a huge number of such combinations, which lead to a huge number of variables and constraints, and therefore the resulting ILP is not scalable.

The authors in [KGD05] propose an ILP model which takes as input path p-cycle candidates. A subset of path p-cycle candidates is pre-enumerated in the following way. Firstly, mutually disjoint route sets (DRSs) is built based on the given working paths using a heuristic. Then, several path p-cycles for each DRS are established such that each p-cycle traverses all end nodes of working paths belonging to the related DRS. Since only a subset of candidate path p-cycles is pre-enumerated, the solution method is scalable, buth the solution quality cannot be ensured.

The authors in [OBG09] propose a hierarchical approach for design of near-optimal path p-cycle network. Therein, firstly, the design problem is formulated as an ILP model without consideration of the failure independent constraints. After the solution of the ILP, the working paths violating such constraints are identified. Finally, the path p-cycle solution is obtained by adding more cycles for protecting these identified working paths. To solve the ILP model, general path p-cycle candidates are off-line enumerated using the proposed generic algorithm.

Jaumard *et al.* [JRBG07] propose a first CG model for path p-cycle design against a single link failure. The candidate path p-cycles are generated on the fly when needed. Based on the CG techniques, the path p-cycle design problem is decomposed into the master problem and the pricing problem. The master problem is used to select path p-cycles from candidates which are generated by the pricing problem dynamically when needed in the course of the optimization process. The improved model for the pricing problem is presented in [RJB09]. Further improvement of the CG model is reported in [RJ12], where two pricing problems are exploited for candidate path p-cycle generation. Thereby, the solution process is much faster than the previous two CG models. Therein, A path p-cycle can protect the pair-wise disjoint working paths. Also, it can protect the pair-wise non-disjoint working paths only if their protection paths are disjoint. Thereby, the capacity efficiency of path p-cycles is greatly improved in comparisons with that in [KG05, KGD05].

Pure heuristic. Zhang and Zhong in [ZZ06] present a heuristic algorithm for design of path p-cycles without using any ILP model. The main idea which is similar to the one proposed for link p-cycle design in [ZYL04], is as follows. In the beginning, one selects the most efficient path p-cycle from the candidate p-cycles according to the proposed efficiency score, and then reduces the number of unprotected working paths accordingly after configuring the selected path p-cycle. This process is iterated until all working paths are protected.

Joint Optimization

The joint optimization of path p-cycle design problem is stated as follows. Given a network topology and traffic matrix, routing traffic and selecting path p-cycle are determined simultaneously such that the overall capacity usage of working paths and path p-cycles is minimized for protection against a single link failure.

The first work on this joint optimization problem is presented by Ge *et. al.* in [GBSZ07]. Therein, a pure heuristic is proposed. With this heuristic, a set of candidate cycles is first enumerated, and then several DRSs are built for each cycle based on multiple route options enumerated for each demand. Finally, based on the protection efficiency metric, the best combinations of cycles and DRSs are selected as path p-cycles.

The authors in [BGK08] formulate as an ILP model the joint optimization of path p-cycle network design against any single link failure. To solve the ILP model, the candidate sets, including the route set and path p-cycle candidate set, are enumerated through extension of the DRS strategy [KGD05]. Specifically, for each demand, the N shortest routes are enumerated to form an eligible route set, where N is an input parameter. Then, eligible

DRSs are constructed based on mutually disjoint route options. For each DRS candidate, a number of eligible cycles are produced as path p-cycle candidates which traverse all end nodes of the working paths in the related DRS. As only a subset of candidates is pre-enumerated, this design method is heuristic and scalable. Therein, the numerical results show that, with the joint optimization design, the resulting networks are at costs that are significantly lower than non-joint designs.

Minimum CAPEX Design

The authors in [GGC$^+$09] evaluate the CAPEX cost of path p-cycles against a single link failure. Due to the great complexity of the CAPEX optimization design, the authors calculate the path p-cycle CAPEX posteriorly from the solution of minimization of spare capacity design in [GGC$^+$07].

Dynamic Protection Provisioning

He *et al.* [HCM07] propose Protected Working Lightpath Envelope (PWLE) for dynamic provisioning survivable service. The PWLE concept is similar to PWCE [Gro04b], and is a path protection approach based on path p-cycles. To design the PWLE, a Mixed Integer Linear Programming (MILP) is developed with the objective of maximizing the PWLE for protection of working paths against a single link failure. To solve the MILP, the pre-request is to enumerate possible candidate cycles and their potentially protected working lightpaths. As a large amount of candidates may exist, the resulting MILP is less tractable for large networks. The same authors in [HCM08] propose a heuristic for pre-enumeration of a subset of candidate cycles, and develop three pure heuristic algorithms for path p-cycle selection.

Metnani and Jaumard [MJ11a] study the path p-cycles stability under dynamic traffic. They formulate as an ILP model the problem of path p-cycle design for dynamic provisioning survivable service. The objective of the ILP model is to minimize the number of OXC port reconfigurations in the context of dynamic traffic such that 100% survivability can be ensured against any single link failure. To solve the ILP model, a CG-based scalable solution method is proposed without any requirement of path p-cycle candidate pre-enumeration. Based on CG, the path p-cycle design problem is decomposed into the master problem and the pricing problem. The master problem is used to select path p-cycles from candidates which are generated by the pricing problem dynamically when needed. To speed up the solution process, the pricing problem is further divided into two pricing problems: the first one is used for generation of a new path p-cycle, and the second one for improving the use of existing p-cycles. It is shown that, using the number of required switching reconfigurations, path p-cycles are highly stable. In the context of incremental traffic, the percentage of required switching reconfigurations follows the percentage of the increased traffic.

Protection against Dual / Multiple Failures

Eiger *et. al.* in [ELS12] investigate the path p-cycle design problem such that demands in the network can survive from single or dual failures depending on their requirement. The problem is formulated as an ILP model with the objective of minimizing spare capacity usage. To solve the ILP model, a subset of path p-cycle candidates are pre-enumerated with the proposed algorithm. As only a subset of path p-cycle candidates is pre-enumerated, the solution accuracy remains unaware.

Hoang and Jaumard in [HJ11b, JHD12] study the path p-cycle design against multiple link failures. The objective is to minimize spare capacity usage. Therein, they propose a generic flow formulation model and the CG-based scalable solution method. The path p-cycle candidates are generated dynamically when needed. With the CG, the original design problem is decomposed into the master problem and the pricing problem. The master problem is formulated for selection of candidate path p-cycles, which are generated by the pricing problem dynamically when needed. In order to speed up the solution process of the pricing problem, a hierarchical decomposition of the pricing problem is utilized, as in [RJ12]. Also, two heuristics is proposed for efficient solution of the pricing problem in large instances. The numerical results show that path p-cycles require much less spare capacity than link p-cycles in order to protect against dual link failures.

Ranjbar and Assi in [RA09] present the first work which addresses the availability-ware path p-cycle design such that the end-to-end unavailability of a working path is no more than a given upper limit. The objective is to minimize spare capacity usage. The design problem is formulated as an ILP model. Given the routed demands, candidate path p-cycles are enumerated using the DRS approach [KGD05]. As only a subset of candidates is enumerated, the solution method is scalable, but the solution accuracy keeps unaware.

2.4.3 Segment p-Cycle Design

Only few studies investigate segment p-cycle designs. The classification of these design problems is shown in Figure 2.10(b). These problems can be divided into two groups according the protected failure scenarios, i.e., single link failures, or single link/node failures. In the former group, the design problems can be further classified into two types according to the traffic pattern, i.e., static or dynamic.

Minimum Bandwidth Usage with Static Traffic

Shen and Grover [SG03] proposed a first method for the design of segment p-cycles. Therein, the design problem is formulated as an ILP model with the objective of minimizing the spare capacity usage for protection against a single link failure. To solve the ILP model, the candidate cycles are pre-enumerated and the *potentially* protected links of working paths are pre-identified. As the number of cycles increases exponentially with the network size increase, this model is not scalable.

In practice, network designers proceed in two steps: firstly, the definition of the working paths (point to point connection with effective guaranteed bandwidth) and secondly with the definition of the protection scheme. The segmentation of the working paths into segments (i.e., optical hops) is usually obtained as the result of the grooming, routing and wavelength assignment (GRWA) step, as in, e.g., Bouffard [Bou05, BJH11]. In Shen and Grover [SG03] (see page 1312, left column), the working segments are post-defined, i.e., "come out implicitly from the choice of p-cycles". This is not quite realistic from a network management point of view. That is the reason why, in this thesis, we assume that working segments are available at the outset of the second step, i.e., the design of the protection scheme. In addition, in [SG03], only the segment intermediate nodes are guaranteed a protection against single node failures, excluding a priori the endpoints of the segments.

Dynamic Survivable Service Provisioning

The work in [LR06a] is the only one to date which investigates dynamic survivable service provisioning based on segment p-cycles. Therein, the following problem is studied. Given a demand request, calculate a working path and a set of segment p-cycles which can protect this path. The objective is to minimize the total capacity cost of the working path and the segment p-cycle set. To address this problem, an ILP model is proposed. To reduce the total capacity cost of the demand just arrived, the ILP model is formulated in such a way that the existing p-cycles (i.e., segment p-cycles configured for protection of the existing demands in the network) can be reused to protect this demand. To solve the ILP model, the combinations of the working path and segment p-cycle candidates are pre-enumerated. Then, the scalability of the ILP model is compromised with the solution quality.

Chapter 3

The Multi-granularity Segment p-Cycle Scheme

3.1 Introduction

Among p-cycles based schemes, segment p-cycles offer the best compromise between the link p-cycles and the path p-cycles in terms of capacity efficiency and recovery delay. However, only very few studies consider segment p-cycle design. In this chapter, we therefore investigate the design of survivable WDM mesh networks based on segment p-cycles.

Most studies on p-cycle based structures have focused on minimizing the spare capacity. While the spare capacity is certainly a decisive design criterion, once optical fibers have been deployed, the nodal equipment cost, i.e., a key component of the CAPital Expenditures (CAPEX), becomes significant in order to set up p-cycle structures. Therefore, the goal here is to investigate the optimal design of segment p-cycles not only with respect to the capacity cost/usage, but also with respect to the nodal cost, in order to ensure 100% survivablity against any single link failure.

The nodal equipment cost will be estimated by the number of transport blades (a pair of input and output ports). It varies with the transport capacity, (for instance, the cost of an OC-192 transport blade is about 2.5 the cost of an OC-48 transport blade). Driven by this, we propose a multi-granularity segment p-cycle design method (see Section 3.5 for the details) that will be able to mix different granularities.

The chapter is organized as follows. Shen and Grover's design method of segment p-cycles [SG03] is presented in Section 3.2. Our proposed design method is presented in Section 3.3. The comparisons of the two design methods are made respectively with the help of an example in Section 3.4 and the numerical results over network instances in Section 3.8. We propose the directed multi-granularity segment p-cycles in Section 3.5. To design directed multi-granularity segment p-cycles, in Section 3.6, we develop an optimization model together with an efficient algorithm in order to solve it. In Section 3.9, computational results are presented with respect to design of multi-granularity segment p-cycles. Conclusion is drawn in Section 3.10.

3.2 The ILP-based Design Method (E-ILP)

In this section, we review the three-step design method of segment p-cycles proposed in [SG03]. There, in the first step (the preprocessing step), a subset of promising segment p-cycle candidates is generated. In the second step (the ILP-based selection step), an ILP model is proposed to select the most promising subset of segment p-cycles. In the third step, working and protection segments are defined.

Step 1: Preprocessing

Link/path/cycle protection relationships

All possible cycles in a network are first enumerated, protection relationships are then determined between cycles and links of given working paths. A cycle c can protect link ℓ of a segment belonging to a working path p if the segment and the cycle have at least two common nodes. With respect to a working path p and a cycle c, a link of a fully or partially on-cycle working segment can be provided one unit of protection segment; A link of a fully straddling working segment can be offered two protection segmented paths. Thereby, the values of the protection-relation parameters $a^p_{\ell,c} \in \{0, 1, 2\}$ are assigned and will be employed in the ILP model (see Section 3.2).

Preselecting a subset of cycle candidates

In order to limit the number of candidate cycles, a metric named Scoring Credit (SC) [SG03] is defined for preselecting a promising subset of segment p-cycles out of the whole cycle candidate set. Scoring credit of a segment p-cycle c is calculated as follows:

$$SC(c) = \frac{\sum\limits_{p \in P, \ell \in \mathrm{L}_p} \text{LENGTH}_p \times d_p \times a^p_{\ell,c}}{\text{COST}_c}$$

where P is the working path set, indexed by p, L_p is the link set on the working path for demand p, d_p is the number of unit requests in path p (i.e., the number of unit connection requests between endpoints of path p), $a^p_{\ell,c}$ is defined as above, and COST_c is the cost of cycle c (e.g., spare capacity).

Step 2: ILP-based Selection

In the second step, an ILP is proposed for selecting the most promising subset of the candidates generated in the first step. The following notations are used:

SETS

L set of links in the WDM network, indexed by ℓ.

C set of segment p-cycle candidates, indexed by c.

P_ℓ set of demands whose working paths traverse link ℓ.

PARAMETERS

$\mathbf{cost}_\ell$ cost of a capacity unit on link ℓ.

$\mathbf{cost}_c$ cost of a cycle c, defined by $\sum_{\ell \in c} \textsc{cost}_\ell$.

VARIABLES

z_c number of copies of cycle c.

$z^p_{\ell,c}$ number of copies of segment p-cycle c needed for protecting working path p from a failure on link ℓ.

The mathematical model can be written as follows.

$$\min \quad \sum_{c \in C} \textsc{cost}_c \, z_c$$

$$\text{subject to:} \qquad \sum_{c \in C} a^p_{\ell,c}\, z^p_{\ell,c} \;\geq\; d_p \qquad \ell \in L,\; p \in P_\ell \tag{3.4}$$

$$z_c \;\geq\; \sum_{p \in P_\ell} z^p_{\ell,c} \qquad \ell \in L,\; c \in C \tag{3.5}$$

$$z_c,\;\; z^p_{\ell,c} \in \mathbb{Z}^+ c \in C,\; \ell \in L,\; p \in P. \tag{3.6}$$

Constraints (3.4) ensure that all demands are protected from any single link failure. A single link failure will disrupt all passing-through working paths. If a segment p-cycle is selected to protect a given link ℓ, the copies of this segment p-cycle must be able to recover from this link failure for all the working paths (demands) containing ℓ. This is ensured by constraints (3.5). A segment p-cycle may protect links with different traffic load. Constraints (3.5) also ensure that the copies of a segment p-cycle must be enough to recover from the failure of any of their protected link with the heaviest traffic load.

Step 3: Working Segment Definition

To completely define the segment p-cycles, one needs to formally define the working segments: it is done in a third step. Once the E-ILP model is solved, the working segments are obtained as follows. If a selected segment p-cycle c protects a largest set of consecutive on-cycle links on a working path p, then this set defines a working segment of the working path ($z^p_{\ell,c} > 0, a^p_{\ell,c} > 0$), and consequently, the protection segments of the protection cycles are fully defined accordingly.

However, some confusion may exist with the definition of the straddling and of the partially straddling/on-cycle segments. Let us first illustrate the difficulties on the example of Figure 3.1.

Two demands A-D and E-C are respectively routed on the working path A-B-C-D and E-B-C, as shown in Figure 3.1. The demands A-D and E-C respectively require one unit and two units of working capacity, see the numbers shown beside both working paths. Two segment p-cycles C_1 and C_2 are selected by E-ILP to protect the two demands. Both segment p-cycles are with one unit of spare capacity. Segment p-cycle C_1 is employed to protect the two units of demand E-C along the path E-B-C. The two protection segmented paths (with endpoints C and E) on segment p-cycle C_1 are used for recovering any link failure on the two-unit working path E-B-C (made of a single working segment). According to the E-ILP solution, this segment p-cycle also protects link A-B (i.e., the associated value of $z^p_{\ell,c}$ is one) but not the whole segment A-B-C along the working path A-B-C-D. Note that link B-C cannot be protected by segment p-cycle C_1 (i.e., the associated value of $z^p_{\ell,c}$ is zero) because there is not enough available spare capacity available on C_1. The other segment p-cycle C_2 is employed to protect the working segment B-C-D of the working path A-B-C-D.

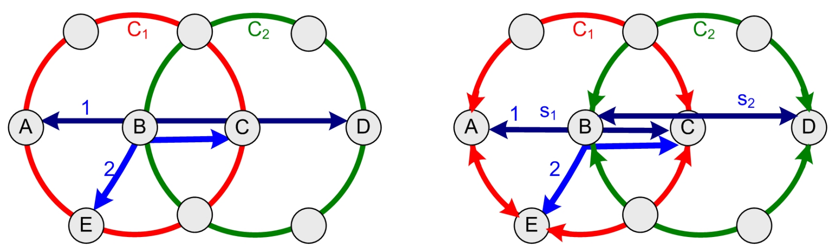

(a) E-ILP solution (b) Working and protection segments

Figure 3.1: An example of segmenting working paths

Obviously, we can take the path E-B-C as a working segment which is an integral part protected by C_1. For the working path A-B-C-D, we take B-C-D as a working segment s_2 because it is an integral part protected by segment p-cycle C_2. For the segment A-B-C which straddles cycle C_1, where link A-B is protected by C_1 while link B-C is protected by C_2, we can then define a segment s_1 = A-B-C protected by C_1; and as s_1 is overlapping s_2, then we will need two copies of C_1 to guarantee 100% link protection.

The above example thus illustrates the possibly extra protection bandwidth that might be required in the E-ILP approach in order to properly define segment p-cycles that fully protect all working segments. Note that no detailed algorithm is provided in [SG03] in order to construct the working and the protection segments.

3.3 Optimal Design of Segment p-Cycles (CG)

We propose an optimization method based on the column generation (CG) techniques for segment p-cycle design, assuming working segments are defined together with the working paths. The objective is to minimize the spare capacity usage such that the given working segment set can survive from any single link failure.

The CG techniques rely on a decomposition of an optimization problem into two sub-problems: the master problem and the pricing problem. The master problem deals with the selection of the most promising segment p-cycles from the candidates, each of which is generated individually and dynamically by the pricing problem at each iteration of the CG algorithm, as illustrated in Figure 3.4. At each iteration, a restricted linear relaxation of the master problem is solved and the associated values of the dual variables are provided to the pricing problem. Next, the pricing problem feeds the master problem with promising segment p-cycles.

3.3.1 The Master Problem

The master problem takes care of segment p-cycle selection to protect the whole working segment set S so that the overall spare cost is minimized. Candidate segment p-cycles are associated with configuration set C. A configuration (segment p-cycle) c consists of a cycle that protects a subset of working segments. Formally, a configuration c is represented by a vector $a^c = (a_c^s)_{s \in S}$, where $a_c^s \in \{2, 1, 0\}$ encodes the number of protection segments provided by configuration c for the failed working segment s (due to the failure of one of its link). For each working segment $s \in S$, let d_s be its capacity (number of capacity units), and SRC_s and DST_s its two endpoints, respectively. Variables z_c encodes the number of copies of configuration c that are selected in the current solution. Then, the mathematical model can be written as follows.

$$\min \quad \sum_{c \in C} \text{COST}_c \, z_c$$

$$\text{subject to:} \qquad \sum_{c \in C} a_c^s \, z_c \ \geq \ d_s \qquad s \in S \tag{3.7}$$

$$z_c \in \mathbb{Z}^+ \qquad c \in C \tag{3.8}$$

Constraints (3.7) ensure that all working segments are protected from a single link failure. Constraints (3.8) are variable domain constraints.

3.3.2 The Pricing Problem

The purpose of the pricing problem is to generate a promising segment p-cycle that, once added to the master problem, will improve the value of the current solution. The pricing problem corresponds to the optimization problem of minimizing the so-called reduced cost of the restricted linear-relaxed master problem subject to a set of segment p-cycle design constraints. The reduced cost is written as follows:

$$\overline{\text{COST}}_c = \text{COST}_c - \sum_{s \in S} u_s a_c^s \qquad c \in C,$$

where u_s are dual variables associated with constraints (3.7). Let us introduce the following notations before describing the set of constraints.

SETS

V set of nodes in a network, indexed by v.

$\omega(V')$ co-cycle of $V' \subseteq V$, i.e., the set of links with exactly one end node belonging to V'. Note that a co-cycle corresponds to a cut in an undirected graph. $\omega(v)$ set of links adjacent to node v (particular case of $\omega(V')$ when $V' = \{v\}$).

PARAMETERS

$\beta^{s,s'}$ = 1, if working segments s, s' are not link disjoint; 0 otherwise.

τ_ℓ^s = 1, if working segment s traverses link ℓ; 0 otherwise.

VARIABLES

$$x_\ell = \begin{cases} 1 & \text{if the current cycle under construction traverses link } \ell; \\ 0 & \text{otherwise.} \end{cases}$$

$$x_\ell^s = \begin{cases} 1 & \text{if link } \ell \text{ protects working segment } s; \\ 0 & \text{otherwise.} \end{cases}$$

Based on these new notations, the reduced cost can be rewritten as follows.

$$\overline{\text{COST}}_c = \overbrace{\sum_{\ell \in L} \text{COST}_\ell \, x_\ell}^{\text{COST}_c} - \sum_{s \in S} u_s \overbrace{\sum_{\ell \in \omega(\text{SRC}_s)} x_\ell^s}^{a_c^s}$$

The pricing problem includes two blocks of constraints. The first block of constraints is defined for generating a simple cycle, which is formulated next.

The first block is defined next.

$$\sum_{\ell \in \omega(v)} x_\ell \leq 2 \qquad v \in V \tag{3.9}$$

$$\sum_{\ell' \in \omega(v): \ell' \neq \ell} x_{\ell'} \geq x_\ell \qquad \ell \in \omega(v),\ v \in V \tag{3.10}$$

$$\sum_{\ell \in \omega(V')} x_\ell \geq x_{\ell'} + x_{\ell''} - 1 \qquad V' \subset V,\ \ell' \in \omega(V'),\ \ell'' \in L,\ \ell'' \notin \omega(V') \tag{3.11}$$

Any on-cycle node must have two incident links on the cycle. This is ensured by the sets of constraints (3.9) and (3.10). Constraints (3.11) prevent generation of a configuration which includes multiple cycles. Otherwise, it burdens the determination of straddling working segments in the next step.

The second block of the constraints is proposed for determining a set of working segments which can be protected by the current cycle under construction.

$$x_\ell^s \leq x_\ell \qquad \ell \in L,\ s \in S \tag{3.12}$$

$$\sum_{\ell \in \omega(\text{SRC}_s)} x_\ell^s = \sum_{\ell \in \omega(\text{DST}_s)} x_\ell^s \qquad s \in S \tag{3.13}$$

$$\sum_{\ell \in \omega(v)} x_\ell^s \leq 2 \qquad s \in S,\ v \in V \tag{3.14}$$

$$\sum_{\ell' \in \omega(v):\, \ell' \neq \ell} x_{\ell'}^s \geq x_\ell^s \qquad \ell \in \omega(v),\ v \in V \setminus \{\text{SRC}_s, \text{DST}_s\},\ s \in S \tag{3.15}$$

$$x_\ell^s + x_\ell^{s'} \leq 2 - \beta^{s,s'} \qquad s, s' \in S,\ \ell \in L \tag{3.16}$$

$$x_\ell^s \leq 1 - \tau_\ell^s \qquad \ell \in L,\ s \in S \tag{3.17}$$

$$x_\ell, x_\ell^s \in \{0, 1\} \qquad \ell \in L,\ s \in S,\ v \in v \tag{3.18}$$

Constraints (3.12) ensure that only on-cycle links can be considered for providing protection.

Constraints (3.13) say that, for any working segment, the associated protection segment(s) must end at its two end nodes. Constraints (3.14) ensure that the current cycle under construction can provide at most two protection segments for any working segment. Constraints (3.14) together with (3.15) guarantee flow conservation in the intermediate nodes along protection segment(s). Constraints (3.16) ensure that only link-disjoint working segments can share protection segments. Constraints (3.17) prevent a link from protecting itself and the related protected working segments.

The above two blocks of constraints are adapted from those proposed in [RJB09]. The pricing problem in [RJB09] is used to generate path-protecting p-cycles.

3.4 Comparison of E-ILP and CG: An Example

We saw in the previous sections that a first difference between E-ILP and CG models is that, while working segments are defined a posteriori in E-ILP, they are part of the inputs in the CG model. We next show that, in spite of using the working segments output by E-ILP, the CG model can find a more bandwidth efficient solution than the E-ILP model.

Let us consider the example instance shown in Figure 3.2(a), where two demands A-C and E-C are routed on paths A-F-C and E-F-C, respectively. Each demand is of one unit capacity.

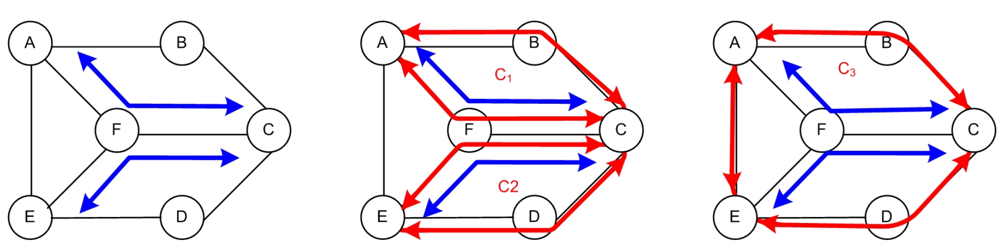

(a) An instance (b) E-ILP solution (c) The CG solution

Figure 3.2: Comparison of the design of segment p-Cycles: E-ILP vs. CG

With E-ILP, protection is determined *independently* for each working path. The segment p-cycle C_1 (i.e., cycle A-B-C-F-A) is selected in the optimal E-ILP solution since its spare-capacity cost is minimum among all possible segment p-cycles to protect working path A-F-C. Likewise, segment p-cycle C_2 (i.e., cycle F-C-D-E-F) is selected to protect working path E-F-C. Both C_1 and C_2 cost each, four units of spare capacity. Thus, the total spare cost is eight units. The corresponding capacity redundancy is $8 \div 4 = 200\%$. (Note that if cycle A-B-C-D-E-A had been selected, two copies of it would have been needed according to E-ILP, to protect working paths A-F-C and E-F-C, respectively. It leads to a total spare capacity cost of 10 units. From the optimal E-ILP solution, we deduce two on-cycle working segments, i.e., A-F-C and E-F-C.

In contrast to E-ILP, the model CG considers protection for all working segments *simultaneously*. Moreover, the CG model allows non-link-disjoint working segments to share a segment p-cycle if their associated protection segments are link-disjoint. Thereby, to protect the working segments deduced from E-ILP, the optimal solution of CG outputs, see Figure 3.2(c), a segment p-cycle C_3 (i.e., cycle A-B-C-D-E-A) for protecting both working segments. The total spare capacity cost is five units and the associated capacity redundancy is $5 \div 4 = 125\%$. The solution of E-ILP is 75% more redundant than CG although both models protect the same working segments.

3.5 Multi-granularity Segment p-Cycles

This section illustrates the proposed multi-granularity segment p-cycles are segment p-cycle scheme. Multi-granularity segment p-cycles are segment p-cycles with multiple transport capacities, e.g., OC-48 (2.5 Gbps), OC-192 (10 Gbps), and OC-768 (40 Gbps). A segment p-cycle with a given transport capacity can be used to protect working segments with the same or smaller transport capacity. We assume, as in practice, that values of the transport capacities are quadruple multiple of OC-48, i.e., OC-48, OC-192 = 4 × OC-48, OC-768, etc. We also assume that any working segment of capacity t can be protected by a set C of segment p-cycles, provided $\sum_{c \in C} t_c \geq t$, where t_c is the capacity of segment p-cycle c.

Multi-granularity segment p-cycles is illustrated in Figure 3.3. A small network instance is depicted in Figure 3.3(a), where two demands, of granularity OC-48 and OC-192, are routed on path $W1$ ($D \rightarrow F \rightarrow A$) and $W2$ ($A \rightarrow F \rightarrow C$), respectively. Both demands are segmented at node F. To protect these working segments from any single link failure, two kinds of configurations based on different granularity segment p-cycles, are needed, as shown in Figure 3.3(b) and 3.3(c).

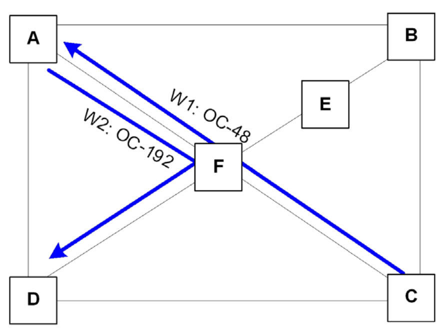

(a) Network topology and working paths

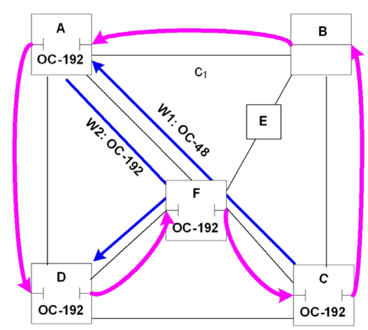

(b) Segment p-cycle c_1

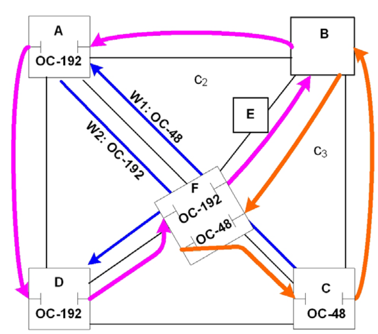

(c) Segment p-cycles c_2 (red) and c_3 (orange)

Figure 3.3: Multi-granularity segment p-Cycles

From the capacity usage point of view, configuration c_1 in Figure 3.3 (b), along cycle $A \rightarrow D \rightarrow F \rightarrow C \rightarrow B \rightarrow A$, is an optimal solution, which requires 5 OC-192 units of spare channels. Moreover, c_1 needs 4 OC-192 transport blades at the end nodes of the protected working segments in order to switch the affected traffic to the protection segments in case of any single link failure. Thus, total nodal cost is $4 \times 10\text{K} = 40\text{K\$}$ where the cost of an OC-192 transport blade is estimated to 10K$.

However, from the nodal cost perspective, it is the configuration in Figure 3.3(b), with c_2 and c_3, that is optimal. Multi-granularity segment p-cycles c_2 and c_3 are with transport capacity OC-192 and OC-48, respectively. In case of any single link failure, three OC-192 blades are needed to switch segments $A \rightarrow F, F \rightarrow A$ and $F \rightarrow D$ in configuration c_2 while 2 OC-48 blades are required in c_3 to switch segment $C \rightarrow F$. Therefore, the total nodal cost equals $3 \times 10\text{K\$} + 2 \times 4\text{K\$} = 38\text{K\$}$. In terms of spare capacity, configuration c_2 requires 4 OC-192 spare channels and c_3 requires 4 OC-48 spare channels, i.e., eight spare channels in total.

Comparing the above two configurations, we observed that performance of the configurations varies with the optimization criterion. The configuration in Figure 3.3(a) outweigh that in Figure 3.3(b) in terms of capacity efficiency. However, this is achieved at the expense of more nodal ports compared with Figure 3.3(b), and vice versa. Based on those observations, we proposed two models (see Section 3.6) to investigate the performances of the resulting optimized configurations.

3.6 Design of Multi-granularity Segment p-Cycles

We propose an optimization model in order to design a directed multi-granularity segment protection p-cycle that entitles to protect all given working segments in such a way that either the nodal equipment cost or spare capacity cost is minimized.

We represent the optical network by a directed graph $G = (V, L)$, where V and L are the sets of nodes and links, respectively indexed by v and ℓ. We denote by $-\ell$ the link in the opposite direction of fiber link ℓ, and by $\omega^+(v)$ (resp. $\omega^-(v)$) the set of outgoing (resp. incoming) links of node v.

3.6.1 Optimization Model: The Master Problem

Each working segment is identified by a 5-tuple (s, SRC_s, DST_s, d_s, w_s), where SRC_s and DST_s are the source and destination of the working segment s, d_s the number of segment copies, and w_s the transport capacity of the segment (e.g., 2.5G, 10G, 40G ...).

In order to set the mathematical model, we introduce the concept of cycle configuration. A cycle configuration c is composed of (i) a set of protection links all with the same transport capacity $t \in T = \{t_1 = OC{-}48, t_2 = OC{-}192, \ldots, t_n = OC{-}n\}$) and (ii) a set of protected working segments. Let C be the overall set of configurations. It is decomposed as follows: $C = \bigcup_{t \in T} C_t$ where C_t is the set of configurations with transport capacity t.

We associate with each configuration $c \in C$, a vector $a^c = (a^c_s)_{s \in S}$ such that a^c_s is equal to 1 if working segment s is protected by the segment p-cycle associated with configuration c, and 0 otherwise.

The mathematical model is written as follows.

$$\min \quad \sum_{c \in C} \text{COST}_c \, z^c \tag{3.19}$$

$$\text{subject to:} \quad \sum_{t \in T} \sum_{c \in C_t} \alpha_t \, a^c_s \, z^c \geq d_s \, w_s \qquad s \in S \tag{3.20}$$

$$z_c \in \mathbb{Z}^+ \qquad c \in C, \tag{3.21}$$

where α_t is a constant $\in \{2.5Gb/s, 10Gb/s, 40Gb/s, \ldots\}$ associated with each transport capacity $t \in T$.

The configuration cost, denoted by COST_c, is either defined by the nodal equipment cost as estimated by the cost of the transport blades, i.e., the cost of a pair of input and output ports on the segment p-cycle, or by the spare capacity cost. Constraints (3.20) guarantee that all given working segments with various transport capacities are protected. Constraints (3.21) define the domain of variables z^c.

One way to approach the solution of the above model is to first enumerate all the candidate configurations (cycles), and then access the solution through a selection of the promising configurations from the candidate set. However, the number of candidate configurations increases exponentially as the network size increases, and the resulting optimization becomes inefficient [SJ08b]. We propose to use the CG techniques to solve the related optimization problem, see section 3.7.

3.6.2 The Pricing Problem: Segment *p*-Cycle Generator

Minimization of nodal cost (node_cost model)

The aim of the pricing problem is to built a potential segment p-cycle of a given transport capacity t that, once added to the master problem, will improve the value of its current solution.

The reduced cost, i.e., the pricing objective is written as follows:

$$\overline{\text{COST}}_c = \text{COST}_c - \sum_{s \in S} \alpha\, u_s a_c^s \qquad c \in C_t, \tag{3.22}$$

where $u = (u_s)_{s \in S}$ is the dual vector associated with constraints (3.20).

We define the following set of parameters and variables.

- Parameters

γ_v^s $= 1$ if node v is an endpoint of segment s, 0 otherwise.

τ_ℓ^s $= 1$ if s traverses link ℓ or $-\ell$, 0 otherwise.

- Variables.

p_v $= 1$ if a transport blade is required at v, 0 otherwise.

The reduced cost is rewritten as follows, in terms of those new variables:

$$\overline{\text{COST}}_c = \overbrace{cost_v \sum_{v \in V} p_v}^{\text{COST}_c} - \sum_{s \in S} \alpha \, u_s \overbrace{\sum_{\ell \in \omega^+(\text{SRC}_s)} x_\ell^s}^{a_c^s}, \tag{3.23}$$

where $cost_v$ designates the cost of a transport blade.

The constraints of the pricing problem are:

$$\sum_{\ell \in \omega^+(v)} x_\ell - \sum_{\ell \in \omega^-(v)} x_\ell = 0 \qquad v \in V \tag{3.24}$$

$$\sum_{\ell \in \omega^+(v)} x_\ell \leq 1 \qquad v \in V \tag{3.25}$$

$$x_\ell + x_{-\ell} \leq 1 \qquad \ell \in L \tag{3.26}$$

$$x_\ell^s \leq x_\ell \qquad \ell \in L, s \in S \tag{3.27}$$

$$\sum_{\ell \in \omega^+(v)} x_\ell^s - \sum_{\ell \in \omega^-(v)} x_\ell^s = 0 \qquad s \in S, v \in V \setminus \{\textsc{src}_s, \textsc{dst}_s\} \tag{3.28}$$

$$\sum_{\ell \in \omega^+(\textsc{src}_s)} x_\ell^s = \sum_{\ell \in \omega^-(\textsc{dst}_s)} x_\ell^s = 0 \qquad s \in S \tag{3.29}$$

$$x_\ell^s + x_\ell^{s'} \leq 2 - \beta^{s,s'} \qquad s, s' \in S, \ell \in L \tag{3.30}$$

$$x_\ell^s \leq 1 - \tau_\ell^s \qquad \ell \in L, s \in S \tag{3.31}$$

$$p_v \geq \sum_{\ell \in \omega^+(v)} x_\ell^s + \gamma_v^s - 1 \qquad v \in V, s \in S \tag{3.32}$$

$$x_\ell,\ x_\ell^s,\ p_v \ \in \ \{0,1\} \qquad \ell \in L,\ s \in S,\ v \in V. \tag{3.33}$$

The first three sets of constraints contribute to the definition of a directed cycle. Constraints (3.26) prevent the generation of cycles made of two links (same fiber) with reverse direction. Constraints (3.27) say that only on-cycle links can protect working segments. Constraints (3.28) are flow conservation, dedicated to guarantee end-to-end protection flow circulation. Constraints (3.30) indicate that two working segments can share a protection segment along the p-cycle only if they are link-disjoint. Constraints (3.31) prevent a link from protecting itself. Constraints (3.32) determine the nodes on which an input/output port should be installed. These constraints ensure that an output (resp. input) port is set on the source (resp. destination) node of working segment s if it is protected by the current cycle under construction.

Minimization of spare capacity (link_cost model)

With respect to minimization of spare capacity, the above pricing problem needs to be changed as follows. The reduced cost in (3.23) is revised as follows.

$$\overline{\text{COST}}_c = \overbrace{\sum_{\ell \in L} \text{COST}_\ell \, x_\ell}^{\text{COST}_c} - \sum_{s \in S} \alpha \, u_s \overbrace{\sum_{\ell \in \omega^+(\text{SRC}_s)} x^s_\ell}^{a^s_c} . \tag{3.34}$$

In addition, constraints (3.32) are irrelevant and thus erased from the design with the spare capacity objective.

3.7 Solution of the Optimization Models

We expose here the details of the solution process for the optimization models described in this chapter. The solution process includes two steps, as illustrated in Figure 3.4. The first step consists in solving the linear relaxation of the optimization model with the column generation (CG) technique. The inner loop (Step 1) illustrates the iterative process of the CG algorithm. The outcome of the first step is a lower bound $\underline{z} = z^\star_{\text{LP}}$ (i.e., the optimal value of the linear relaxation) on the optimal integer solution of the model that is solved. The second step consists in building an integer solution of value $\tilde{z}_{\text{ILP}}$, as shown by the outer arrow (Step 2).

3.7.1 Column Generation Technique

In order to deal with the optimization models arising in the design of p-cycle-based schemes, decomposition techniques are required in order to overcome their large number of variables. They allow an iterative solution scheme where p-cycle configurations are on-line generated as long as there exists an augmenting configuration, i.e., a configuration such that its addition

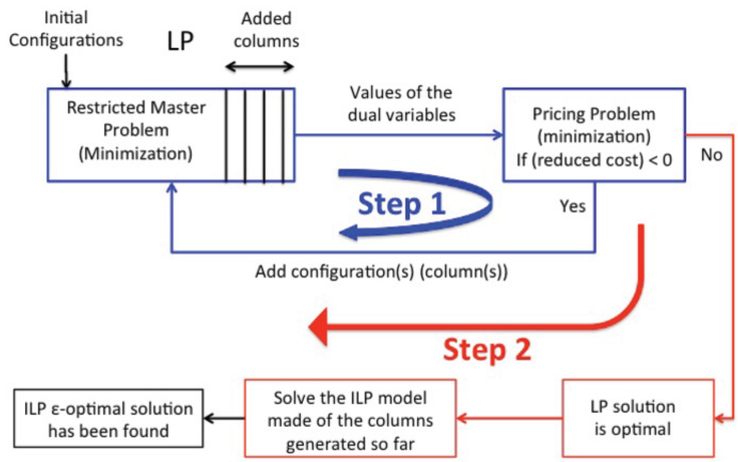

Figure 3.4: Classical CG and ILP Solutions

means an improvement of the current solution of the linear relaxation of the master problem. If no configuration with the negative reduced cost can be produced by the pricing problem, the optimal LP solution is achieved.

The master problem model is used to select configurations as formulated in Section 3.6. The pricing problem models are present next for generation of configurations.

3.7.2 How to Get an Optimal (near Optimal) Integer Solution

Once the optimal solution of the linear relaxation of an ILP model has been reached, the next step consists in computing an integer solution, ideally an optimal one. However, in order to guarantee reaching an optimal integer solution, one must use a branch-and-price method (see, e.g., [BJN+98]) when a column generation model is used. It requires some effort in order to identify an efficient and scalable branching scheme. Instead, let $\tilde{z}_{\text{ILP}}$ be the optimal integer solution of the ILP model such that its constraint matrix is associated with the last solved restricted master problem. It is well known that $\tilde{z}_{\text{ILP}}$ is not necessarily the value $z^\star_{\text{ILP}}$ of an optimal integer solution of the master problem. However, $z^\star_{\text{LP}}$, the optimal value of the linear relaxation of the master problem provides a lower bound on $z^\star_{\text{ILP}}$. It follows that the accuracy ε of $\tilde{z}_{\text{ILP}}$ can be measured by the following optimality gap (in percentage):

$$\varepsilon = 100 \times \frac{\tilde{z}_{\text{ILP}} - z^{\star}_{\text{LP}}}{z^{\star}_{\text{LP}}}. \tag{3.35}$$

3.8 Computational Results Based on Segment *p*-Cycles

In this section, with respect to the design of segment p-cycles for protection against a single link failure, we compare the performances of our CG-based design method with the one based on classical ILP (E-ILP) proposed in [SG03]. We compare the two methods regarding their capacity redundancy, the number of candidate segment p-cycles considered in the final solution, and their running time.

Data instances

We use four sample networks in the evaluation and comparison processes. The network names for reference and associated characteristics are present in Table 3.1. For each network, we present its number of nodes, number of links, average nodal degree for approximately representing connectivity, number of demands, and the working capacity cost. Each element in the traffic matrices indicates the number of unit requests.

Table 3.1: Network instances

Networks	Nodes	Edges	Node Degree	Num. Demands	Working Cost
NSF [HBB+04]	14	21	3.0	91	585
BELLCORE [SG03]	15	28	3.7	105	684
NJ LATA [YAK03]	11	23	4.2	55	213
SmallNet [SG03]	10	22	4.4	45	258
COST239 [BDH+99]	11	26	4.7	55	288

Recall that both design methods (i.e., E-ILP and CG) take as inputs the identical data instances, but with different traffic formats. The traffic input to CG is a working segment set, while the input to the E-ILP [SG03] model is a set of working paths. In order to fairly compare both designs, we perform the following process to protect the same set of working segments for each instance.

In general, we first conduct the experiments using E-ILP for each instance; we then obtain a working segment set from the E-ILP optimal solutions; finally, the results of CG are computed using the input of the working segment set.

For large networks with, e.g, 40 nodes, it may be impossible to enumerate all simple cycles included. Thus, E-ILP is intractable. Although our CG may solve the associated design problem, it is too time-consuming. Therefore, a heuristic needs to be developed to balance the solution quality and the running time.

Computation time

In this section, we present numerical results obtained respectively from the five network instances using E-ILP and CG design approaches. Table 3.2 compares the performances of the two designs, E-ILP and CG, in terms of the number of candidates considered as well as of the associated running times. The first column lists the network instances. The following two columns present the number of candidates considered in each design method. The last two columns show the running times needed by both designs. We observe that the number of candidate segment p-cycles in E-ILP increases as the network size increases as well as the running time. In contrast with E-ILP, CG considers a much smaller number of segment p-cycles in each network instance. For the first three network instances, which are either sparse or moderately dense, E-ILP runs faster than CG. However, for the last two dense networks, CG is much faster than E-ILP. Especially, for BELLCORE, CG runs ten times faster than E-ILP.

Table 3.2: Number of candidates and running time: E-ILP vs. CG

Network instance	Num. candidates		Running time (sec.)	
	E-ILP	CG	E-ILP	CG
NJ LATA	307	38	8.1	35.9
NSF	139	58	12.1	82.1
SMALLNET	833	128	67.0	303.1
BELLCORE	976	101	6,915.4	701.5
COST239	3531	113	1,407.8	816.4

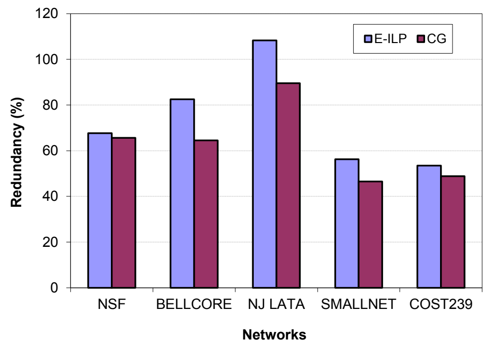

(a) Capacity redundancy: E-ILP vs. CG

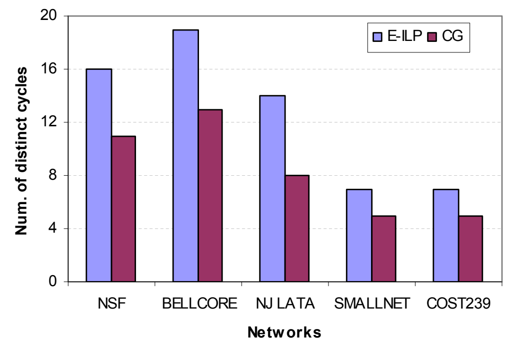

(b) Num. of distinct cycles: E-ILP vs. CG

Figure 3.5: E-ILP vs. CG

Capacity redundancy

Figure 3.5(a) shows the variation of the capacity redundancy of E-ILP versus CG in the five network topologies. In each network, the solution of CG is more capacity efficient (i.e., less capacity redundant) than the E-ILP one. Differences in the capacity redundancy between E-ILP and CG lies in the interval [3%, 20%].

Number of distinct cycles

Figure 3.5(b) shows a variation of the number of distinct cycles output by the E-ILP and CG approaches in the five test networks. For each network instance, E-ILP method requires more distinct segment p-cycles than CG. The differences on the number of distinct cycles between these two designs vary from ∼29% to ∼43% over the five networks. Thereby, from the networking and management point of view, CG method leads to better solutions than

E-ILP, in addition to be more realistic with the definition of the working segments together with the working paths.

3.9 Computational Results Based on Multi-granularity Segment *p*-Cycles

We compare the two design models of multi-granularity segment p-cycles proposed in Section 3.6. Two protection metrics, node cost redundancy and capacity redundancy, are considered for comparisons. We define the node cost redundancy as the ratio of protection nodal cost over working nodal cost, i.e., extra nodal cost that is required in order to ensure 100 % segment survivability against any single link failure.

Data instances

Four network instances are used in the comparison, see Table 3.3 for their characteristics. Traffic is given as a set of working segments (# WS). They are derived as the output of a grooming, routing and wavelength assignment (GRWA) algorithm ([BHJ06]) on traffic instances, generated according to [HBB$^+$04]. We use the following cost values: 10K$ for an OC-192 transport blade and 4K$ for a OC-48 one.

Table 3.3: Network instances

Networks	Nodes	Edges	Node Degree	# WS	% OC-48
Atlanta [OPTW07]	15	22	2.9	126	12.7%
NSF [HBB$^+$04]	14	21	3.0	132	17.4%
BELLCORE [SG03]	15	28	3.7	95	27.4%
COST239 [BDH$^+$99]	11	26	4.7	66	22.7%

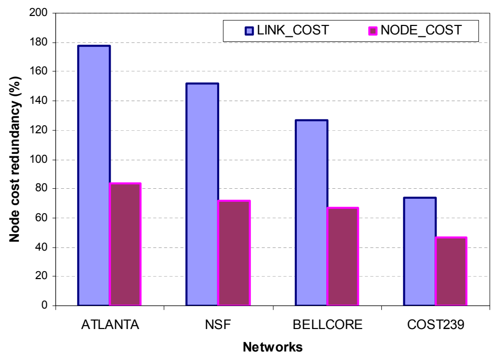

(a) CAPEX redundancy

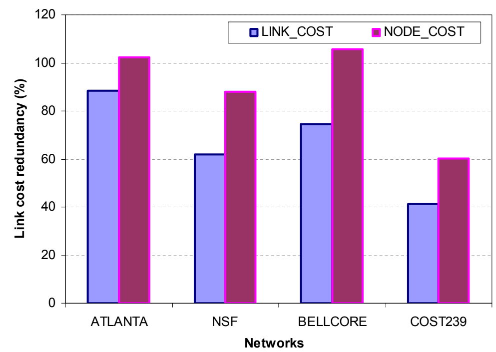

(b) Capacity redundancy

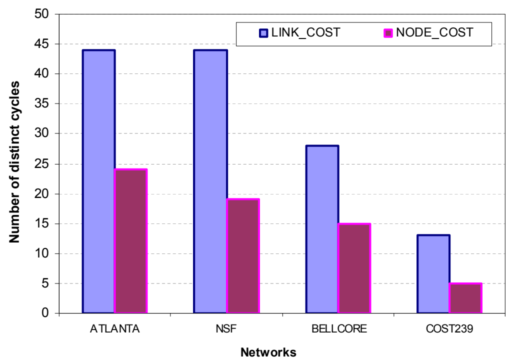

(c) Number of distinct selected cycles

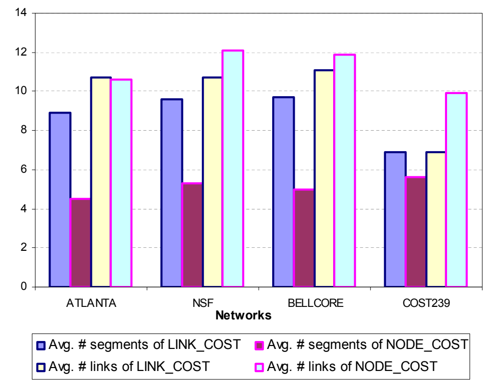

(d) Average number of links and average number of segments

Figure 3.6: Performance analysis

Node cost redundancy

Figure 3.6(a) depicts the node cost redundancy of the LINK_COST versus NODE_COST solutions for the four network instances. For each network, the NODE_COST segment p-cycle solutions are less cost redundant than the LINK_COST ones, which is in line with the example in Section 3.5. The cost redundancy differences between the LINK_COST and NODE_COST solutions range from ∼23% to ∼94%. Differences decrease as the network connectivity increases.

Capacity redundancy

Figure 3.6(b) describes the capacity redundancy of the LINK_COST versus NODE_COST solutions. For each network, the LINK_COST solutions show less capacity redundancy than the NODE_COST ones, in line again with the example in Section 3.5. Differences range from ∼14% to ∼48%.

Number of distinct cycles

In Figure 3.6(c), we provide the number of distinct cycles for both model solutions. For each network instance, the NODE_COST model produces protection with less distinct segment p-cycles than with the LINK_COST model. Differences are similar, ∼45%, for each network. The advantage in terms of management is therefore considerable.

Solution structure

Figure 3.6(d) shows the solution structure of the LINK_COST versus NODE_COST models. For each network, the average size of the segment p-cycles derived with the NODE_COST model is larger than that of the segment p-cycles of LINK_COST, as measured by the average number of links. The reason is that the more links are used for cycles, the more likely it is to have working segments with straddling segments sharing transport blades with other protected working segments. As such, the NODE_COST model is less capacity efficient than the LINK_COST one. With respect to the number of protection segments, the NODE_COST model has a smaller number, on average, than the LINK_COST one. Each protection segment needs one pair of ports, i.e., the equivalent of a transport blade. As such, the NODE_COST model is less costly than the LINK_COST one.

Overall, the NODE_COST design outperforms the LINK_COST one in terms of nodal cost and operational efforts of deployment of segment p-cycles and recovery switching. If capacity efficiency is more of a concern than the nodal cost, the LINK_COST design outperforms the NODE_COST one. Trade off exists between node cost and capacity cost.

3.10 Conclusion

In this chapter, we developed a design method of survivable WDM mesh networks based on segment p-cycles. Using the CG techniques, we proposed a scalable design method where only few segment p-cycles are explicitly dynamically generated when needed during the optimization process. The computational results show that CG-based design outperforms the prevalent three-step approach (E-ILP) of Shen *et al.* [SG03] in terms of capacity efficiency, manageability, and scalability. With respect to the running times, the CG model is shown much more effective and faster than E-ILP in large networks.

Moreover, we proposed a new multi-granularity segment scheme to protect a set of working segments with different granularities. Scalable ILP models, solved with the use of the CG techniques, are developed with the objective of minimizing the nodal cost (NODE_COST) and of minimizing the spare capacity cost, respectively. The computation results show that differences between the models are significant. When nodal cost is more of a concern than spare capacity, the model NODE_COST outperforms the LINK_COST one.

Chapter 4

The Node *p*-Cycle Scheme

4.1 Introduction

The overwhelming majority of studies explored the protection of WDM networks against single link failures, the dominant failure scenario in WDM mesh networks, and did not worry about single node failures. However, the failure of a single node can occur, even though not so often, as a result of disasters such as fires or floods. A single node failure is equivalent to the failure of all its incident fiber links and their connections through that node. The consequences of a node failure are therefore devastating.

This chapter investigates the design of p-cycle-based schemes for 100% node protection, and proposes a new scheme for node protection using p-cycles. The underlying idea comes from the observation that a node is protected if its two adjacent links on the working path are protected by the same p-cycle. It resembles the two hop approach of Grover and Onguetou [GO09], with one additional feature, detailed in Section 4.3. We develop a new Column Generation (CG) model to design p-cycles with node protection in order to adequately address the scalability issue afflicting the classical design of p-cycles. In order to make a quantitative comparison of the proposed node-protecting p-cycles with path p-cycles, we adapt the CG model for the design of FIPP p-cycles of [RJ12] so as to guarantee 100% protection against a single node / link failure.

The chapter is organized as follows. In Section 4.2, we first explain how p-cycles can be used to guarantee node protection and then present a comprehensive example for illustrating the distinctive characteristics of the four compared p-cycle-based protection schemes. In Section 4.3, we develop an original and scalable optimization model for the design of node p-cycles, i.e., p-cycles ensuring 100 % node protection. In Section 4.4, we re-use the same optimization model framework to design a scalable model for the node p-cycle scheme of Grover and Onguetou [GO09]. In Section 4.5, we then adapt the column generation model of [RJ12, RJ08] for the design of FIPP p-cycles in order to guarantee 100% node protection. In Section 4.6, we present the solution methods to the column generation models developed in Sections 4.3 to 4.5. Intensive comparative numerical results are presented in Section 4.7. Conclusion is drawn in Section 4.8.

4.2 Node p-Cycles

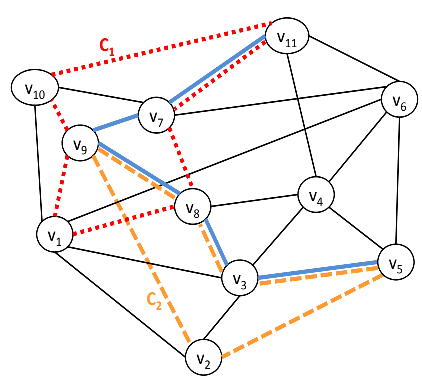

Figure 4.1: p-Cycles for node protection

In order to protect an intermediate node of a working path, a p-cycle can be constructed in such a way that two adjacent links ℓ and ℓ' of a node v on a given working path p are protected by the same p-cycle. We denote such link pairs by $(\ell, \ell')_{v,p}$, or equivalently by $\omega_p(v)$, i.e., the co-cycle of v restricted to the links of p. Upon the failure of such an intermediate node, the two closest (adjacent) nodes on the working path can detect the failure and switch the disrupted traffic automatically onto the p-cycle(s), as in the link failure scenario.

An illustration is provided in Figure 4.1. In order to offer node and link protection to the request demand between nodes v_5 and v_{11}, one needs two p-cycles c_1 (short dashes) and c_2 (long dashes). All links of the working path are protected as each of them is either an on-cycle link or a straddling link of c_1 or c_2. Each intermediate node is also protected as the two adjacent links on its working path are protected by the same p-cycle. For instance, node v_7 has its two adjacent links $\{v_7, v_9\}$ and $\{v_7, v_{11}\}$ protected by c_1. It follows that, if node v_7 fails, the subpath $v_9 - v_7 - v_{11}$ is rerouted on, e.g., $v_9 - v_{10} - v_{11}$.

Node protection with p-cycles was previously investigated by Grover and Onguetou [GO09]. Their study relies on a 2-hop strategy which allows a p-cycle to protect a node with respect to one working path. Our proposal is more general as it allows the protection of a node lying on several working paths by the same p-cycle if the working paths use link disjoint protection entities following the failure of that node. As we will see in the numerical results, this allows reducing the spare bandwidth requirement.

Figure 4.2 illustrates the idea with a network topology comprising eight nodes and three demands routed on primary paths w_1, w_2 and w_3. Figure 4.2(a) shows the solution of the design strategy proposed in [GO09]. Therein, three p-cycles, c_1, c_2 and c_3, are required to provide full node protection. The resulting spare capacity requirement amounts to 12 channel units. However, with our node p-cycle scheme, as shown in Figure 4.2(b), only one

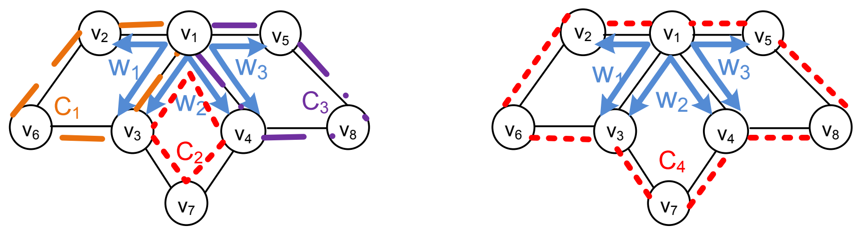

(a) Grover and Onguetou (2009) Node p-Cycle Scheme

(b) Our Node p-Cycle Scheme

Figure 4.2: Comparison of our node p-cycle scheme with that of Grover and Onguetou (2009)

p-cycle, c_4, is required in order to provide full node protection. Upon the failure of node v_1, on-cycle protection paths $v_2 - v_6 - v_3, v_3 - v_7 - v_4$ and $v_4 - v_8 - v_5$ can be used to recover the three disrupted demands routed on w_1, w_2 and w_3, respectively. The associated spare capacity cost is eight units of channels. Compared with the strategy of [GO09], our solution reduces by 33% the amount of required bandwidth.

Literature Review

In order to provide node protection, p-cycles have been generalized to path-segment-protecting p-cycles (flow p-cycles for short) in [SG03], where a flow p-cycle can protect on-cycle and straddling working segments. Thus, the intermediate nodes of the working segments can be inherently protected but not the end nodes of the working segments. Kodian and Grover in [KG05] proposed Failure-Independent Path-Protecting (FIPP) p-cycles to provide end-to-end path protection. Note that flow p-cycles and FIPP p-cycles are usually more capacity efficient than link protection schemes [SG03, KG05]. However, optical recovery is slower as for any path or segment protection schemes.

In most previous works, comparisons were performed with heuristics as the classical model for the design of p-cycle-based schemes relies on an Integer Linear Program (ILP) model where each variable is associated with a potential cycle. Then, the solution of such an ILP model involves the off-line generation of either the whole set of potential p-cycles [GS98, Sch05b, SGA02], or a restricted set of promising candidate p-cycles [GD02, RT05], leading to a huge ILP or to a heuristic solution with unknown accuracy, respectively. Indeed, it has been shown in [JRBG07], in the case of FIPP p-cycles, that heuristics may provide quite inaccurate solutions in some cases.

Most studies on FIPP p-cycles did not pay attention to node protection, but merely to path versus link protection with respect to bandwidth requirements, as in [KG05, JRBG07, RJ08, RJB09]. FIPP p-cycle design may vary from one study to the next (see [RJ12] for a thorough analysis of their differences). Indeed, as a path protection scheme, FIPP p-cycles can inherently provide node protection assuming protection and working paths are pairwise node disjoint, and the set of working paths which are protected by the same unit FIPP p-cycle are node disjoint.

To simplify notations and to improve the readability of the chapter, in the sequel, we will talk about link, segment, path p-cycles instead of p-cycles, flow p-cycles and FIPP p-cycles. Link p-cycles with node protection capability will be referred to as node p-cycles.

4.2.1 Motivation and a Comprehensive Example

Path p-cycles are known to be more capacity efficient than link p-cycles in the context of protection against a single link failure [RJ08,RJB09]. With respect to single node failures, to the best of our knowledge, comparisons can only be found in [GO09], where the conclusion is that node p-cycles hold a capacity efficiency comparable to path p-cycles and, therefore, are an attractive approach for link and node protection. Our conclusions are slightly different, depending on the data instances. The motivation of this chapter is to go one step further with our enhanced node p-cycle scheme on the one hand, and exact solution of the ILP models on the other hand, rather than heuristic solutions or exact solutions on very small network and traffic instances.

Before going into the details of the optimization models, we propose to first explore the distinctive characteristics between the various protection schemes on a small example. We use the BELLCORE network topology with two unit demand requests, see Figure 4.3(a). Therein, the number on each link is the link geographical length [MK98], expressed in thousands of kilometers. Three protection schemes are illustrated: link p-cycles in Figure 4.3(b), node p-cycle in Figure 4.3(c) as our newly proposed node p-cycle scheme described in Section 4.2, and path p-cycle in Figure 4.3(d), i.e., the so-called FIPP p-cycle with the required adaptations in order to guarantee node protection, as discussed in Section 4.5. Note that, on that simple example, both our node p-cycle protection scheme and that of Grover and Onguetou give the same results. For differences, see the example illustrated in Figure 4.2 or to Section 4.7.

The protection schemes, which are illustrated in Figure 4.3, can be described as follows. To protect traffic against a single link failure, two link p-cycles, c_1 and c_2 as shown in Figure 4.3(b) are used, with a spare capacity requirement of 14.5. To provide protection not only against single link failures, but also against single node failures, we need again two node p-cycles, c_3 and c_4, different from c_1 and c_2, as depicted in Figure 4.3(c). Their overall spare capacity is equal to 31.5. If, instead of link p-cycles, we now consider path p-cycles, again two p-cycles c_5 and c_6 are needed, as shown in Figure 4.3(d), with a spare capacity equal to 38.8.

This example shows that, as expected, the node p-cycles require more spare capacity than the link p-cycles for node protection. On the other hand, while it would have been expected that node p-cycles might have required more spare bandwidth than path p-cycles,

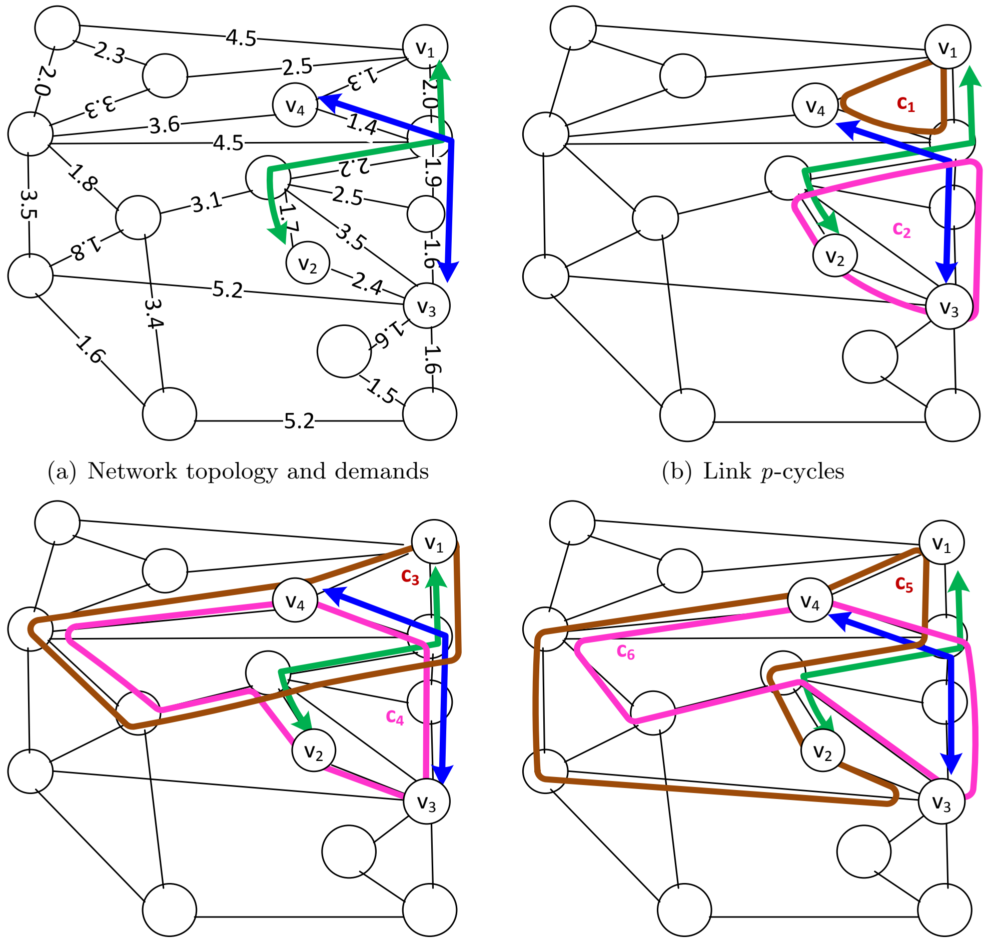

(a) Network topology and demands (b) Link p-cycles

(c) Node p-cycles (d) Path p-cycles

Figure 4.3: Illustration of different p-cycle-based protection schemes

it is not the case for the above example. As will be seen in the sequel, node p-cycles are sometimes more bandwidth efficient, sometimes less bandwidth efficient than path p-cycles, which depends on the network topologies.

4.3 A New Scalable Optimization Model for Node p-Cycles

4.3.1 Notations

For a given working path $p \in P$, let d_p be the number of connection requests carried on it, and let $V_p^\star$ be the set of its intermediate nodes.

We propose a model for the design of p-cycle-based schemes against any single link or node failures with minimum bandwidth requirements. The model relies on p-cycle configurations, where a p-cycle configuration consists of a one unit p-cycle and the set of links and nodes it protects.

Before setting the details of the model, we need to introduce some notations.

Sets

C	set of p-cycle configurations, indexed by c.

Parameters

$a_\ell^c \in \{0, 1, 2\}$	number of working capacity units on link ℓ protected by p-cycle c. $a_\ell^c = 1$ (resp. 2) if link ℓ is an on-cycle (resp. a straddling) link, 0 otherwise.
$a_{pv}^c \in \{0, 1\}$	number of protection paths provided by p-cycle c for working path p against the failure of node v.

We can observe that by assuming $a_{pv}^c \in \{0, 1, 2\}$ rather than $\{0, 1\}$, we can easily embed some additional cases for node protection as illustrated in Figure 4.4. Indeed, if a node v belonging to a working path is on a 2-hop chord of the p-cycle, then the latter one can provide 2 units of protection to that node. Such a node will be called a *straddling* node. Note that the links adjacent a straddling node will be protected together or one at a time by another p-cycle(s) as, in this case, they cannot be protected by the same p-cycle than node v. For instance, in Figure 4.4, demand $v_1 - v_5$ is routed on path $v_1 - v_2 - v_3 - v_4 - v_5$, with p-cycle c_1 built to protect node v_3. If v_3 fails, its adjacent nodes v_2 and v_4 can switch the disrupted traffic on c_1, which can offer two protection paths. However, note that neither link $v_2 - v_3$ nor $v_3 - v_4$ can be protected by c_1. We included straddling nodes in

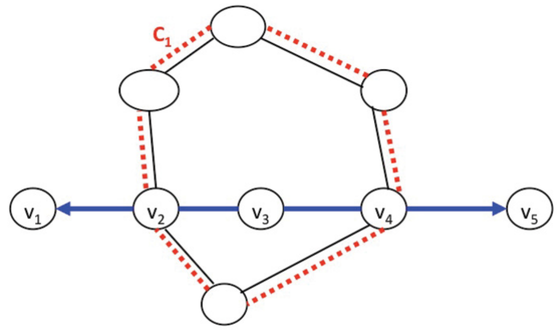

Figure 4.4: A straddling node

our formulations in order to facilitate the comparisons with the node protection scheme of Grover and Onguetou [GO09]. However, we observed that very few such nodes are encountered in the solutions, most probably due to the fact that the protection of their adjacent links requires another p-cycle (possibly two more).

From now on, we will therefore assume that $a^c_{pv} \in \{0, 1, 2\}$.

4.3.2 An Enhanced Optimization Model for Node p-Cycles

We propose an optimization method based on Column Generation (CG) techniques for the design of node p-cycles according to the description given in Section 4.2. Following a CG modelling, the design problem is decomposed into two subproblems: the master problem and the pricing problem. The master problem selects the best combination of p-cycles in order to guarantee the node/link protection while the pricing problem dynamically generates new p-cycles, which iteratively contribute to the improvement of the current value of the objective of the (continuous relaxation of the) master problem. This way, the number of generated cycles remain reasonable without jeopardizing the solution optimality. See Section 4.6 for the details.

The Master Problem

The master problem relies on the concept of configurations, where a p-cycle configuration c is represented by a vector $(a_\ell^c)_{\ell \in L}$ and a matrix $(a_{pv}^c)_{p \in P,\, v \in V_p^\star}$.

The optimization model can then be written as follows.

$$\min \quad \sum_{c \in C} \text{COST}_c \, z_c \tag{4.1}$$

subject to:

$$\sum_{c \in C} a_\ell^c \, z_c \geq d_\ell \qquad \ell \in L \tag{4.2}$$

$$\sum_{c \in C} a_{pv}^c \, z_c \geq d_p \qquad p \in P,\ v \in V_p^\star \tag{4.3}$$

$$z_c \in \mathbb{Z}^+ \qquad c \in C. \tag{4.4}$$

Constraints (4.2) ensure that the overall traffic is protected against a single link failure. Constraints (4.3) ensure that all demands are protected against a single failure at node v with respect to working path p, for all intermediate nodes on all working paths. Constraints (4.4) define the domains of variables z_c.

The Pricing Problem

The role of the pricing problem is to generate a promising p-cycle that, once added to the master problem, will improve the value of the current solution of the linear relaxation of the master problem. Its objective corresponds to the minimization of the so-called reduced cost subject to a set of constraints for the generation of not only a p-cycle but also of the set of its protected links/nodes. Readers who are not familiar with linear programming are referred to, e.g., Chvatal [Chv83].

The objective function can be written as follows.

$$\min \qquad \text{COST}_c - \sum_{\ell \in L} u_\ell \, a^c_\ell - \sum_{p \in P} \sum_{v \in V^\star_p} u_{pv} \, a^c_{pv} \tag{4.5}$$

where u_ℓ and u_{pv} are the dual variables associated with constraints (4.2) and (4.3) respectively.

Before presenting the set of constraints of the pricing problem, we need to introduce the following notations.

Parameters

v^1_{pv}, v^2_{pv} the two nodes adjacent to node v on path p.

Variables

$s_\ell =$ 1 if link ℓ straddles the cycle under construction; 0 otherwise.

$y_v =$ 1 if node v lies on the cycle under construction; 0 otherwise.

$x^\ell_{pv} =$ 1 if link ℓ is used to protect working path p against the failure of intermediate node v; 0 otherwise.

The objective function of the pricing problem can then be re-written as follows:

$$\min \qquad \overbrace{\sum_{\ell \in L} \text{COST}_\ell x_\ell}^{\text{COST}_c} - \sum_{\ell \in L} u_\ell \overbrace{(x_\ell + 2 s_\ell)}^{a^c_\ell} - \sum_{p \in P} \sum_{v \in V^\star_p} u_{pv} \overbrace{\sum_{\ell \in \omega(v^1_{pv})} x^\ell_{pv}}^{a^c_{pv}} . \tag{4.6}$$

The set of constraints can be subdivided into two groups of constraints. The first group of constraints is associated with the generation of a simple cycle and the identification of the set of links which are protected by this cycle. The second group takes care of determining pairs (p, v), made of a working path p and one of its intermediate node v, such that node v

is protected by the cycle with respect to p.

The first group of constraints can be written as follows:

$$\sum_{\ell \in \omega(v)} x_\ell = 2\, y_v \qquad v \in V \tag{4.7}$$

$$s_\ell \leq y_v - x_\ell \qquad v \in V,\ \ell \in \omega(v) \tag{4.8}$$

$$s_\ell \geq y_v + y_{v'} - x_\ell - 1 \qquad v, v' \in V, \ell = \{v, v'\} \in L \tag{4.9}$$

$$\sum_{\ell \in \omega(V')} x_\ell \geq y_v + y_{v'} - 1 \qquad 3 \leq |V'| \leq |V| - 3, V' \subset V, v \in V',\ v' \in V \backslash V'. \tag{4.10}$$

Each node on a given cycle must have two incident links on that cycle. This is ensured by constraints (4.7). Constraints (4.8) and (4.9) are used to identify straddling links. A link straddles a cycle if its two end nodes are on the cycle, but the link itself is not. Constraints (4.10) prevent from generating a p-cycle configuration which includes multiple cycles. Otherwise, the identification of the straddling links would become too difficult.

Before describing the second group of constraints, we introduce one more notation: $P^\star_v$, the set of working paths going through node $v \in V$, with v being an intermediate node of the path.

$$x^\ell_{pv} \leq x_\ell \qquad p \in P,\ v \in V^\star_p,\ \ell \in L \tag{4.11}$$

$$x^\ell_{pv} = 0 \qquad p \in P,\ v \in V^\star_p,\ \ell \in \omega(v) \tag{4.12}$$

$$\sum_{\ell \in \omega(v^1_{pv})} x^\ell_{pv} = \sum_{\ell \in \omega(v^2_{pv})} x^\ell_{pv} \qquad p \in P,\ v \in V^\star_p \tag{4.13}$$

$$\sum_{\ell \in \omega(v')} x^\ell_{pv} \leq 2 \qquad p \in P,\ v \in V^\star_p,\ v' \in V \tag{4.14}$$

$$\sum_{\ell \in \omega(v') | \ell \neq \ell'} x_{pv}^{\ell} \geq x_{pv}^{\ell'} p \in P,\ v \in V_p^{\star},\ v' \in V \setminus \{v_{pv}^1, v_{pv}^2\}, \ell' \in \omega(v') \quad (4.15)$$

$$\sum_{p \in P_v^{\star}} x_{pv}^{\ell} \leq 1 \qquad \ell \in L,\ v \in V \quad (4.16)$$

$$x_{\ell},\ s_{\ell} \in \{0, 1\} \qquad \ell \in L \quad (4.17)$$

$$y_v \in \{0, 1\} \qquad v \in V \quad (4.18)$$

$$x_{pv}^{\ell} \in \{0, 1\} \qquad \ell \in L,\ p \in P,\ v \in V_p^{\star}. \quad (4.19)$$

Constraints (4.11) ensure that only on-cycle links are eligible for protecting an intermediate or a straddling node of working path p against a single node failure. Constraints (4.12) say that, if a link is adjacent to an intermediate node v of working path p, the link cannot be used for protection of node v, i.e., cannot be on a protection path going around node v. Constraints (4.13) - (4.15) are flow conservation constraints for defining the protection paths. Constraints (4.13) say that a protection path, which protects node v, must go through the two nodes which are adjacent to node v on working path p. Constraints (4.13), together with (4.14), ensure that a p-cycle can provide at most two protection paths for the protection of a node lying on a working path. Constraints (4.14) and (4.15) ensure that protection paths are simple paths (without any loop), meaning that, a given node is either not on the protection path, or only encountered once. Upon the failure of a node, working paths passing through the failing node are all disrupted. Constraints (4.16) say that a link channel can only be used for recovering one unit of disrupted working paths. The last sets of constraints (4.17), (4.18), and (4.19) define the domains of the variables.

4.4 A Column Generation Reformulation of the Model of Grover and Onguetou (2009)

In order to compare our node p-cycle scheme with the one by Grover and Onguetou (2009) [GO09], we next rewrite their integer linear program in a column generation (CG) framework so as to obtain a scalable model which can solve larger instances than in their original chapter. Note that instead of a two step process as in [GO09] (firstly, identify the best p-cycles, secondly, decide for each node which p-cycle protects it), the proposed CG model corresponds to an equivalent one step solution process.

We first recall their original ILP model with unified notations, and then reformulate it in a column generation framework.

4.4.1 ILP Model by Grover and Onguetou (2009)

While re-using notations of the previous section, we need two additional sets of variables, which are defined as follows:

z^c_{pv} number of copies of p-cycle c to protect intermediate node v of path p.

t^c_{pv} number of demand units of node v in path p, which are protected by p-cycle c in the event of a failure of node v.

The mathematical model of [OG08b] can be written as follows (with unified notations):

$$\min \quad \sum_{c \in C} \text{COST}_c \, z_c \tag{4.20}$$

subject to:

$$\sum_{c \in C} a_\ell^c \, z^c \geq d_\ell \qquad \ell \in L \tag{4.21}$$

$$t_{pv}^c \leq a_{pv}^c \, z_{pv}^c \qquad p \in P, \, v \in V_p^\star, \, c \in C \tag{4.22}$$

$$\sum_{c \in C} t_{pv}^c \geq d_p \qquad p \in P, \, v \in V_p^\star \tag{4.23}$$

$$z_{pv}^c \leq M \, a_{pv}^c \qquad p \in P, \, v \in V_p^\star, \, c \in C \tag{4.24}$$

$$\sum_{p \in P_v} z_{pv}^c \leq z^c \qquad v \in V, \, c \in C \tag{4.25}$$

$$z_c \in \mathbb{Z}^+ \qquad c \in C \tag{4.26}$$

$$z_{pv}^c, \, t_{pv}^c \in \mathbb{Z}^+ \qquad c \in C, \, p \in P, \, v \in V_p^\star. \tag{4.27}$$

The objective is to minimize the spare capacity requirements. Constraints (4.21) ensure 100% guaranteed protection against a single link failure. Constraints (4.22) determine the units of protection that a p-cycle can provide for a single intermediate or straddling node of a working path upon the node failure. Constraints (4.23) ensure that all intermediate nodes of all working paths are protected against a single node failure. Constraints (4.24) indicate that, a p-cycle can be used to protect an intermediate (resp. straddling) node if $(\ell, \ell')_{v,p}$ link pair is on the cycle (resp. straddle the cycle, as illustrated in Figure 4.4). Constraints (4.25) say that, for a given path p going through node v, if node v is protected by p-cycle c with respect to p, the reserved copies of unit p-cycle c should be enough to recover all impaired traffic on p against node v failure. Constraints (4.26) and (4.27) define the domains of the variables.

4.4.2 CG Reformulation of the Model by Grover and Onguetou (2009)

In order to reformulate the above ILP in a column generation framework, the design problem is decomposed into two problems which will be solved alternately: the master problem and the pricing problem. The master problem selects p-cycles which are calculated on the fly by the pricing problem at each iteration of the CG algorithm. The p-cycle candidates are associated with configuration set C. A configuration c consists of a cycle that protects a set of links and a set of intermediate (possibly straddling) nodes of working paths. Unlike the p-cycle configuration defined in Section 4.3.2, a node p-cycle configuration can only be used to protect a given node for a single impaired working path.

The CG reformulation leads to a master problem, which is the same as the model (4.1) - (4.4), i.e., our newly proposed model. However, while the objective of the pricing problem is the same as (4.5), its constraints differ. Before presenting it, we need to introduce the following sets and variables.

Sets

$\omega_p(v)$ Pair of links on a working path p which are adjacent to an intermediate or a straddling node v. Those link pairs will be denoted by $(\ell, \ell')_{v,p}$ in the sequel.

$V_{p,v}$ Pair of nodes that are adjacent to node v on working path p.

Variables

$b_p^v =$ 1 if the cycle under construction protects node v in path p, with v lying on the cycle; 0 otherwise.

$s_p^v =$ 1 if the cycle under construction protects node v in path p, with v being a straddling node; 0 otherwise.

Using these notations, the objective (4.5) can then be rewritten as follows.

$$\min \quad \overbrace{\sum_{\ell \in L} \text{COST}_\ell x_\ell}^{\text{COST}_c} - \sum_{\ell \in L} u_\ell \overbrace{(x_\ell + 2s_\ell)}^{a^c_\ell} - \sum_{p \in P} \sum_{v \in V^\star_p} u^v_p \overbrace{(b^v_p + 2s^v_p)}^{a^c_{pv}} . \tag{4.28}$$

Again, the pricing problem contains two blocks of constraints. The first one consists of the constraints for defining a cycle, which are identical to constraints (4.7) to (4.10). The second block of constraints is as follows:

$$b^v_p \leq x_\ell + s_\ell \qquad p \in P,\ v \in V^\star_p,\ \ell \in \omega_p(v) \tag{4.29}$$

$$s^v_p \leq y_{v'} \qquad p \in P,\ v \in V^\star_p,\ v' \in V_{p,v} \tag{4.30}$$

$$s^v_p \leq 1 - y_v \qquad p \in P,\ v \in V^\star_p \tag{4.31}$$

$$\sum_{p \in P_v} (b^v_p + s^v_p) \leq 1 \qquad v \in V \tag{4.32}$$

$$x_\ell,\ s_\ell \in \{0,1\} \qquad \ell \in L \tag{4.33}$$

$$y_v \in \{0,1\} \qquad v \in V \tag{4.34}$$

$$b^v_p,\ s^v_p \in \{0,1\} \qquad p \in P,\ v \in V^\star_p . \tag{4.35}$$

Constraints (4.29) say that an intermediate node on a working path p can be protected in an on-cycle manner, i.e,. the node belongs to the cycle under construction, if its two adjacent links on p are also protected by the cycle under construction. Constraints (4.30) and (4.31) together say that the cycle under construction can protect a straddling node v on a working path p if its two adjacent nodes on p belongs to the cycle (i.e., are on-cycle nodes), but not v itself. Upon node failure of v, all working paths transmitting the failed node are disrupted, but the cycle under construction can offer node protection only for a single path with respect to node v, which is stated by constraints (4.32).

This last CG-ILP model, through its pricing problem, is not fully equivalent to the model of Grover and Onguetou [OG08b], but corresponds to where they aim at with their two phase process. Details follow.

Firstly in the above pricing problem of the CG-ILP model, we directly generate a unique p-cycle for the protection of a given node, as obtained with the two step process in [GO09]. Indeed, a candidate p-cycle consists of a unit cycle, the protected links and the *potential* protected intermediate nodes of working paths, in such a way that a node can be protected by a pcycle for a *unique* working path. As shown in Figure 4.5, two candidates, c_1 and c_2 are generated respectively for protecting node v of path p_1 and for v of p_2. The master problem then determines how many units of c_1 and c_2 are required in the solution.

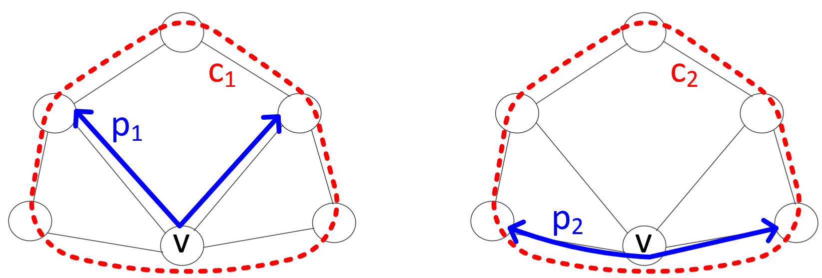

(a) A candidate for node v of path p_1

(b) A candidate for v of path p_2

Figure 4.5: Example candidates for the CG model

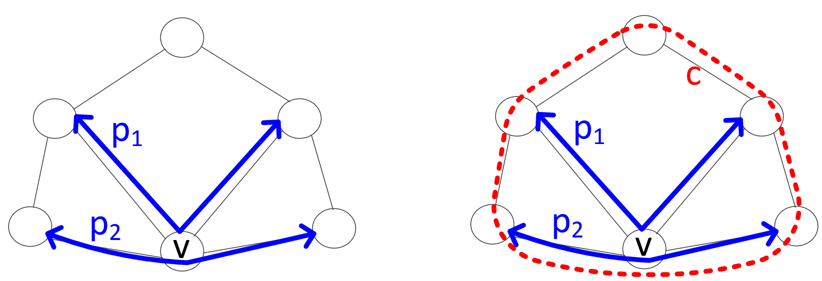

(a) An example instance

(b) A candidate

Figure 4.6: An example candidate for the ILP model by Grover and Onguetou

Figure 4.6(a) presents a network topology, and two demands carried respectively on paths p_1 and p_2. Both paths pass through node v. Figure 4.6(b) illustrates a candidate

p-cycle, which is made up of an unit cycle c, the protected (on-cycle and straddling) links and the potential protected node v of p_1 and of p_2. The model by Grover and Onguetou then determines in turn how many units of cycle c are allocated for node v of p_1 and for node v of p_2.

4.5 Column Generation Model for Design of FIPP p-Cycles

We adapt the column generation formulation of [RJ12] in order to guarantee 100% node protection. Note that we consider here, as in [RJ12], a decomposition of the pricing problem in order to further enhance the CG model scalability as path p-cycles are more costly (with respect to computing times) to compute than link p-cycles.

4.5.1 The Master Problem

As for the models in Sections 4.3 and 4.4, the master problem selects path p-cycles for protection of all working paths against single link or node failures so that the overall spare capacity is minimized. A configuration c is made of a cycle and the set of working paths it protects against single node/link failures, represented by vector a^c. The vector element $a_p^c \in \{2, 1, 0\}$ encodes the number of protection paths provided by this configuration c for working path p. The mathematical model is next formulated.

$$\min \quad \sum_{c \in C} \text{COST}_c \, z_c$$

$$\text{subject to:} \qquad \sum_{c \in C} a_p^c \, z_c \geq d_p \qquad p \in P \tag{4.36}$$

$$z_c \in \mathbb{Z}^+ \qquad c \in C. \tag{4.37}$$

Constraints (4.36) express that all working paths should be protected against a single link or node failure. Constraints (4.37) define the domains of the variables.

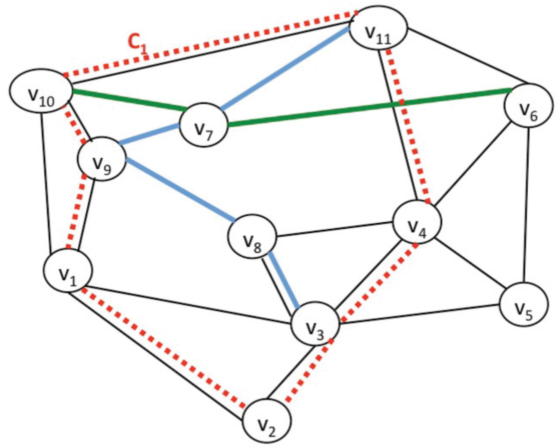

Figure 4.7: Link disjoint paths which are not node disjoint

4.5.2 The Pricing Problem

The goal of the pricing problem is to generate a valid augmenting configuration, i.e., a unit path p-cycle with the set of requests it protects against single node/link failures. We are discussing below the changes to the previous model of [RJ12] so to guarantee protection against single node failures.

The first one is due to the fact that link disjoint paths are not necessarily node disjoint, as shown in Figure 4.7. Therein, node v_7 can not be protected if both working paths $v_3 - v_{11}$ (blue path) and $v_1 - v_{10}$ (green path) are protected by the path p-cycle c_1(in red in Figure 4.7). The second one deals with the case of (partially) straddling working paths with one intermediate node belonging to a path p-cycle. For instance, see working path $v_3 - v_{11}$ (blue path) in Figure 4.7. Indeed, for protection against single link failures, it is required that working and backup paths to be pairwise link disjoint. Similarly, in order to guarantee node protection, working and backup paths must be pairwise node disjoint. Back to the example with working path $v_3 - v_{11}$, path p-cycle c_1 offers only one unit of protection through the backup path $v_3 - v_4 - v_{11}$ as one of its intermediate node, v_9, is on the cycle, even if the working path is a straddling one.

The pricing problem generates a promising configuration for the master problem in each iteration of the CG algorithm such that the value of the current solution (linear relaxation) may be improved. Its objective corresponds to the minimization of the so-called reduced cost of the linear relaxation subject to the configuration constraints, and can be written as follows.

$$\overline{\text{COST}_c} = \text{COST}_c - \sum_{p \in P} u_p a_p^c \qquad c \in C, \tag{4.38}$$

where u_p are the dual variables related to constraints (4.36).

Before describing the constraints of the pricing problems, we need to define some additional notations. Previously defined notations still hold.

Parameters

$\beta^{p,p'} =$ 0 if working paths p and p' are node disjoint (and hence, link disjoint); 1 otherwise.

$\tau_\ell^{p,v} =$ 1 if link ℓ is adjacent to an intermediate node v of working path p; 0 otherwise.

$v_p^1,\ v_p^2$ end nodes of working path p.

Variables

$x_\ell^p =$ 1 if link ℓ is used to protect working path p; 0 otherwise.

Using these notations, the reduced cost (4.38) can then be rewritten:

$$\overline{\text{COST}_c} = \overbrace{\sum_{\ell \in L} \text{COST}_\ell \, x_\ell}^{\text{COST}_c} - \sum_{p \in P} u_p \overbrace{\sum_{\ell \in \omega(v_p^1)} x_\ell^p}^{a_p^c}$$

Once more, constraints can be subdivided into two subsets. The first subset takes care of the generation of a cycle which consists of constraints (3.9) - (3.11). The second subset of constraints deals with the identification of the protected working paths by the current cycle.

$$x_\ell^p \leq x_\ell \qquad p \in P,\ \ell \in L \qquad (4.39)$$

$$x_\ell^p \leq 1 - \tau_\ell^{p,v} \qquad p \in P,\ v \in V_p^\star, \ell \in \omega_p(v) \qquad (4.40)$$

$$\sum_{\ell \in \omega(v_p^1)} x_\ell^p = \sum_{\ell \in \omega(v_p^2)} x_\ell^p \qquad p \in P \qquad (4.41)$$

$$\sum_{\ell \in \omega(v)} x_\ell^p \leq 2 \qquad p \in P,\ v \in V \qquad (4.42)$$

$$\sum_{\ell' \in \omega(v):\, \ell' \neq \ell} x_{\ell'}^p \geq x_\ell^p \qquad p \in P,\ v \in V,\ \ell \in \omega(v) \qquad (4.43)$$

$$\sum_{p \in P_v^\star} x_\ell^p \leq 1 \qquad v \in V, \ell \in L \qquad (4.44)$$

$$x_\ell \in \{0, 1\} \qquad \ell \in L \qquad (4.45)$$

$$x_\ell^p \in \{0, 1\} \qquad p \in P,\ \ell \in L. \qquad (4.46)$$

Constraints (4.39) say that only on-cycle links are eligible for protection of working paths. Constraints (4.40) ensure that a working path and its corresponding protection path are node disjoint. Constraints (4.41) say that, for any working path, its protection path(s) must end at its two end nodes. Constraints (4.41) and (4.42) ensure that the configuration under construction can provide at most two protection paths for any working path.

Constraints (4.42) together with (4.43) guarantee flow conservation in the intermediate nodes along protection path(s). Constraints (4.44) ensure that only link-and-node-disjoint working paths can share protection paths.

4.6 Enhanced Solution of the Optimization Models

Basically, the solution process for all the optimization models described in the last three sections is as described in Section 3.7.

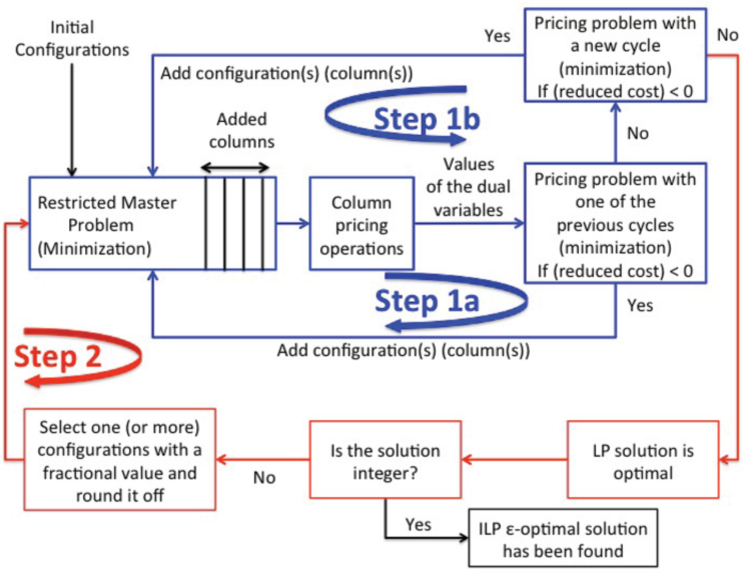

Figure 4.8: Enhanced CG and ILP Solutions

In order to speed up the CG algorithm, based on the observation that we may have the same cycle belonging to different configurations, we first generate the augmenting configurations using the cycles which have already been used in the previously generated configurations. This iterative process is illustrated by Step 1a in Figure 4.8. Note that the search of a configuration is advantageously speeded up if a cycle has been already selected, meaning that the first group of constraints of the pricing problems disappear. If no augmenting configuration can be generated with the last generated cycles, then we solve the complete pricing problem, which includes the first group of constraints, i.e., the search of a cycle. This iterative process is illustrated by Step 1b in Figure 4.8. The resulting cycle can either be a brand new one, or one of the cycles generated with one of the earliest configurations. We observe, in practice, that very few complete pricing problems need to be solved, usually the number is of the order of the number of distinct cycles among the overall set of configurations.

Column generation algorithms which are described in the early chapters often assume that we eliminate at each iteration the columns associated with nonbasic variables in order to keep the size of the constraint matrix as small as possible. However, in practice, this often entails regenerating several times some columns (or managing a column buffer), and therefore, the most efficient strategy is to "price out columns" only when the constraint matrix becomes too large, so say every 50 to 100 iterations in practice. Column pricing is conducted looking at the variables/columns with the largest reduced cost. This technique corresponds to the box entitled "Column pricing operations" in Figure 4.8.

4.6.1 How to Get an Optimal (near Optimal) Integer Solution

In this study, we used the so-called rounding up method. It consists in an iterative algorithm, which, at each iteration, selects the configuration variable with the largest fractional value, round it up, and set the variable to that rounded value. The linear relaxation of the resulting problem is updated, and then the algorithm iterates. This process is illustrated by Step 2 in Figure 4.8.

4.7 Computational results

In this section, we evaluate the performances of the newly proposed scheme for node protection using p-cycles (node p-cycles), and compare it with three other schemes:

(i) the OG p-cycle scheme of [GO09] (OG p-cycle) using a column generation reformulation as described in Section 4.4;

(ii) the path p-cycle scheme using the model of Section 4.5;

(iii) the link p-cycle scheme corresponding to the original p-cycles using the column generation model of [RJ08].

Note that the column generation does not change the models initially proposed (in relation with the constraint set), but only the scalability of the solution process. In addition, they allow an exact and scalable solution of the models, and hence make their comparison more efficient and equitable.

We estimate the bandwidth cost in two different ways, the number of link channels on the one hand, and the sum of the geographical distances of the links on the other hand, while assuming the cost to be proportional to these parameters. For performance evaluation and comparison, we use three metrics.

- Capacity redundancy - $R^{\text{P/W}}$, i.e., the ratio of spare capacity cost over working capacity cost.

- Dual link failure recovery ratio - R_2 (as in Grover [Gro04a] (formula (8.3), p. 510) and Schupke [Sch03b]):

$$R_2 = 1 - \frac{\sum\limits_{\ell,\ell' \in L \times L : \ell \neq \ell'} \textsc{loss}(\ell, \ell')}{\sum\limits_{\ell,\ell' \in L \times L : \ell \neq \ell'} (d_\ell + d_{\ell'})} \tag{4.47}$$

where d_ℓ is the number of traffic units carried on link ℓ (see notations in Section 4.3.1), $\text{LOSS}(\ell, \ell')$ is the total number of unprotected traffic units under the dual failure of links ℓ and ℓ'.

- Number of topologically distinct p-cycles which need to be configured upon the deployment of a p-cycle scheme, a measure of the complexity of the protection management overhead.

Table 4.1: Data instances

			Networks					
			NSF [HBB+04]	GERMANY [HBB+04]	BELLCORE [MK98]	NJLATA [MK98]	COST239 [BDH+99]	EON2004 [HBB+04]
	#	nodes	14	17	15	11	11	28
	#	edges	21	26	28	23	26	41
Node	degree	average	3.0	3.1	3.7	4.2	4.7	2.9
		deviation	0.6	1.2	1.3	2.1	0.6	0.9
Link	length	min	387	36	130	250	210	218
		max	3,529	353	520	950	1,310	1,500
		avg.	1,303.5	170.3	262.5	553.9	578.7	625.4
Network	diameter	[hops]	3	6	4	4	3	8
		[km]	5,316	951	1,160	1,800	1,660	5,051
Avg. alter.	distance	[hops]	3.6	4.2	3.2	2.3	2.2	5.6
		[km]	4,181.9	722.7	886.6	1,179.8	996.3	3,277.9
Avg. link	pair dist.	[hops]	3.7	3.5	2.9	2.2	2.2	3.8
		[km]	4,247.1	600.8	778.3	1,130.2	997.7	2,136.6
Network	connectivity	DV	1.8	1.3	1.6	1.6	3.4	1.6
		DP	1.7	1.2	1.4	1.6	3.4	1.3
# Demands			91	136	105	55	55	378
Working cost			1,970	4,050	2,610	943	792	2,984

Data Instances

We use six different network instances, which are described in Table 4.1, together with some key characteristics of the traffic instances. For each network instance, we provide the number of nodes, the number of edges, the nodal degree (average and standard deviation values) as an indicator of the regularity of the network connectivity, and the link length (minimum, average, maximum).

In order to go one step further in the analysis of the results, we added three more characteristics for the network instances. They are all expressed in two units, number of hops and km. We therefore computed the network diameter, i.e., the length of the longest path among the shortest paths for any node pair in the network. Moreover, for all working paths, we provide the average distance of the alternate shortest path, which is link and $(\ell, \ell')_{v,p}$ link disjoint respectively, see the columns entitled Avg. alter. distance (resp. Avg. Link pair dist.).

At last, we added two parameters for characterizing the network connectivity in the context of path p-cycles and node p-cycles, which are defined below.

For a path p-cycle protection scheme, we define the DP parameter as the average number of node disjoint protection paths (for construction of path p-cycles) over the set $\mathcal{SD}$ of node pairs, i.e., the set of node pairs with some traffic:

$$DP = \frac{\sum\limits_{\{s,d\} \in \mathcal{SD}} DP_{sd}}{|\mathcal{SD}|}$$

where DP_{sd} is the maximum number of node disjoint protection paths for a node pair $\{s, d\}$.

For a node p-cycle protection scheme, we define the parameter DV as follows:

$$DV = \frac{\sum\limits_{p \in P, v \in V_p^\star} DV_{p,v} + \sum\limits_{\ell \in L} DL_\ell}{\sum\limits_{p \in P} \left|V_p^\star\right| + |L|}$$

where $DV_{p,v}$ and DL_ℓ denote the maximum number of node disjoint protection paths for the $(\ell, \ell')_{v,p}$ link pair and for link ℓ (a one-hop working path), respectively.

Traffic instances are described by their number of demand requests and working capacity (i.e., number of link wavelength channels which are required for the primary paths), in the last two lines of Table 4.1. For each network, the number of demand units between a given node pair is randomly generated (uniform distribution) in the interval [1..20] for the first five networks, and in the interval [1..3] for EON2004. Working paths are computed in such a way as to guarantee that they are of minimum length subject to the condition that there exists at least one potential protection path that is link and node disjoint with the working path.

4.7.1 Capacity Redundancy

We first compare the four protection schemes, link p-cycle (LpCycle), OG p-cycle (OGpCycle), node p-cycle (LNpCycle) and path p-cycle (PpCycle), with respect to capacity redundancy. Results are summarized in Figures 4.9(a) and 4.9(b) for the hop and the geographical distance (km) metrics, respectively. Except for Germany instance, the behavior (ranking of the four protection schemes according to the capacity redundancy) is identical for the two bandwidth cost metrics.

As expected, extra spare capacity is required by p-cycles for node protection compared with those providing only link protection for each network instance. As for node p-cycle with hop metric (resp. for the geographical distance metric), from 1.3% to 25.3% (from 1.7% to 28.7%) more bandwidth is required than link p-cycle, while providing 100% protection

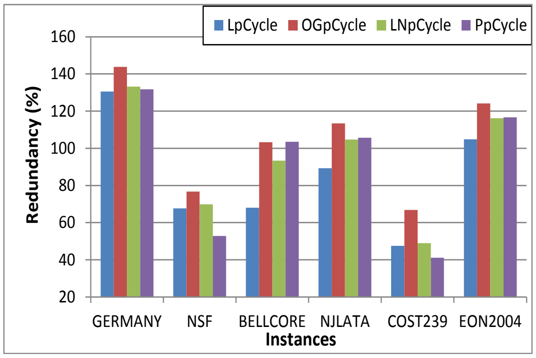

(a) Hop metric

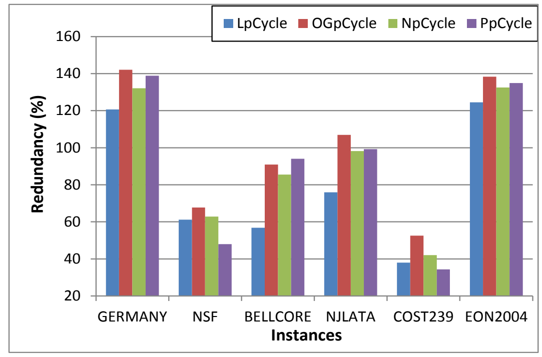

(b) Distance metric (km)

Figure 4.9: Capacity redundancies

against single link and node failures.

Node p-cycle is more capacity efficient than OG p-cycle for all network instances, keeping in line with the comparison of these two protection schemes in the example presented in Section 4.2 (see Figure 4.2). The redundancy differences vary from 7% to 18% for the hop metric, and from 5% to 11% for the geographical distance metric.

For path p-cycle vs. node p-cycle, for NSF and COST239 with the small deviation of node degree (0.6 shown in Table 4.1), the path p-cycle scheme has an advantage over the node p-cycle one in terms of capacity efficiency, following the belief that a shared path protection approach is more capacity efficient than a shared link one. The difference ranges from 7.8% to 17.1% for the channel metric, and from 7.7% to 14.9% for the geographical distance metric. However, for the four other instances with a high node degree deviation, node p-cycle outperforms path p-cycle, with respect to capacity efficiency. This is in accordance with the example illustrated in Section 4.2.1. The differences vary from 0.5% to 10.2% (resp. 1.1% to 8.6%) for the hop (resp. distance) metric. We analyze further those results in the next paragraph throughout the impact of the network topology.

Impact of the Network topology

In order to understand the impact of the network topologies, we calculate the average distance of the shortest node disjoint protection paths for all working paths. The average distance is provided in the row with the header of Avg. alter. distance in Table 4.1. Also, for all $(\ell, \ell')_{v,p}$ link pairs, we calculate the average distance of their shortest node-disjoint protection paths, see the row entitled by Avg. link pair distance in Table 4.1.

We can observe from Table 4.1 that, for NSF and COST239, the average path distance for the intermediate node protection is equal to or longer than that for the path protection. However, for the other four instances, the average path distance for the node protection is shorter than that for the path protection. Note that, in the optimal solution of node p-cycles (resp. path p-cycles), the shortest protection paths are most probably used for the construction of node p-cycles (resp. path p-cycles) in order to keep spare capacity usage minimal. As a result, node p-cycles require less spare capacity, and therefore are more capacity efficient than path p-cycles in these four instances. Thereby, the experimental results shown in Figure 4.9(b) are verified.

We next investigate further how the capacity efficiency of path p-cycles (resp. node p-cycles) varies with the topology characteristics, and on which kind of topology path p-cycles (resp. node p-cycles) can achieve better performance. To this end, we calculate the indicator DP (resp. DV) for each working path (resp. each $(\ell, \ell')_{v,p}$ link pair with respect to an intermediate node of each working path), and present its value in Table 4.1. The relationship of DP (resp. DV) with the capacity redundancy is shown in Figure 4.10(a) (resp. 4.10(b)) for path p-cycles (resp. node p-cycles) respectively.

Figures 4.10(a) and 4.10(b) suggest that the average number DP (resp. DV) of alternate paths in a network is a key factor impacting the performance of path p-cycles (resp. node

p-cycles) with respect to the capacity efficiency. In general, the more protection paths, the more efficient path p-cycles (resp. node p-cycles) are in the context of protection against a single link/node failure. The reason is as follows. For each working path (resp. $(\ell, \ell')_{v,p}$ link pair), if more protection paths, and thereby more p-cycles are available, more opportunities then exist for the sharing of spare bandwidth with other node-disjoint working paths.

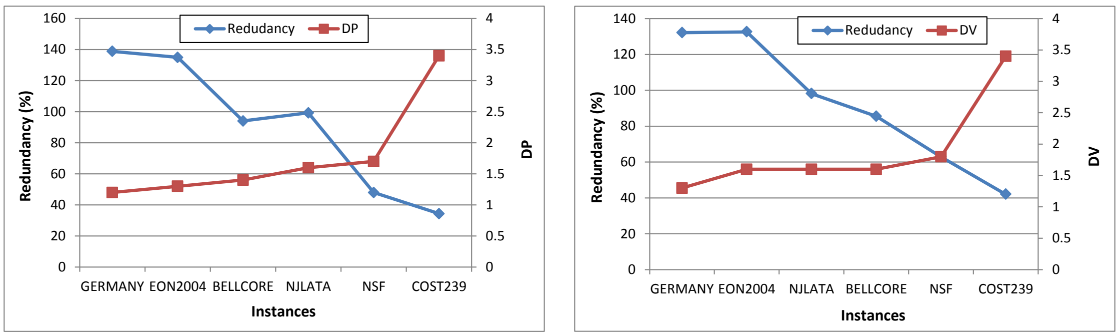

(a) Redundancy vs. DP (b) Redundancy vs. DV

Figure 4.10: Capacity redundancies vs. connectivity

4.7.2 Number and Length of the Cycles

Assuming no restriction on the length of the p-cycles, in Figure 4.11, we present respectively the number and length of the cycles in the optimal solutions of link p-cycle (LpCycle), OG p-cycle (OGpCycle), node p-cycle (LNpCycle) and path p-cycle (PpCycle). Since the excessive length of p-cycles has been often criticized (see, e.g., [SG03, CJ07]), we will study, in Section 4.7.4, the impact of shortening the p-cycles on the performance metrics.

Here, we observe more differences when comparing the four protection schemes, depending on the selected bandwidth metric. With respect to the number of distinct cycles, comparative performance (ranking of the four protection schemes) is the same for BELLCORE, NJLATA and EON2004. With respect to the average length of the cycles (weighted with the number of cycle occurrences), comparative performance (the protection scheme ranking) is the same for the GERMANY, BELLCORE and EON2004 instance, while it differs for the other three instances. A first observation is therefore that the number of hops is not necessarily a good approximation of the geographical length depending on the network structure (the variance of the link length is not enough to predict the different ranking).

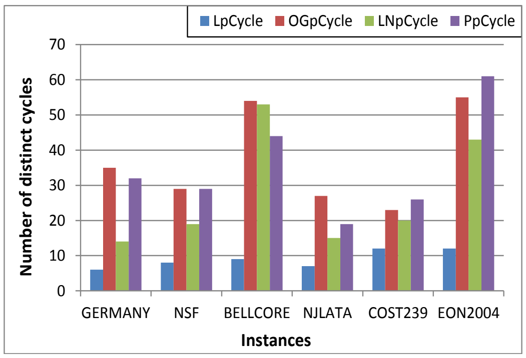

(a) Number of distinct cycles (hops)

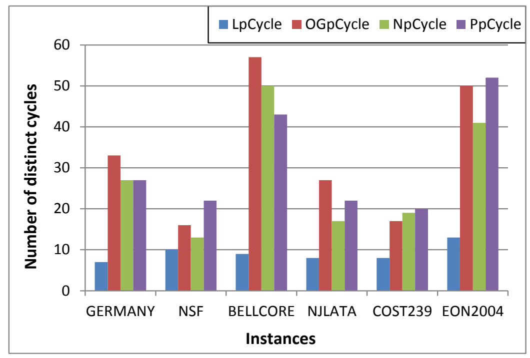

(b) Number of distinct cycles (km)

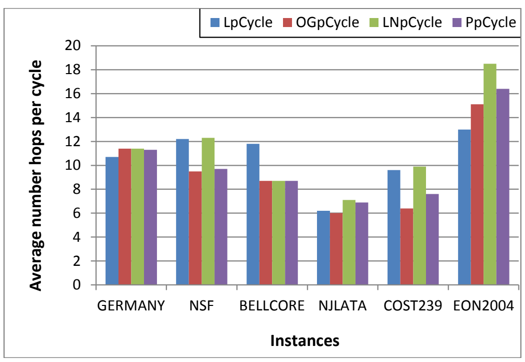

(c) Average number of links/cycle (hops)

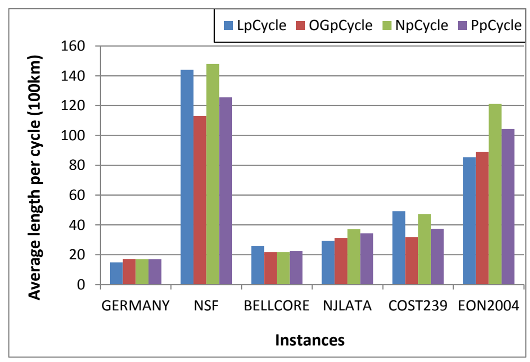

(d) Average length of a cycle (km)

Figure 4.11: Number and Length of the Cycles

Overall, the link p-cycle scheme requires the smallest number of distinct cycles among the four protection schemes for all instances (independently of the topologies). For the distance metric, there is no clear winner among the three other protection schemes for the number of distinct cycles, while for the hop metric, if we exclude the BELLCORE instance, the node p-cycle scheme requires the smallest number of distinct cycles, a possible advantage for the cycle management. Regarding OG p-cycle versus path p-cycle, the ranking varies with the network topologies, and there is no systematic ranking between them.

From the perspective of the average length of the p-cycles ensuring node protection, node p-cycle is equal to or larger than the other two protection schemes (OG p-cycle and path p-cycle). In contrast with link p-cycle, the average length of node p-cycle is larger in the GERMANY, NJLATA and EON2004 instances.

4.7.3 Protection against Dual Link Failures

We next compare the four protection schemes with respect to the dual link failure restoration ratio (R_2) over the six network instances. Note that here the protection against dual link failures comes for free from the solutions ensuring 100% link or link/node protection. Results are displayed in Figure 4.12(a) and 4.12(b) with the hop and distance metrics respectively.

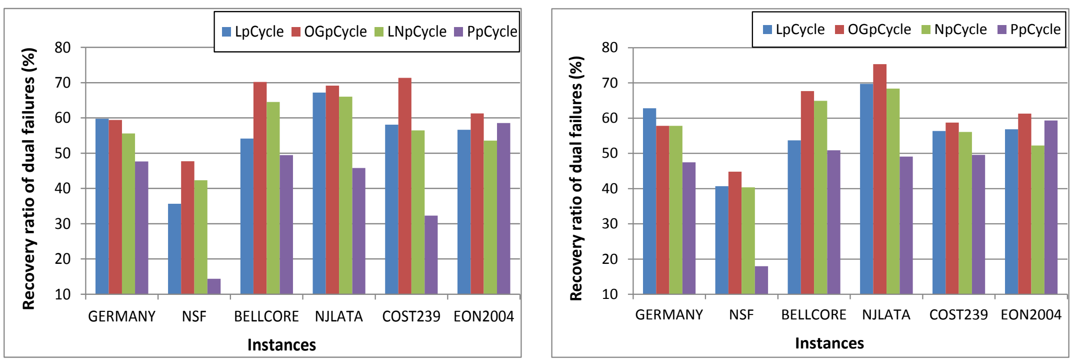

(a) Hop Metric (b) Distance Metric

Figure 4.12: Traffic Weighted Dual Recovery Ratio

The ranking of the four schemes with the hop metric is similar to the one with the distance metric except for NSF and GERMANY instances. OG p-cycle holds the largest value of R_2 for all instances except for GERMANY. This comes from the fact that OG p-cycle is the most capacity redundant among these four schemes. The R_2 differences between node p-cycle and OG p-cycle range from 3.1% to 15% (resp. from 0.1% to 9.1%) for the hop metric (resp. the distance metric).

Except for EON2004 instance, node p-cycle outperforms path p-cycle. Node p-cycle can provide from 8% to 27.9% (resp. 6.5% to 22.4%) more R_2 than path p-cycle for the hop (resp. distance) metric. In contrast with link p-cycle, the node p-cycle scheme provides comparable R_2 value for all instances except for BELLCORE and NSF. This can be explained by the fact that the average length of the cycles in the solutions based on node p-cycle is larger than those based on link p-cycles. In BELLCORE, however, node p-cycles can provide 10% more R_2 than link p-cycles for both bandwidth metrics.

4.7.4 Impacts of Cycle Length Limitation on Performance Metrics

The numerical results in the previous sections have been obtained without any limitation on the p-cycle length (whether for link, node or path protection), as for most of the related studies in the literature. However, length restrictions may have to be taken into account, if the delay of a connection is limited, especially if we assume that wavelength conversion is available at each node (the assumption of this study). For those reasons, we next investigate further the performance of the node protection schemes (node p-cycle and path p-cycle), while some restrictions are applied on the length of the p-cycles. We added the following constraint in the pricing problems:

$$\sum_{\ell \in L} \text{LENGTH}_\ell \, x_\ell \leq \overline{\text{LENGTH}}, \tag{4.48}$$

where $\overline{\text{LENGTH}}$ is the length limit on the p-cycles.

Experiments are carried out on the COST239 and EON2004 instances, and the numerical results are summarized in Figure 4.13 and 4.14 respectively.

For COST239 (resp. EON2004) network, $\overline{\text{LENGTH}}$ value ranges between 3,000 km (resp. 7,000 km) and 6,000 km (resp. 15,000 km), and no limit on the length of the p-cycles. Those values have been selected in order to guarantee that solutions exist for node p-cycle with

100% node protection. Note that for values slightly smaller, neither of these two instances can be fully protected by any of these two protection schemes.

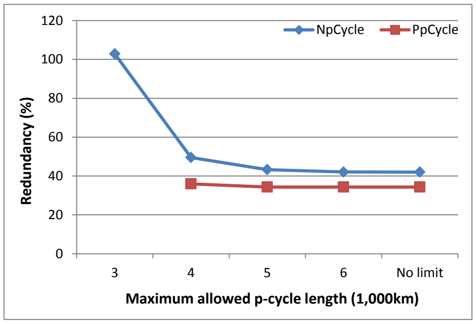

(a) Capacity redundancy

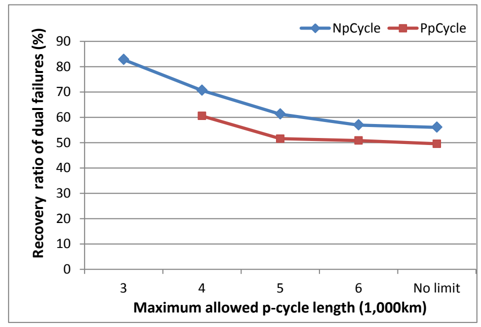

(b) Dual link failure restorability

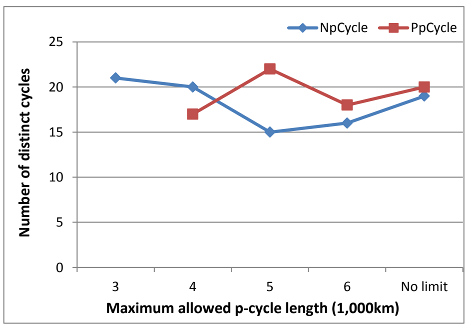

(c) Number of distinct cycles

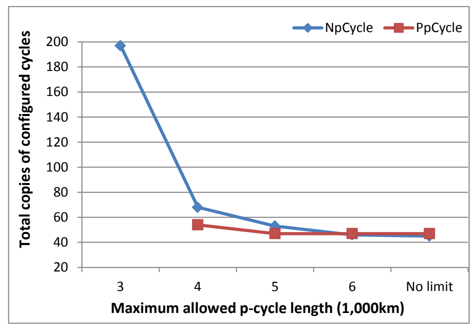

(d) Total copies of configured p-cycles

Figure 4.13: Effects of maximum allowed physical p-cycle length: COST239

Figures 4.13(a) and 4.14(a) show the decrease of the redundancy ratio as the length of the p-cycles increases for COST239 and EON2004 respectively. Note that for both instances, especially, for EON2004, there is no path p-cycle protection ensuring full link/node protection much earlier than for the node p-cycle scheme ($\overline{\text{LENGTH}}$ = 7,000 vs. 12,000) as the length limit of p-cycles decreases. The reason is as follows.

For path p-cycles, the length limit on the cycle length should be at least twice as much as the network diameter (1,660km for COST239 and 5,051km for EON2004, as shown in Table 4.1) to ensure 100% guaranteed link and node protection for all demands. With respect to node p-cycle, however, there is no such restriction, and the length limit on cycles only needs to be larger than the size of any cycle ensuring 100% link protection. This implies

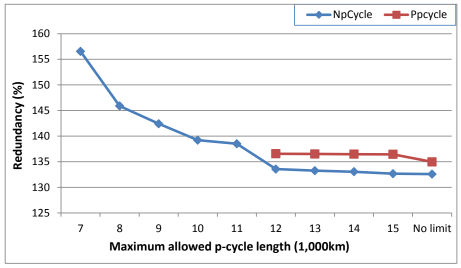

(a) Capacity redundancy

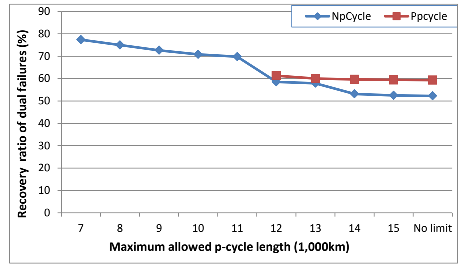

(b) Dual link failure restorability

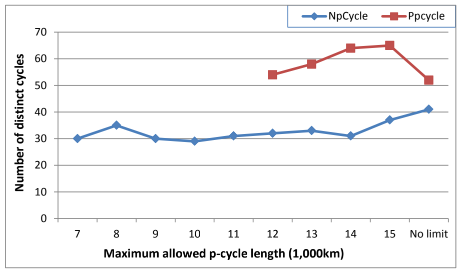

(c) Number of distinct cycles

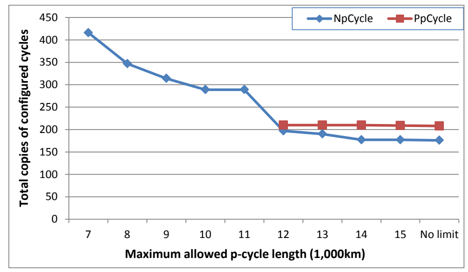

(d) Total copies of configured p-cycles

Figure 4.14: Effects of maximum allowed physical p-cycle length: EON2004

that, node p-cycle is an interesting scheme for link and node protection in the context of the existence of very restricted length limit.

For both instances, there is a length threshold (5,000 for COST239 and 12,000 for EON2004) beyond which the redundancy of these two protection schemes does not decrease significantly.

One of the advantages of short p-cycles, both for path and node p-cycles, but more so for node p-cycles, is the protection for dual link failures which reaches, e.g., 83% for node p-cycles when $\overline{\text{LENGTH}} = 3,000$, as shown in Figure 4.13(b). Although here, we evaluate the protection against dual failures which comes for free when ensuring protection against a single node/link failure, it shows that it should be rather easy to ensure protection against targeted dual failures (e.g., shared risk link group (SRLG) failures) while ensuring protection against a single link/node failure without requiring extra bandwidth.

For the overall number of p-cycles, there is a sharp increase of their number as the length limit decreases, especially for the node p-cycles, as shown in Figure 4.13(d) and

4.14(d). However, the number of distinct cycles (with respect to the links they use) remains rather stable. This suggests that the length limit has a minor impact on the management overhead.

4.8 Summary and Conclusion

In this chapter, we proposed an enhanced node p-cycle scheme, which improves the first node p-cycle of Onguetou and Grover [GO09]. Also, we have studied the comparison of it with the other three p-cycle-based schemes in WDM mesh networks for single link or node failures. Unified column generation models have been written and developed for all compared protection schemes.

Numerical results show that ensuring node protection in addition to link protection against a single failure is not significantly more costly in terms of spare capacity than for link protection against a single failure.

Contrary to a wide belief that path p-cycles have an advantage of capacity efficiency over p-cycles for link and node protection, numerical results reveal that, in some network instances with high standard deviation for the node degree, p-cycles ensuring node protection hold comparable capacity efficiency as path p-cycles. In some network instances, node p-cycles are even more capacity efficient than path p-cycles. In addition, results show that p-cycles with node protection can achieve higher recovery ratio of dual link failures than path p-cycles. In the context of restricted length cycles, node p-cycle solutions exist for much smaller cycles than path p-cycle for full link and node protection. The above observations suggest that p-cycles with node protection are a promising alternative of path p-cycles for full link and node protection.

Chapter 5

The Segment p-Cycle with Full Node Protection Scheme

5.1 Introduction

Segment p-cycles offer an interesting compromise between the classical (link) p-cycles and the path p-cycles (also known as FIPP p-cycles), inheriting most advantages of both p-cycle schemes. In their original form, segment p-cycles do not offer 100% node protection, i.e., do not guarantee any protection against node failure for the endpoints of the segments.

We propose a new efficient design approach for segment p-cycles, called segment Np-cycles, which ensure 100% protection against any single failure, either link or node (endpoints of requests are excluded). In order to evaluate the performances of segment Np-cycles, we compare segment Np-cycles with original segment- and path-protecting p-cycles mainly from the perspectives of the network cost and the failure recovery time.

We consider the network cost respectively from two aspects: the bandwidth usage and the capital expenditures (CAPEX). To this end, we develop two optimization models: One optimization model is to minimize spare capacity usage, as in conventional designs, the other is to minimize CAPEX. Definition of the protection segments (i.e., optical hops) takes into account the fact that equipment cost varies with the optical reach: longer reach means less equipment, but more expensive equipment. In order to identify the best trade-offs, we develop a new set of flow conservation constraints in order to optimize the length of the protection segments. These optimization models are solved using the column generation (CG) techniques. The use of such techniques eliminates the need to explicitly enumerate all segment Np-cycle configurations, but instead leads to a process where only improving segment Np-cycle configurations are generated.

Besides these, we develop three new formulas respectively for estimation of the recovery time based on these p-cycle schemes in order to compare quantitatively their recovery speed.

The rest part of this chapter is structured as follows. Section 5.2 introduces our proposed segment Np-cycles followed by the bandwidth minimization model present in Section 5.4. Section 5.3 illustrates respectively the CAPEX model of segment Np-cycles, segment p-cycles and path p-cycles. In Section 5.5 and Section 5.6, accordingly, we present the CG-based optimization models. The formulas for the recovery time estimation are reported in Section 5.7. The numerical results are shown in Section 5.8 followed by conclusion made in Section 5.10.

5.2 Segment Np-Cycles

In order to provide full node protection with the segment p-cycle scheme, we propose a new protection scheme, named as segment Np-cycle. The first key idea is to pair consecutive segments belonging to the same lightpath, and to ensure that both segments are protected by the same segment p-cycle. Let us see Figure 5.1 for an illustration. Therein, we have one request supported by a lightpath made of three segments s_1, s_2, s_3, with their endpoints represented by squares, and their intermediate nodes by circles. There are two segment p-cycles, the first one (c_1) protects segments s_1 and s_2 (both are on-cycle segments), the second one (c_2) protects segments s_2 and s_3 (again, both are on-cycle segments). If the common endpoint v_1 of s_1 and s_2 fails, then the lightpath is protected, using the counter part of c_1 with respect to s_1 and s_2. It is similar for the v_2 failure. Protection of nodes v_1 and v_2 comes at the expense of an overlapping of the two p-cycles with respect to s_2.

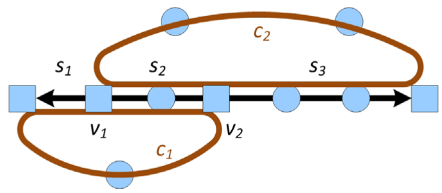

Figure 5.1: Segment Np-cycles which ensure 100% intermediate node protection

Several different relationships may exist between segment Np-cycles and the pair of working segments they protect. Some cases are illustrated in Figure 5.2. For a given pair of segments, the two segments may be, e.g., one on-cycle one and one straddling one (see Figure 5.2(a)), one straddling and one hybrid one (see Figure 5.2(b)).

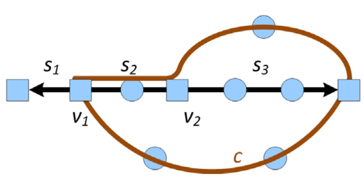

(a) Pairing of one straddling and one on-cycle segment

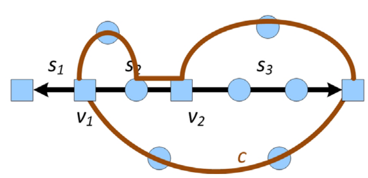

(b) Pairing of one straddling and one hybrid segments

Figure 5.2: Two possible configurations of segment Np-cycles

5.3 Capex Cost Model

In this section, we propose a new segment Np-cycle (p-cycle) framework based on the node architecture in [OG11]. We then illustrate respectively, based on this framework, how to calculate the CAPEX cost for deployment of segment Np-cycles, segment- and path-protecting p-cycles.

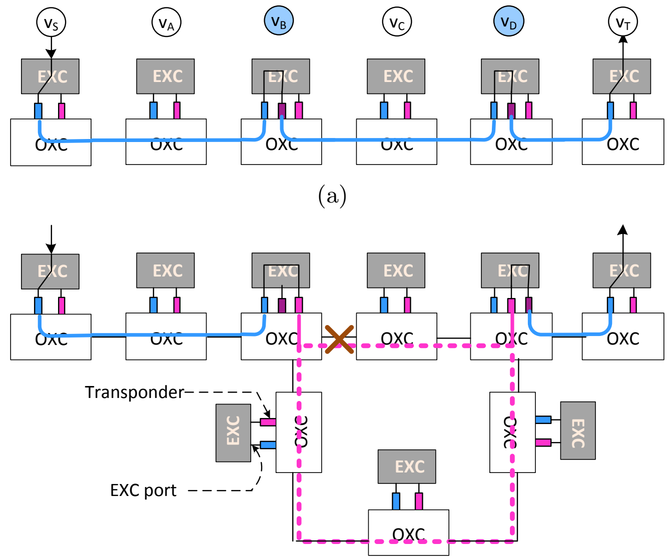

(a)

(b)

Figure 5.3: A segmented path and a segment p-cycle

5.3.1 p-Cycle Framework

In optical WDM mesh networks, we assume that each node hosts a transparent OXC/OADM together with an EXC (e.g., node $v_{\rm A}$ in Figure 5.3). We propose accordingly a new segment p-cycle (Np-cycle) framework in such WDM networks, as illustrated in Figure 5.3. A demand $v_{\rm S} - v_{\rm T}$ is carried on path $v_{\rm S} - v_{\rm A} - v_{\rm B} - v_{\rm C} - v_{\rm D} - v_{\rm T}$, as shown in Figure 5.3(a), which is segmented at nodes $v_{\rm B}$ and $v_{\rm D}$. In each segment (e.g., $v_{\rm S} - v_{\rm A} - v_{\rm B}$), the signal keeps in the optical domain. A segment p-cycle is shown in Figure 5.3(b). Upon a link failure (e.g, $v_{\rm B} - v_{\rm C}$), the end nodes (e.g., $v_{\rm B}$ and $v_{\rm D}$) of the affected working segment (e.g., $v_{\rm B} - v_{\rm C} - v_{\rm D}$), with the help of the EXC switching, switch the traffic to the transponders for access to the p-cycle. The signal switched onto such segment p-cycle remains in optical domain. A pair of a transponder and an EXC port is required at each end node of working segment for access to the related segment Np-cycle.

We assume that each OXC/OADM holds wavelength conversion functionality, and consequently, we do not consider wavelength continuity constraints in the present study. Other assumptions are those: *(i)* EXCs are only for protection switching, *(ii)* there are enough deployed fibers for accommodating p-cycles required, *(iii)* we only consider the network equipment usage with respect to p-cycle construction.

5.3.2 CAPEX of Segment Np-Cycles

We next illustrate the calculation of segment Np-cycle CAPEX, which comes from three CAPEX components: transmission cost, link cost and node cost. For illustration, Figure 5.4(a) is used as an example network topology, the number beside each link denotes the link length in km. In this network, two demands, each with one unit request, are routed along segmented working paths: $v_A - v_H$ and $v_D - v_K$ are routed on path $v_A - v_C - v_D - v_H$ and $v_D - v_F - v_G - v_I - v_K$, and segmented at node v_D and v_F, respectively. Another demand $v_G - v_H$ with two units of requests is carried on path $v_G - v_H$.

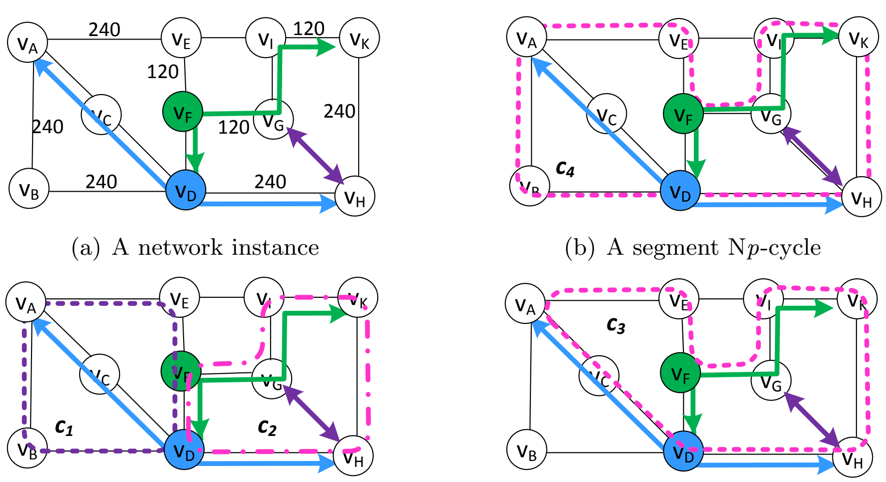

(a) A network instance (b) A segment Np-cycle

(c) Segment p-cycles (d) A path p-cycle

Figure 5.4: Link and node protection

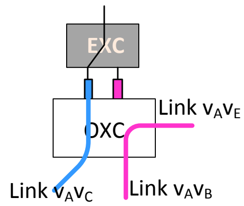

(a) Node v_{A}

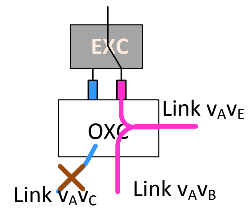

(b) Node v_{A} with $v_{\text{A}}v_{\text{C}}$ cut

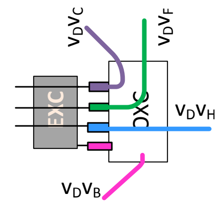

(c) Node v_{D}

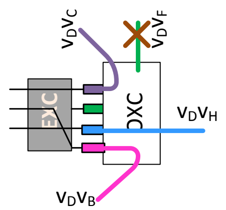

(d) Node v_{D} with $v_{\text{D}}v_{\text{F}}$ cut

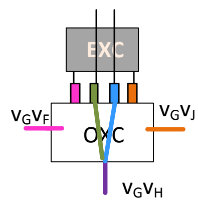

(e) Node v_{G}

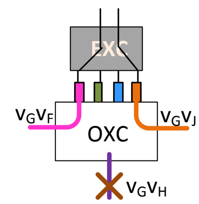

(f) Node v_{G} with $v_{\text{G}}v_{\text{H}}$ cut

Figure 5.5: Details of nodes in a segment Np-cycle

- Transmission cost

The transmission cost includes the cost of the transponders and of the EXC ports for access to segment Np-cycles. Each end node of each unit working segment requires one transponder and one EXC port to switch the affected traffic to a segment Np-cycle.

As shown in Figure 5.5(a) and 5.5(b), node v_{A} of $v_{\text{A}} - v_{\text{C}} - v_{\text{D}}$ in Figure 5.4(b) requires one transponder and one EXC port for access to c_4.

Segments with a common end node, say v and protected by the same Np-cycle can share the transponder and EXC port at v if these segments are node disjoint except for node v. As shown in Figure 5.5(c) and 5.5(d), node v_{D} only requires one transponder and one EXC port for switching traffic to segment Np-cycle c_4. For each unit straddling segment (e.g., $v_{\text{G}} - v_{\text{H}}$), each end node (e.g., v_{G} and v_{H}) requires one transponder and one EXC port, as shown in Figure 5.5(e) and 5.5(f).

The optical reach of a transponder should fulfill the length of the associated protection segment. If a transponder is shared by different working segments, its optical reach should match the longest protection segment which it spans.

In the NOBEL cost model [HGMS08], the normalized cost of an EXC port is 0.67, and the cost of a 750 km (LH) (resp. 1500 km, ELH) transponder is 1 (resp. 1.25). Table 5.1 summarizes the transmission cost of segment Np-cycle c_4 in Figure 5.4(b).

Table 5.1: Transmission cost of a segment Np-cycle

End node	W-segment or segmentation node	Max. segment Np-cycle Length (km)	Reach	Cost
v_{A}	$v_{\text{A}} - v_{\text{C}} - v_{\text{D}}, v_{\text{D}}$	960	ELH	1.92
v_{D}	$v_{\text{D}} - v_{\text{C}} - v_{\text{A}}$, $v_{\text{D}} - v_{\text{F}}, v_{\text{D}} - v_{\text{H}}$	1,440	ELH	1.92
v_{F}	$v_{\text{F}} - v_{\text{D}}$, $v_{\text{F}} - v_{\text{G}} - v_{\text{J}} - v_{\text{K}}$	1,320	ELH	1.92
v_{K}	$v_{\text{K}} - v_{\text{J}} - v_{\text{G}} - v_{\text{F}}, v_{\text{F}}$	1,320	ELH	1.92
$v_{\text{G}}, v_{\text{H}}$	$v_{\text{G}} - v_{\text{H}}$	480	LH	2×1.67
	$v_{\text{G}} - v_{\text{H}}$	1,220	ELH	2×1.92
	Total cost			14.86

- Link cost

The link cost comprises the costs of the following network elements: *(i)* optical line amplifiers (OLAs); *(ii)* dispersion compensating fibers (DCFs); *(iii)* dynamic gain equalizers (DGEs). An OLA and a DCF are required every 80km between two transparent nodes, and a DCF is required every fourth OLA [HGMS08]. These network elements operate in the fiber level, and therefore are priced per fiber link. With respect to a optical fiber, the optical signals may have different optical reach, and the optical reach of OLAs and DCFs on this fiber should meet the longest signal reach.

In Np-cycle c_4, each link may carry the ELH signal depending on utilization of the protection segments, then requires OLAs and DCFs with ELH optical reach. Given that one OLA (resp. a DGE) costs 2.77 (resp. 3.17) for the ELH optical reach [HGMS08], the link cost is then:

$$5 \times (\left\lceil \frac{240}{80} \right\rceil - 1) \times (2.77 + 3.17) + 4 \times (\left\lceil \frac{120}{80} \right\rceil - 1) \times (2.77 + 3.17) = 83.16.$$

- Node cost

The node cost involves the cost of OADMs/OXCs. An OADM/OXC is priced by the fiber port number. The fiber ports on an OADM/OXC should be enough for the overall fibers on the links adjacent to the node for carrying the crossing Np-cycles.

Each node on the Np-cycle c_4 in Figure 5.4(b) requires an OADM for cross connection of on-cycle links. Given that an OADM costs 18.8, the c_4 node cost is $18.8 \times 9 = 169.2$.

This leads to the overall CAPEX of $14.86 + 83.16 + 169.2 = 267.22$ for segment Np-cycle c_4.

5.3.3 CAPEX of Segment- and Path-protecting *p*-Cycles

- Segment p-cycles

The CAPEX of segment p-cycles is calculated in the same way as that of segment Np-cycles. It also consists of three components: transmission cost, link cost and node cost.

Recall that segment Np-cycles are segment p-cycles with full node protection. Thus, c_4 in Figure 5.4(b) can act as a segment p-cycle, and is less costly than configurations c_1 and c_2 in Figure 5.4(c). In Figure 5.4(c), for node v_{D}, two transponders are required to get the respective access to c_1 and c_2. In addition, node v_{D} needs to equip an OXC with three fiber ports. However, in Figure 5.4(b), only one transponder and an OADM on v_{D} are needed. Therefore, we will consider c_4 as a segment p-cycle (no protection for segmentation nodes) and calculate its CAPEX cost.

With respect to segment p-cycles, the calculation of transmission cost is similar to the one shown in Table 5.1. The only difference exists in that node v_A is only used to switch working segment $v_A - v_C - v_D$, whose protection path spans 480 km. Then, node v_A requires a LH transponder with an EXC port, the cost is 1.67. Thus, the total transmission cost is 14.61. The link cost and the node cost are the same as those for the segment Np-cycle. Then, the overall CAPEX cost amounts to $14.61 + 83.16 + 169.2 = 266.97$ if c_4 is exploited as a regular segment p-cycle.

This example manifests that, in contrast with segment p-cycles, segment Np-cycles can provide full node and link protection with very small extra CAPEX cost.

- Path p-cycles

The CAPEX cost of path p-cycles also consists of the three components, as in segment p-cycles. In contrast with segment p-cycles, path p-cycles only require the end nodes of working paths to be equipped with the transponder-and-EXC-port pairs for switching traffic onto p-cycles. Therefore, path p-cycles require less number of transponders, and thus, need the less transmission cost than segment p-cycles.

Let us calculate the CAPEX of path p-cycle c_3 in Figure 5.4(d). Two transponders are required by the end nodes of working path $v_A - v_C - v_D - v_H$ ($v_D - v_F - v_G - v_K$), whose protection path spans 960 km (480 km). Then, these two transponders should be with ELH (LH) optical reach. For working path $v_G - v_H$ carrying two unit requests, two pairs of transponders are needed at each end node. The length of one protection path is 480 km while the other is 1220 km. This suggests that one pair of transponders should be with LH optical reach, the other pair with ELH optical reach. Note that, two disjoint working paths $v_A - v_C - v_D - v_H$ and $v_G - v_H$ have the same end node v_H, they can then share one transponder for access to c_3. Therefore, the total transmission cost is $4 \times 1.67 + 3 \times 1.92 = 12.44$.

The link(resp. node) cost is calculated as the same as that of Np-cycle c_4, and the link (resp. node) cost value is 83.16 (169.2). Therefore, the overall CAPEX cost of c_3 is $12.44 + 83.16 + 169.2 = 264.8$.

This example shows that path p-cycles can be less costly than segment p-cycles and Np-cycles.

5.4 Minimum Bandwidth Usage Design of Segment Np-Cycles

To design segment Np-Cycles, we follow a sequential method where the working segments have been established prior to defining the segment p-cycles. The input of the proposed optimization model is therefore a set P of working lightpaths together with the set S of associated working segments. Traffic is defined by a set of requests of various granularities, which are groomed in order to define the working segments, using the algorithm of [BJH11, Bou05], with the objective of minimizing the bandwidth requirements.

In order to deal with the scalability issue suffered by the past conventional designs, we developed an optimization model based on a column generation (CG) formulation. In this way, we avoid the explicit enumeration of all potential segment Np-cycle configurations (see next section for a formal definition), and replace it with an iterative process, where after the selection of an initial set of configurations, we only generate the segment Np-cycle configurations, one at a time, which improve the value of the current solution. This way, we can reach an optimal solution (or a near optimal solution) after the generation of a very small number of cycles. The associated column generation algorithm is identical to the one described in Section 3.7.

5.4.1 The Master Problem

For a working segment $s \in S$, let d_s be its bandwidth capacity (the number of capacity units).For a given working lightpath $p \in P$, let d_p be the number of bandwidth units it carries on and $V_p^\star$ the set of its segmentation nodes ($V_p^\star = V_p \setminus \{$ endpoints of $p\}$), where V_p is the set of segment endpoints.

The CG model makes use of a set C of segment Np-cycle configurations defined as follows. A configuration c consists in: *(i)* a cycle; *(ii)* a subset of working segments protected by the p-cycle, and *(iii)* a subset of segmentation nodes protected by the p-cycle. Note that the intermediate nodes of the segments protected by a given p-cycle are protected. More formally, a configuration c is defined by the following parameters:

− a vector $(a_\ell^c)_{\ell \in L}$ such that $a_\ell^c \in \{0, 1\}$ is equal to 1 if link ℓ is an on-cycle link of the p-cycle, and 0 otherwise.

− a vector $(a_s^c)_{s \in S}$ such that $a_s^c \in \{2, 1, 0\}$ encodes the number of protection units associated with a protected working segment s (depending on whether the working segment is an on-cycle, hybrid or straddling one).

− a matrix $(a_{pv}^c)_{p \in P,\, v \in V_p^\star}$ such that $a_{pv}^c \in \{2, 1, 0\}$ represents the number of protection segments provided by the configuration c for the working path p against the failure of its segmentation node v.

The optimization model can be written as follows.

$$\min \quad \sum_{c \in C} \text{COST}_c \, z_c$$

$$\text{subject to:} \qquad \sum_{c \in C} a_s^c \, z_c \;\geq\; d_s \qquad\qquad s \in S \tag{5.1}$$

$$\sum_{c \in C} a_{pv}^c \, z_c \geq \; d_p \qquad p \in P, \; v \in V_p^\star \tag{5.2}$$

$$z_c \in \mathbb{Z}^+ \qquad\qquad c \in C \tag{5.3}$$

where $\text{COST}_c = \sum\limits_{\ell \in L} \text{COST}_\ell \, a_\ell^c$, COST_ℓ being the spare capacity requirement for link ℓ.

The objective is to minimize the cost of the selected segment Np-cycles, defined here by the overall amount of required bandwidth for the set of selected configurations. Constraints (5.1) ensure that all working segments are protected from a single failure of one of their link or of one of their intermediate node. Constraints (5.2) guarantee that segment endpoints (excluded the endpoints of the requests) are protected against a single failure. Constraints (5.3) are variable domain constraints.

5.4.2 The Pricing Problem

The pricing problem corresponds to the optimization problem for calculation of a segment Np-cycle configuration. The objective is to minimize the so-called reduced cost (denoted by $\overline{\text{COST}}$) of the master problem. The reduced cost of configuration c is as follows:

$$\overline{\text{COST}}_c = \text{COST}_c - \sum_{s \in S} u_s \, a_s^c - \sum_{p \in P} \sum_{v \in V_p^\star} u_{pv} \, a_{pv}^c,$$

where u_s and u_{pv} are the dual variables associated with constraints (5.1) and (5.2), respectively.

We next introduce some notations before setting the mathematical model for the pricing problem. First, some sets:

P_v set of working lightpaths with v as a segmentation node.

S_v set of working segments going through node v.

Parameters

$\beta_s^{s'}$ $= 1$ if working segments s and s' are not link-and-intermediate-node disjoint, 0 otherwise.

τ_ℓ^s $= 1$ if link ℓ belongs to working segment s, or is adjacent to one of its intermediate node, 0 otherwise.

Note that [$\beta_s^{s'}$ and [τ_ℓ^s are with the different definitions than those in Section 3.3.2.

Let p be a working lightpath. It can be defined by a sequence of one or more segments. Assuming p contains more than 2 segments, let v be one of the segment endpoints, different from the endpoints of p. Let s_1 and s_2 be the two segments of p such that s_1 and s_2 intersects at v. Let e_{pv}^1, e_{pv}^2 be the end nodes, $\neq v$, of the segments of p intersecting at v.

Variables

x_{pv}^ℓ $=$ 1 if link ℓ is used to protect segmentation node v on working path p, 0 otherwise.

The reduced cost can be rewritten:

$$\overline{\text{COST}}_c = \sum_{\ell \in L} \text{COST}_\ell \overbrace{x_\ell}^{a_\ell} - \sum_{s \in S} u_s \overbrace{\sum_{\ell \in \omega(v_s^1)} x_\ell^s}^{a_s^c} - \sum_{p \in P} \sum_{v \in V_p^\star} u_{pv} \overbrace{\sum_{\ell \in \omega(v_{pv}^1)} x_{pv}^\ell}^{a_{pv}^c}.$$

The set of constraints includes three blocks of constraints. The first block takes care of the generation of a simple cycle, which is made up of constraints (3.9) - (3.11).

The second block takes care of identifying the set of working segments to be protected by the segment Np-cycle under construction. This block consists of constraints (3.12) -

(3.15) together with the following two sets of constraints.

$$x_\ell^s + x_\ell^{s'} \leq 2 - \beta_s^{s'} \qquad s, s' \in S,\ \ell \in L \tag{5.4}$$

$$x_\ell^s \leq 1 - \tau_\ell^s \qquad \ell \in L,\ s \in S. \tag{5.5}$$

Constraints (5.4) ensure that only link-and-node-disjoint working segments can share protection segments. Constraints (5.5) prevent a link from protecting itself and the related protected working segments.

The third block of the constraints identifies the segmentation nodes protected by the segment Np-cycle under construction.

$$x_{pv}^\ell \leq x_\ell \qquad p \in P,\ v \in V_p^\star,\ \ell \in L \tag{5.6}$$

$$x_{pv}^\ell \leq 0 \qquad p \in P,\ v \in V_p^\star,\ \ell \in \omega(v) \tag{5.7}$$

$$\sum_{\ell \in \omega(v_{pv}^1)} x_{pv}^\ell = \sum_{\ell \in \omega(v_{pv}^2)} x_{pv}^\ell \qquad p \in P,\ v \in V_p^\star \tag{5.8}$$

$$\sum_{\ell \in \omega(v')} x_{pv}^\ell \leq 2 \qquad p \in P,\ v \in V_p^\star,\ v' \in V \tag{5.9}$$

$$\sum_{\ell \in \omega(v') | \ell \neq \ell'} x_{pv}^\ell \geq x_{pv}^{\ell'} \qquad p \in P,\ v \in V_p^\star,\ \ell' \in \omega(v')$$

$$v' \in V \setminus \{e_{pv}^1, e_{pv}^2\} \tag{5.10}$$

$$\sum_{p \in P_v} x_{pv}^\ell + \sum_{s \in S_v} x_\ell^s \leq 1 \qquad \ell \in L,\ v \in V \tag{5.11}$$

$$x_\ell,\ x_\ell^s,\ x_{pv}^\ell \in \{0,1\} \qquad \ell \in L,\ s \in S, p \in P,\ v \in V_p^\star \tag{5.12}$$

Constraints (5.6) say that only on-cycle links are eligible for the protection of a segmentation node. Constraints (5.7) say that a link cannot be used to protect a segment endpoint if the link is incident to the endpoint. Constraints (5.8)-(5.10) are the flow conservation constraints for defining the links defining the protection of a segment endpoint: they need to define a path from one endpoint ($\neq v$) to the other endpoint ($\neq v$) of the two segments having v in common (i.e., nodes v' and v' in Figure 5.6).

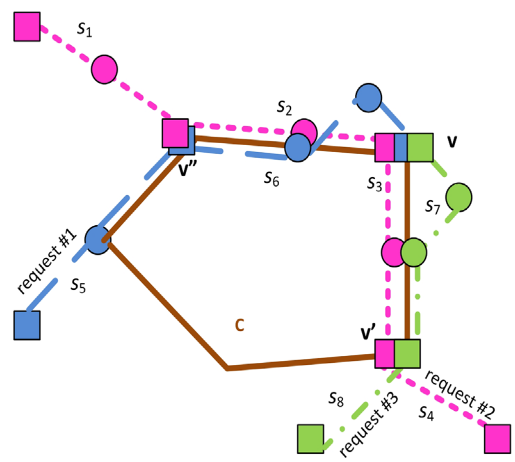

Figure 5.6: Protection of segment endpoints

Note that with the above constraints, we do not necessarily protect the common endpoint of a segment pairing (see Section 5.2 for the definition) with the same segment Np-cycle than the one protecting each or both segments of the pairing, see Figure 5.6. Therein, we have one Np-cycle (solid brown line), and three requests. A possible configuration c is as follows: a cycle made of the solid brown lines, protecting segments s_6 of request #1 (blue dashed lines) and s_7 of request #3 (green dash-dot lines), and segment endpoints v with respect to request #2 (pink dotted lines). Additional constraints can be easily added ($x_\ell^{pv} \leq x_\ell^s$ for v being an endpoint of s and s belonging to p) in order to ensure the protection of the adjacent segments of any segment endpoints if desired.

5.5 Minimum CAPEX Design of Segment Np-Cycles

In this section, we develop two optimization models for design of segment Np-cycles. The column generation (CG) model I is the restricted one, with which, the transponders on each generated Np-cycle candidate are with the same optical reach. The CG model II is the generalized one, with which, the transponders on each generated Np-cycle candidate may be with the different optical reach.

5.5.1 Column Generation Model I

The Master Problem

The objective of the master problem is to minimize the overall CAPEX of the segment Np-cycles in order to ensure a protection of all segments against any single failure of a link or a node (except for the working path endpoints).

Let M = {LH, ELH, ULH} be the optical reach value set, indexed by m, where LH (resp. ELH and ULH) stands for long haul (resp. extended long haul and ultra long haul) optical reach, i.e., 750km, 1,500km and 3,000km. The number i of fiber ports on an OADM/OXC belong to the set I = {2,3, …, 10}. The cost of an OXC with i fiber ports is denoted by $\text{COST}^{i}_{\text{OXC}}$.

The optimization model relies on the concept of configurations, where each configuration c is associated with a potential segment Np-cycle and the set of segments and segmentation nodes it protects. A configuration (segment Np-cycle) c consists of a cycle, where each transponder is with the same optical reach m. Formally, it is described by: *(i)* Vector $(a^c_\ell)_{\ell \in L}$, *(ii)* Vector $(a^c_s)_{s \in S}$ and *(iii)* Matrix $(a^c_{pv})_{p \in P,\, v \in V^*_p}$ are as defined in Section 5.4.1. *(iv)* Vector $(t^c_{\ell m})_{m \in M}$, with $t^c_{\ell m} = 1$ if each protection segment along the cycle c is with the optical reach m, 0 otherwise.

For a configuration c with optical reach m, let COST_c be the cost of its on-cycle transponders and EXC ports. Let COST_{TA} be the cost of a transparent node amplifier, and $\text{COST}^{\text{FB}}_{\ell m}$ the cost of a fiber, on which the equipment is within a m reach. The number of wavelengths in each fiber is denoted by W_{FB}.

We define the following sets of variables. Let $z_c \in \mathbb{Z}^+$ represent the copies of configuration c that are selected in the current solution. Let $\varphi^m_\ell \in \mathbb{Z}^+$ be the fiber number variable of link ℓ with a m reach. The binary variable ψ^i_v is equal to 1 if the OXC/OADM at node v has i fiber ports, 0 otherwise.

The mathematical model is next formulated.

$$\min \quad \sum_{c \in C} \text{COST}_c \, z_c + \sum_{\ell \in L} \sum_{m \in M} \text{COST}^{\text{FB}}_{\ell m} \, \varphi^m_\ell + \sum_{v \in V} \sum_{i \in I} i \, (\text{COST}^i_{\text{OXC}} + \text{COST}_{\text{TA}}) \, \psi^i_v$$

subject to:

$$\sum_{c \in C} a^c_s \, z_c \; \geq \; d_s \qquad s \in S \tag{5.13}$$

$$\sum_{c \in C} a^c_{pv} \, z_c \geq \; d_p \qquad p \in P, \; v \in V^*_p \tag{5.14}$$

$$\text{W}_{\text{FB}} \, \varphi^{\text{ULH}}_\ell \geq \sum_{c \in C} a^c_\ell \, t^c_{\text{ULH}} \, z_c \qquad \ell \in L \tag{5.15}$$

$$\text{W}_{\text{FB}}(\varphi^{\text{ULH}}_\ell + \varphi^{\text{ELH}}_\ell) \geq \sum_{c \in C} a^c_\ell (t^c_{\text{ULH}} + t^c_{\text{ELH}}) z_c \qquad \ell \in L \tag{5.16}$$

$$\text{W}_{\text{FB}} \sum_{m \in M} \varphi^m_\ell \geq \sum_{c \in C} \sum_{m \in M} a^c_\ell \, t^c_m \, z_c \qquad \ell \in L \tag{5.17}$$

$$\sum_{i \in I} \psi^i_v = 1 \qquad v \in V \tag{5.18}$$

$$\sum_{i \in I} i \, \psi^i_v \geq \sum_{\ell \in \omega(v)} \sum_{m \in M} \varphi^m_\ell \qquad v \in V. \tag{5.19}$$

Constraints (5.13) and constraints (5.14) have respectively the same functionality of constraints (5.1) and (5.2). Each link may consist of multiple fibers, each of which may carry the recovered signals with the different optical reach along Np-cycles. Recall that the equipment on fibers should meet the longest reach of signals carried on it. Constraints (5.15) (resp. (5.16), (5.17)) are formulated to determine, for each link, the number of fibers with the ULH (resp. ELH, LH) equipment. Specifically, constraints (5.15) say that, for each link, the number of fibers equipped with ULH optical reach equipment must be enough to accommodate the crossing Np-cycles, along which the protection segments are with ULH optical reach. Constraints (5.16) ensure that, for each link, the number of ELH fibers together with ULH fibers must be sufficient to carry all recovered ELH reach signals along the crossing Np-cycles. Constraints (5.17) ensure that, for each link, the number of LH fibers together with that of fibers with ELH or ULH equipment must be enough for carrying the recovered LH reach optical signal on the the crossing Np-cycles. OADMs/OXCs have several options to set the fiber port number (i.e., 2, 3, ..., 10). However, each OADM/OXC can only choose one option from these available ones. This is ensured by constraints (5.18). Constraints (5.19) say that, for any node, the fiber ports of an OXC/OADM must be adequate for all fibers adjacent to it.

Model Solution and The Pricing Problem

Based on the CG techniques, the solution process of the master problem model is identical to the one described in Figure 3.4.

The objective of the pricing problem consists of the minimization of the so-called reduced cost of the z_c variable of the master problem.

$$\overline{\text{COST}_c} = \text{COST}_c - \sum_{s \in S} u_s \, a_s^c - \sum_{p \in P} \sum_{v \in V_p^*} u_{pv} \, a_{pv}^c$$

$$+ \sum_{\ell \in L} u_\ell^2 \, t_{\text{ULH}}^c \, a_\ell^c + \sum_{\ell \in L} u_\ell^1 (t_{\text{ULH}}^c + t_{\text{ELH}}^c) a_\ell^c + \sum_{\ell \in L} \sum_{m \in M} u_\ell^0 \, t_m^c a_\ell^c$$

where u_s and u_{pv} are dual variables associated respectively with constraints (5.13) and (5.14). u_ℓ^2, u_ℓ^1 and u_ℓ^0 are dual variables related to constraints (5.15) – (5.17), respectively.

Let us introduce the following notations before presenting the pricing problem model.

Sets and Parameters

$\mathbf{cost_{ep}}$ the cost of an EXC port.

$\mathbf{cost}_m^{\mathbf{tp}}$ the cost of a WDM transponder with optical reach m.

$J = \{0, 1\}$, the index set of unit protection flows, indexed by j. For a straddling segment (e.g., as drawn in blue solid line in in Figure 5.7(a)), one unit p-cycle can offer two units of protection flows (e.g., as drawn in red dash line). These two protection flows are indexed by 0 and 1 respectively. While for a on-cycle working segment (as blue solid line shown in Figure 5.7(b)), one unit p-cycle provides one unit protection flow (red dash line in Figure 5.7(b)), indexed by 1. The other flow does not exist and therefore set as 0.

R_m maximal transmission distance of reach m.

$\sigma_v^s = 1$ if node v belongs to $\{v_s^1, v_s^2\}$, 0 otherwise.

$\sigma_{v'}^{pv} = 1$ if node v' belongs to $\{v_{pv}^1, v_{pv}^2\}$, 0 otherwise.

$\rho_{ss'}^v = 1$ if working segments s and s' share end node v and the adjacent link, 0 otherwise.

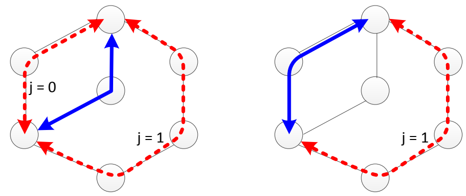

Figure 5.7: Protection flow index

Variables

$x_s^{\ell j}$ = 1 if link ℓ on the j^{th} protection segment is used to protect working segment s, 0 otherwise.

y_v ∈ $\{0, 1, 2\}$ represents the number of the pairs of transponders and EXC ports required at node v.

t_m = 1 if each protection segment along the current cycle is with the optical reach m, 0 otherwise.

With these notations, the reduced cost can be rewritten as follows.

$$\overline{\text{COST}}_c = \overbrace{\sum_{v \in V} \sum_{m \in M} \text{COST}_m^{\text{TP}} \, t_m \, y_v + \sum_{v \in V} \text{COST}_{\text{EP}} \, y_v}^{\text{COST}_c} - \sum_{s \in S} u_s \overbrace{\sum_{\ell \in \omega(v_s^1)} x_\ell^s}^{a_s^c} - \sum_{p \in P} \sum_{v \in V_p^*} u_{pv} \overbrace{\sum_{\ell \in \omega(v_{pv}^1)} x_{pv}^\ell}^{a_{pv}^c}$$

$$+ \sum_{\ell \in L} u_\ell^2 \, t_{\text{ULH}} \, x_\ell + \sum_{\ell \in L} u_\ell^1 \, (t_{\text{ULH}} + t_{\text{ELH}}) \, x_\ell + \sum_{\ell \in L} \sum_{m \in M} u_\ell^0 \, t_m \, x_\ell$$

We also introduce variables β_v^m and α_ℓ^m in order to linearize the quadratic terms $t_m \, y_v$ and $t_m \, x_\ell$ in the expression of the reduced cost. The quadratic terms

$$\beta_v^m = t_m \, y_v \quad \text{and} \quad \alpha_\ell^m = t_m \, x_\ell,$$

are then linearized thanks to the following constraints:

$$\beta_v^m \geq t_m + y_v - 1,\ \beta_v^m \leq y_v,\ \beta_v^m \leq t_m \quad v \in V,\ m \in M$$

$$\alpha_\ell^m \geq t_m + x_\ell - 1,\ \alpha_\ell^m \leq t_m,\ \alpha_\ell^m \leq x_\ell \quad \ell \in L,\ m \in M.$$

The pricing problem includes five blocks of constraints. The first block defines a simple cycle, which consists of constraints (3.9) - (3.11). The second block, which includes constraints (5.6) - (5.11), deals with the identification of a set of segmentation nodes which can be protected by the cycle under construction. The third block of constraints is defined next for determining the working segments protected by and for differentiating the protection segments along the cycle under construction.

$$x_\ell^s \leq \sum_{j \in J} x_{\ell j}^s \qquad \ell \in L,\ s \in S \tag{5.20}$$

$$\sum_{j \in J} x_{\ell j}^s \leq 1 \qquad \ell \in L,\ s \in S \tag{5.21}$$

$$x_s^{\ell j} \leq x_\ell \qquad \ell \in L,\ j \in J,\ s \in S \tag{5.22}$$

$$\sum_{\ell \in \omega(v_s^1)} x_s^{\ell j} = \sum_{\ell \in \omega(v_s^2)} x_s^{\ell j} \qquad j \in J,\ s \in S \tag{5.23}$$

$$\sum_{\ell \in \omega(v_s^1)} x_s^{\ell j} \leq 1 \qquad s \in S,\ j \in J \tag{5.24}$$

$$\sum_{\ell \in \omega(v)} x_s^{\ell j} \leq 2 \qquad s \in S,\ j \in J,\ v \in V \setminus \{v_s^1, v_s^2\} \tag{5.25}$$

$$\sum_{\ell' \in \omega(v):\, \ell' \neq \ell} x^s_{\ell' j} \geq x^{\ell j}_s \qquad \ell \in \omega(v),\ v \in V \backslash \{v^1_s, v^2_s\}, s \in S,\ j \in J \tag{5.26}$$

$$x^{\ell j}_s + x^{s'}_{\ell j} \leq 2 - \beta^{s,s'} \qquad s, s' \in S,\ \ell \in L,\ j \in J \tag{5.27}$$

$$x^{\ell j}_s \leq 1 - \tau^s_\ell \qquad \ell \in L,\ j \in J,\ s \in S \tag{5.28}$$

Constraints (5.20) say that, if a link is used to protect a segment, it must be on either of protection segment(s) along the current cycle. Constraints (5.21) state that two possible protection segments on the current cycle must be disjoint. Constraints (5.22) ensure that only on-cycle links are qualified for providing protection. Constraints (5.23) say that, for any working segment, its protection segment must end at its two end nodes. Constraints (5.24) ensure that each protection segment along the current cycle can only provide one unit protection for a working segment. Constraints (5.25) together with (5.26) guarantee flow conservation in the intermediate nodes along a protection segment. Constraints (5.27) ensure that only disjoint working segments can share protection segments. Constraints (5.28) prevent a link from protecting itself and the related working segments.

The next block of constraints is developed for determining the number of pairs of transponders and EXC ports required by the on-cycle nodes.

$$y_v \leq \sum_{\ell \in \omega(v)} x_\ell \qquad v \in V \tag{5.29}$$

$$y_v \geq \sigma^s_v \sum_{\ell \in \omega(v^1_s)} x^s_\ell \qquad v \in V, s \in S \tag{5.30}$$

$$y_{v'} \geq \sum_{\ell \in \omega(v^1_{pv})} x^\ell_{pv} + \sigma^{pv}_{v'} - 1 \qquad v' \neq v \in V, p \in P \tag{5.31}$$

$$y_v \geq \rho^v_{ss'}(\sigma^s_v \sum_{\ell \in \omega(v^1_s)} x^s_\ell + \sigma^{s'}_v \sum_{\ell \in \omega(v^1_{s'})} x^{s'}_\ell) \qquad v \in V, s, s' \in S \tag{5.32}$$

Constraints (5.29) express that only on-cycle nodes require transponders and EXC ports. Constraints (5.30) and (resp. (5.31)) ensure that, for a protected working segment (resp. a protected segmentation node of a working path), if an on-cycle node is its end node (resp. its adjacent segmentation node or one end node), the number of the pairs of transponders and EXC ports must match the protected units of segments (resp. segmentation nodes of working paths). Constraints (5.32) express that if two working segments share a link adjacent to their common end node, then two pairs of transponders and EXC ports are required in this end node for switching the failed segments.

The last block of constraints deals with the determination of the optical reach of the protection segments along the cycle under construction:

$$\sum_{m \in M} t_m = 1 \tag{5.33}$$

$$\sum_{\ell \in L} \text{LEN}_\ell \, x_s^{\ell j} \le \sum_{m \in M} R_m \, t_m \qquad s \in S, \, j \in J \tag{5.34}$$

$$\sum_{\ell \in L} \text{LEN}_\ell \, x_{pv}^{\ell} \le \sum_{m \in M} R_m \, t_m \qquad p \in P, \, v \in V_p^*. \tag{5.35}$$

Constraints (5.33) force the selection of a unique optical reach value for the protection segments along the cycle under construction. Constraints (5.34) and (5.35) guarantee that the length of each protection segment on the cycle under protection cannot exceed the selected optical reach value.

5.5.2 Column Generation Model II

The Master Problem

The main difference of the CG model II with the CG model I in Section 5.5.1 exists in the configuration definition. Herein, An one-unit configuration (segment Np-cycle) c consists of a one-unit cycle that protects a set of working segments and a set of segmentation nodes. With respect to a configuration, on-cycle transponders and link equipment may have different optical reach. Formally, a one-unit configuration c is made up of one vector and two matrices:

– Vector $(a_s^c)_{s \in S}$ and Matrix $(a_{pv}^c)_{p \in P,\, v \in V_p^*}$ are defined as in Section 5.4.1.

– Matrix $(t_{\ell m}^c)_{m \in M}$ is related to the link equipment optical reach. Its elements $t_{\ell m}^c = 1$ if on-cycle link ℓ requires link equipment with optical reach m, 0 otherwise.

The mathematical model is next formulated.

$$\min \quad \sum_{c \in C} \text{COST}_c \, z_c + \sum_{\ell \in L} \sum_{m \in M} \text{COST}_{\ell m}^{\text{FB}} \, \varphi_\ell^m + \sum_{v \in V} \sum_{i \in I} i \, \text{COST}_{\text{OXC}}^i \, \psi_v^i \tag{5.36}$$

subject to:

$$\sum_{c \in C} a_s^c \, z_c \ \geq \ d_s \qquad s \in S \tag{5.37}$$

$$\sum_{c \in C} a_{pv}^c \, z_c \geq \ d_p \qquad p \in P,\ v \in V_p^* \tag{5.38}$$

$$\mathrm{W_{FB}}\, \varphi_\ell^{\mathrm{ULH}} \geq \sum_{c \in C} t^c_{\ell,\mathrm{ULH}}\, z_c \qquad \ell \in L \tag{5.39}$$

$$\mathrm{W_{FB}}(\varphi_\ell^{\mathrm{ULH}} + \varphi_\ell^{\mathrm{ELH}}) \geq \sum_{c \in C} (\, t^c_{\ell,\mathrm{ULH}} + t^c_{\ell,\mathrm{ELH}}\,) z_c \qquad \ell \in L \tag{5.40}$$

$$\mathrm{W_{FB}} \sum_{m \in M} \varphi_\ell^m \geq \sum_{c \in C} \sum_{m \in M} t^c_{\ell m}\, z_c \qquad \ell \in L \tag{5.41}$$

$$\sum_{i \in I} \psi_v^i = 1 \qquad v \in V \tag{5.42}$$

$$\sum_{i \in I} i\, \psi_v^i \geq \sum_{\ell \in \omega(v)} \sum_{m \in M} \varphi_\ell^m \qquad v \in V \tag{5.43}$$

Constraints (5.37) and (5.38) have the same functionality respectively as the ones (5.1) and (5.2). The descriptions of constraints (5.39) - (5.43) are respectively identical to constraints (5.15) - (5.19).

The Pricing Problem

The objective of the pricing problem is minimization of the so-called reduced cost of the z_c variable of the master problem. The reduced cost is written next.

$$\overline{\mathrm{COST}_c} = \mathrm{COST}_c - \sum_{s \in S} u_s\, a_s^c - \sum_{p \in P} \sum_{v \in V_p^*} u_{pv}\, a_{pv}^c \, + \sum_{\ell \in L} u_\ell^2\, t^c_{\ell,\mathrm{ULH}}$$
$$+ \sum_{\ell \in L} u_\ell^1 (t^c_{\ell,\mathrm{ULH}} + t^c_{\ell,\mathrm{ELH}}) + \sum_{\ell \in L} \sum_{m \in M} u_\ell^0\, t^c_{\ell m}$$

where u_s and u_{pv} are the dual variables associated respectively with constraints (5.37) and (5.38). u_ℓ^2, u_ℓ^1 and u_ℓ^0 are the dual variables related to constraints (5.39) – (5.41), respectively.

Let us first introduce the following notations before presenting the formulations of the pricing problem.

Parameters

δ_ℓ^{pv} For segmentation node v of working path p, there are two working segments on p with v as their common end node. $\delta_\ell^{pv} = 1$ if link ℓ is adjacent to node v or the intermediate node of these two working segments, 0 otherwise.

o_s^{pv} $= 1$ if working segment s belongs to working path p and with node v as its one end node, 0 otherwise.

Variables

$x_{pv}^{\ell j} =$ 1 if link ℓ sits on the j^{th} protection flow, and is employed to protect one-unit traffic carried on working path p against the node v failure, 0 otherwise.

y_v^j $=$ 1 if a transponder with an EXC port is required at the end node v of the j^{th} protection flow, 0 otherwise.

$t_m^{vj} =$ 1 if the end node v of the j^{th} flow requires a transponder with optical reach m, 0 otherwise.

$t_m^\ell =$ 1 if the on-cycle link ℓ asks for the equipment with optical reach m, 0 otherwise.

With these notations, the reduced cost can be rewritten as follows.

$$\overline{\text{COST}}_c = \overbrace{\sum_{j \in J} (\sum_{v \in V} \sum_{m \in M} \text{COST}_m^{\text{TP}} \, t_m^{vj} \, y_v^j + \sum_{v \in V} \text{COST}_{\text{EP}} \, y_v^j)}^{\text{COST}_c} - \sum_{s \in S} u_s \overbrace{\sum_{\ell \in \omega(v_s^1)} \sum_{j \in J} x_s^{\ell j}}^{a_s^c}$$
$$- \sum_{p \in P} \sum_{v \in V_p^*} u_{pv} \overbrace{\sum_{\ell \in \omega(v_{pv}^1)} \sum_{j \in J} x_{pv}^{\ell j}}^{a_{pv}^c} + \sum_{\ell \in L} u_\ell^2 \, t_{\text{ULH}}^\ell + \sum_{\ell \in L} u_\ell^1 \, (t_{\text{ULH}}^\ell + t_{\text{ELH}}^\ell) + \sum_{\ell \in L} \sum_{m \in M} u_\ell^0 \, t_m^\ell$$

We also introduce variable γ_m^{vj} for linearization of item $t_m^{vj} y_v^j$ in the expression of the reduced cost. Let

$$\gamma_m^{vj} = t_m^{vj} y_v^j.$$

The quadratic term is then linearized thanks to the following constraints:

$$\gamma_m^{vj} \geq t_m^{vj} + y_v^j - 1, \quad \gamma_m^{vj} \leq t_m^{vj}, \quad \gamma_m^{vj} \leq y_v^j$$

The pricing problem includes five blocks of constraints. The first block defines a simple cycle which includes constraints (3.9) - (3.11). The second block, which is made up of constraints (5.20) - (5.28), is to identify a set of working segments which can be protected by the current cycle. The third block is defined next for the identification of the protected segmentation nodes by the current cycle.

$$x_{pv}^{\ell j} \leq x_\ell \qquad p \in P,\ v \in V_p,\ \ell \in L \tag{5.44}$$

$$\sum_{j \in J} x_{pv}^{\ell j} \leq 1 \qquad p \in P,\ v \in V_p,\ \ell \in L \tag{5.45}$$

$$\sum_{\ell \in \omega(v_{pv}^1)} x_{pv}^{\ell j} = \sum_{\ell \in \omega(v_{pv}^2)} x_{pv}^{\ell j} \qquad p \in P,\ v \in V_p,\ j \in J \tag{5.46}$$

$$\sum_{\ell \in \omega(v')} x_{pv}^{\ell j} \leq 1 \qquad p \in P,\ v \in V_p,\ v' \in \{v_{pv}^1, v_{pv}^2\},\ j \in J \quad (5.47)$$

$$\sum_{\ell \in \omega(v')} x_{pv}^{\ell j} \leq 2 \qquad p \in P,\ v \in V_p,\ v' \in V \backslash \{v_{pv}^1, v_{pv}^2\},\ j \in J \quad (5.48)$$

$$\sum_{\ell \in \omega(v') | \ell \neq \ell'} x_{pv}^{\ell j} \geq x_{pv}^{\ell'} \qquad p \in P,\ v \in V_p,\ \ell' \in \omega(v'), v' \in V \backslash \{v_{pv}^1, v_{pv}^2\},\ j \in J \quad (5.49)$$

$$x_{pv}^{\ell j} \leq 1 - \delta_{\ell}^{pv} \qquad p \in P,\ v \in V_p,\ \ell \in L,\ j \in J \quad (5.50)$$

$$\sum_{p \in P_v} \sum_{j \in J} x_{pv}^{\ell j} + \sum_{s \in S_v} \sum_{j \in J} x_s^{\ell j} \leq 1 \qquad \ell \in L,\ v \in V \quad (5.51)$$

$$\sum_{\ell \in \omega(v_{pv}^1)} \sum_{j \in J} x_{pv}^{\ell j} \leq \sum_{s \in S} (o_s^{pv} \sum_{\ell \in \omega(v_s^1)} \sum_{j \in J} x_s^{\ell j}) \qquad p \in P,\ v \in V_p^* \quad (5.52)$$

Constraints (5.44) say that only on-cycle links are eligible for protection of a segmentation node. Constraints (5.45) say that, two protection flows must be disjoint for a segmentation node protection. Constraints (5.46) ensure that the protection flow for a segmentation node of a working path must be ended at the adjacent segmentation nodes or end nodes of the working path. Constraints (5.47) state that one unit Np-cycle can only protect one unit traffic through a segmentation node. Constraints (5.48) and (5.49) ensure the flow conservation in the intermediate nodes of the protection flow for recovery of a segmentation node. Constraints (5.50) say that a link cannot be used to protect a segmentation node if the link is adjacent to a segmentation node. For the working segment of a working path adjacent to the segmentation node, if a link is adjacent to its intermediate node, the link is not eligible for protection of the segmentation node. This is also ensured by constraints (5.50). The failure of a node affects all working segments through it and all working paths segmented at this node. Constraints (5.51) state that one unit protection flow can only protect one unit disrupted working segments or paths. Constraints (5.52) say that a segmentation node of a working path can be protected by the current p-cycle only if one of its adjacent working segments of the working path is also protected by the current p-cycle.

The following block of constraints is developed for determination of the number of transponders and EXC ports required by the on-cycle switching nodes.

$$y_v^j \geq \sum_{\ell \in \omega(v_s^1)} x_s^{\ell j} + \sigma_v^s - 1 \qquad v \in V,\ s \in S,\ j \in J \tag{5.53}$$

$$y_{v'}^j \geq \sum_{\ell \in \omega(v_{pv}^1)} x_{pv}^{\ell j} + \sigma_{v'}^{pv} - 1 \qquad v, v' \in V,\ v' \neq v, p \in P,\ j \in J \tag{5.54}$$

$$\sum_{j \in J} y_v^j \geq \rho_{ss'}^v \Big(\sum_{\ell \in \omega(v_s^1)} \sum_{j \in J} x_s^{\ell j} + \sum_{\ell \in \omega(e_{s'}^1)} \sum_{j \in J} x_{\ell j}^{s'} \Big) \qquad v \in V, s, s' \in S, s \neq s' \tag{5.55}$$

For a one-unit working segment (resp. one unit traffic through a segmentation node) protected by the current Np-cycle, there exists a one-unit on-cycle protection flow for recovery of the segment (resp. the segmentation node). Constraints (5.53) (resp. (5.54)) say that each end node of such one-unit protection flow must be equipped with a transponder together with an EXC port. Constraints (5.55) say that, for two working segments (e.g., segments s and s' in Figure 5.8(a)) which share a link (e.g., $v_{\text{A}} - v_{\text{D}}$) adjacent to the common end node (e.g., v_{A}), if both of them are protected by the current unit cycle (e.g., c), then two pairs of transponders with EXC ports are required in this common end node (e.g., v_{A} as shown in Figure 5.8(b) and Figure 5.8(c)) for switching the affected working segments upon a failure (e.g., the failure of link $v_{\text{A}} - v_{\text{D}}$).

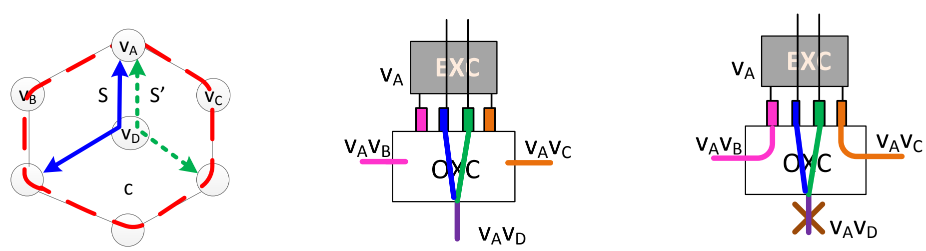

(a) (b) (c)

Figure 5.8: Two transponders required by a node

The last block of constraints is next present for determination of the equipment optical reach based on the current cycle under construction.

$$\sum_{\ell \in L} \mathrm{LEN}_\ell \, x_s^{\ell j} \; \leq \; R_{\mathrm{ULH}} \qquad s \in S, \; j \in J \tag{5.56}$$

$$\sum_{\ell \in L} \mathrm{LEN}_\ell \, x_{pv}^{\ell j} \; \leq \; R_{\mathrm{ULH}} \qquad p \in P, \; v \in V_p^*, \; j \in J \tag{5.57}$$

$$\sum_{m \in M} t_m^{vj} \; = \; 1 \qquad v \in V, \; j \in J \tag{5.58}$$

$$\sum_{m \in M} R_m \, t_m^{vj} \; \geq \; \sigma_v^s \sum_{\ell \in L} \mathrm{LEN}_\ell \, x_s^{\ell j} \qquad v \in V, s \in S, \; j \in J \tag{5.59}$$

$$\sum_{m \in M} R_m \, t_m^{v'j} \; \geq \; \sigma_{v'}^{pv} \sum_{\ell \in L} \mathrm{LEN}_\ell \, x_{pv}^{\ell j} \qquad p \in P, v \in V_p^*, v' \in V, j \in J \tag{5.60}$$

$$\sum_{m \in M} t_m^{\ell} = x_\ell \qquad \ell \in L \tag{5.61}$$

$$t_m^{\ell} \; \geq \; x_s^{\ell j} + \sigma_v^s \, t_m^{vj} - 1 \qquad \ell \in L, \; m \in M, \; s \in S, v \in V, \; j \in J \tag{5.62}$$

$$t_m^{\ell} \; \geq \; x_{pv}^{\ell j} + \sigma_{v'}^{pv} \, t_m^{v'j} - 1 \qquad \ell \in L, \; m \in M, \; p \in P, v \in V_p^*, v' \in V, \; j \in J \tag{5.63}$$

Constraints (5.56) and (5.57) say that a protection segment length cannot be longer than ULH optical reach (3000km), which is the longest optical reach of equipment available in the NOBEL cost model. Constraints (5.58) ensure that a transponder can only be with one type of optical reach. Constraints (5.59) and (5.60) say that a transponder optical reach should meet the associated protection segment length. If a transponder on a switching node is shared by several working segments for access to the current cycle under construction, the transponder optical reach should meet the associated longest protection segment length. Constraints (5.61) say that the on-cycle link equipment can only be with one kind of optical reach. Constraints (5.62) (resp. (5.63)) say that if link ℓ is used to protect working segment

s (resp. segmentation node v of working path p), then optical reach of link equipment should match the associated protection segment length. If link ℓ is shared for protection of several disjoint working segments (resp. segmentation nodes of working paths), the link equipment optical reach should meet the longest protection segment length.

Enhancing the Solution Process

In order to speed up the CG-based solution process, as illustrated in Fig. 5.9, we propose the following two techniques to facilitate the calculation of columns (configurations). The first one lies in the solution of successive MILP (mixed integer linear program) pricing problems rather than the original ILP one to generate a configuration. The second one relies on the decomposition of the pricing problem into two pricing problems, as in [RJ12].

Solution of the pricing problem model In order to speed up the computation of a new configuration (i.e., solution of the pricing problem), we solve a sequence of MILP pricing subproblems. Each MILP pricing problem originates from the original ILP pricing problem by re-defining temporarily the domains of some integer variables, with the following procedure:

Step 1. The first MILP pricing subproblem is deduced from the original pricing problem by keeping as integer the cycle flow x_ℓ and segment protection flow $x_s^{\ell j}$ while temporarily redefining the other variables as continuous variables. We then solve the resulting MILP, and fix the values of x_ℓ and $x_s^{\ell j}$ to their integer optimal values in the MILP.

Step 2. We next define a second MILP pricing subproblem, starting again from the original pricing problem with the variable setting as defined at the end of the solution of the first MILP, and then maintaining as integer variables the node-protection flow $x_{pv}^{\ell j}$ and switching node flow y_v^j variables, while temporarily redefining the other variables as continuous variables. We then solve the resulting MILP, and fix the values of $x_{pv}^{\ell j}$ and y_v^j to their integer optimal values after solving the second MILP pricing subproblem.

Step 3. We next solve the original pricing problem with the above fixed integer values for variables x_ℓ, $x_s^{\ell j}$, $x_{pv}^{\ell j}$ and y_v^j, and obtain integer values for all variables. Thereby, we obtain a new configuration.

The above iterative technique allows to go around the scalability issues of solving the original pricing problem. While it corresponds to a heuristic method, it allows to significantly speed up the overall solution process.

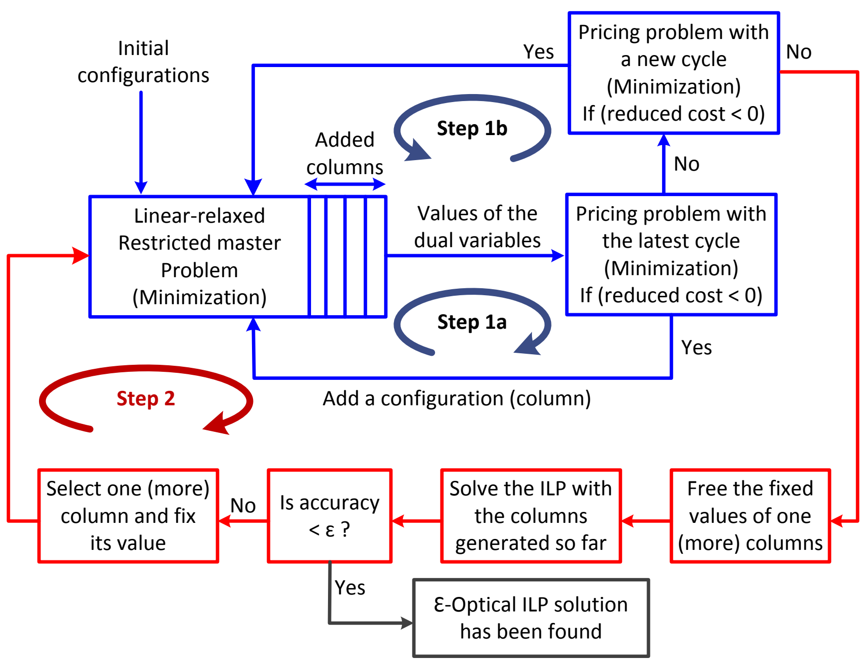

Figure 5.9: Classical CG and ILP solutions

Decomposition of the pricing problem Based on the observation that the same cycle may be used in different configurations, we then first calculate the augmenting configurations using the cycle which has been used in the latest generated configuration. This process is iterative, as shown by **Step 1a** in Fig. 4.8. Note that the calculation of a configuration with a given cycle can be greatly accelerated as it suggests that the first group of constraints of the pricing problem disappears. If no such augmenting configuration can be found, we solve the complete pricing problem, which includes the first group of constraints, i.e., the search of a cycle. This iterative process is illustrated by **Step 1b** in Fig. 4.8.

We observe, in practice, that very few complete pricing problems need to be solved. Usually, their number is of the order of the number of distinct cycles among the overall set of configurations. In this way, we can significantly speed up the CG algorithm.

How to Get an Optimal (near Optimal) Integer Solution After reaching the optimal solution of the linear relaxation of an ILP model, we need to calculate an integer solution, ideally an optimal one. When a column generation solution method is used, one must use a branch-and-price method (see, e.g., [BJN+98]) in order to guarantee reaching an optimal integer solution. However, it requires some effort in order to identify an efficient and scalable branching scheme, see, e.g., [BJN+98].

Note that, With the technique described in Section 5.5.2 for solving the pricing problem, we only get an approximation (indeed a lower bound) of $z^{\star}_{\text{LP}}$, denoted by $\tilde{z}_{\text{LP}}$, so that the accuracy is estimated by:

$$\varepsilon' = \frac{\widetilde{z}_{\text{ILP}} - \tilde{z}_{\text{LP}}}{\tilde{z}_{\text{LP}}}.$$

If the accuracy is less than ϵ (or ϵ'), we stop the solution process and obtain an ϵ- or an ϵ'-optimal ILP solution. Otherwise, as illustrated by **Step 2** in Fig. 4.8, we attempt to obtain a better ILP solution with the following process: we fix some integer variables (columns) to their values in the last obtained ILP solution, and go on iterating with the CG algorithm on the remaining 'free' variables in order to generate more configurations, and proceed again with the search of an ILP solution using the enhanced set of configurations.

5.6 Minimum CAPEX Designs of Segment- and Path p-cycles

5.6.1 Segment p-Cycle Design

With respect to the segment p-cycle design, the objective is the same as in the segment Np-cycle design in Section 5.5, i.e., minimization of CAPEX for p-cycle deployment such that all working segments are protected against a single failure. As in the design of segment Np-cycles, we develop a CG model which consists of the master problem and the pricing problem. The master problem takes responsible for the selection of the configurations (segment p-cycles) which are produced by the pricing problem, one at each iteration.

The configuration c is defined by a cycle and the protected working segments. The configuration c cost, COST_c is defined as the overall cost of on-cycle transponders and EXC ports. A configuration c can be formally represented by a vector $(a_s^c)_{s \in S}$ and a matrix $(t_{\ell m}^c)_{m \in M, \ell \in L}$. The elements $a_s^c \in \{2, 1, 0\}$ and $t_{\ell m}^c \in \{1, 0\}$ hold respectively the same definitions as those in Sec. 5.5.2.

The master problem model is with the same objective function as shown in (5.36), and is subject to constraints (5.37) and (5.39) - (5.43).

Regarding the pricing problem, the objective is to minimize the so-called reduced cost, formulated as follows.

$$\overline{\text{COST}}_c = \overbrace{\sum_{j \in J} \Big(\sum_{v \in V} \sum_{m \in M} \text{COST}_m^{\text{TP}} \, t_m^{vj} \, y_v^j + \sum_{v \in V} \text{COST}_{\text{EP}} \, y_v^j \Big)}^{\text{COST}_c} - \sum_{s \in S} u_s \overbrace{\sum_{\ell \in \omega(v_s^1)} \sum_{j \in J} x_s^{\ell j}}^{a_s^c}$$
$$+ \sum_{\ell \in L} u_\ell^2 \, t_{\text{ULH}}^\ell + \sum_{\ell \in L} u_\ell^1 \, (t_{\text{ULH}}^\ell + t_{\text{ELH}}^\ell) + \sum_{\ell \in L} \sum_{m \in M} u_\ell^0 \, t_m^\ell$$

where, the notations are defined as in Sec. 5.5.2.

The pricing problem consists of four blocks of constraints. The first block defines a simple cycle by the constraints (3.9) - (3.11). The second block is facilitated by constraints (5.20) - (5.28) for identification of the working segments which can be protected by the current cycle. The third block of constraints is used for determination the number of transponders and EXC ports required for protection switching. This block comprises constraints (5.53) and (5.55). The last block is formulated to settle on-cycle transponder optical reach, and possible equipment optical reach of on-cycle links. This block encompasses constraints (5.56), (5.58), (5.59), (5.61) and (5.62).

5.6.2 Path p-Cycle Design

Recall that a working segment is a set of contiguous links along a working path. If a segment covers all links of a working path, the segment is equivalent to the working path. Therefore, if we take each working path as one working segment, we can exploit the optimization model for the segment p-cycle design in the previous section for path p-cycle design. Note that path p-cycles are designed in such a way that overall CAPEX is minimized with 100% guranteed survivability against a single link/node failure.

5.7 Calculation of Failure Recovery Times

In this section, we study the estimation of the recovery time of p-cycle schemes from a single link/node failure. The optical recovery time refers to the time difference between the instant at which the failure occurs and the instant when the affected traffic arrives from protection paths.

For shared (segment) protection approaches, the computation of the recovery time is exploited in [THV$^+$08, Ram08]. There, protection paths are cross connected after a failure happens. For link-based pre-configured protection approaches, e.g., link p-cycles, the formulation of the recovery time is studied in [HS07,SJ11]. We next propose the new formulas respectively for the calculation of the recovery time under protection of segment p-cycles, path p-cycles and segment Np-cycles. Let us introduce the following new notations before present these new formulas.

V_s^* Intermediate node set of working segment s.

L_s, L_p Link set of working segment s and of working path p respectively.

$L_s(v, v')$ Link set between two nodes v and v' along a segment s.

$L_p(v, v')$ Link set between two nodes v and v' along a path v.

$\alpha_{pv}^1, \alpha_{pv}^2$ Two adjacent nodes of segmentation node v of working path p.

$a_{s\ell}^c$ = 1 if the on-cycle link ℓ is used to protect working segment s, 0 otherwise.

$a_{pv\ell}^c$ = 1 if the on-cycle link ℓ protects segmentation node v of working path p, 0 otherwise.

$T_{\mathbf{d}}$ Failure detection time. A failure is detected by the adjacent nodes through periodical exchange of the packet, say, 'Hello'. Therefore, we assume that T_{D} is constant, and set as 4 ms [Ram08].

$T_{\mathbf{p}}$ Message processing and forwarding time at a node. Without loss of generality, we assume that each node has the same processing capability and set T_{P} as 4 ms [Ram08].

$T_{\mathbf{g}}^{\ell}$ Signal propagation time on link ℓ, set as 5 μs per kilometer.

$T_{\mathbf{sw}}$ Traffic switching time, the time needed by a node (an EXC) for switching traffic from a working segment (path) to a protection segment (path). We assume that each node needs the same switching time, i.e., 500 μs [Ram08].

Upon a link failure, the end nodes (the adjacent nodes) of the failed link (the failed node) detect the failure. Then, these end nodes (the adjacent nodes) generate failure notification message and send it to the switching nodes along the affected working segments or paths. Let $T_{\mathrm{N}}^{s\ell'}$ be the failure notification time, i.e., the time difference between the instant at which the failure is detected and the instant at which the switching nodes get the failure notification message.

Recall that p-cycles are pre-configured, i.e., the OXCs en route are pre-cross-connected. Upon getting failure notification message, the switching nodes can therefore automatically switch the affected traffic to the corresponding protection segments (paths). Let T_{G}^{s} denote the overall propagation time required for the failed traffic transmission along the protection segments.

Let $RT_s^{\ell'}$ (RT_s^{v}) be the overall recovery time of segment s from the failure of a single link ℓ (node v) en route. $RT_s^{\ell'}$ (RT_s^{v}) is calculated as the summation of the recovery time of each unit working segment in case of the link ℓ' failure.

The network-wide *average recovery time* is defined as the summation of the overall recovery time of each segment (path) upon each link or node failures divided by the number of all possible failure scenarios of each unit working segment (path). The network-wide *maximal recovery time* is the maximum of the recovery time of each unit working segment (path) over all possible combinations of segments (paths) and links and nodes.

5.7.1 Segment- and Path p-Cycles

For working segment s carrying D_s units of demands, the overall recovery time $RT_s^{\ell'}$ from link ℓ' failure is calculated as follows.

$$RT_s^{\ell'} = D_s \times (T_{\mathrm{D}} + T_{\mathrm{N}}^{s\ell'} + T_{\mathrm{SW}}) + T_{\mathrm{G}}^{s}$$

where, for each unit of working segment s, the failure notification time $T_{\mathrm{N}}^{s\ell'}$ is next formulated.

$$
\begin{aligned}
T_{\mathrm{N}}^{s\ell'} = \quad & \max\{\left| L_s(e_s^1, e_{\ell'}^1)\right| \times T_{\mathrm{P}} + \sum_{\ell \in L_s(e_s^1, e_{\ell'}^1)} T_{\mathrm{G}}^{\ell} \, \mathrm{LEN}_{\ell}, \\
& \left| L_s(e_{\ell'}^2, e_s^2) \right| \times T_{\mathrm{P}} + \sum_{\ell \in L_s(e_{\ell'}^2, e_s^2)} T_{\mathrm{G}}^{\ell} \, \mathrm{LEN}_{\ell}\}
\end{aligned}
$$

After the affected segment s is switched to segment p-cycles, total traffic propagation time T_{G}^{s} along protection segments can be calculated as follows.

$$
T_{\mathrm{G}}^{s} = \sum_{c \in C} \sum_{\ell \in L} T_{\mathrm{G}}^{\ell} \, \mathrm{LEN}_{\ell} \, a_{s\ell}^{c} \, z_c
$$

With segment p-cycles, the network-wide *average recovery time* from a single link failure is calculated as:

$$
\frac{\sum_{s \in S} \left(\sum_{\ell \in L_s} RT_s^{\ell} + \sum_{v \in V_s^*} RT_s^{v} \right)}{\sum_{s \in S} \left(\left| L_s \right| + \left| V_s^* \right| \right) \times D_s} \tag{5.64}
$$

Working segments are generalization of working paths. Therefore, we can easily derive from the formula (5.64) a new formula for calculation of the network-wide *average recovery time* under protection of path p-cycles.

5.7.2 Segment Np-Cycles

Recall that segment Np-cycles are segment p-cycles with full node (segmentation node) protection. Thus, the recovery time under protection of segment Np-cycles is calculated in the way similar to the formula (5.64). In contrast with segment p-cycles, we also need to take into account the overall recovery time RT_p^{v} upon the failure of a segmentation node v

of a working path p. RT_p^v is computed as follows.

$$RT_p^v = D_p \times (T_{\text{D}} + T_{\text{N}}^{pv} + T_{\text{SW}}) + T_{\text{G}}^{pv}$$

where, T_{N}^{pv} is the failure notification time computed as:

$$T_{\text{N}}^{pv} = \max\{\left| L_p(v_{pv}^1, \alpha_{pv}^1)\right| \times T_{\text{P}} + \sum_{\ell \in L_p(v_{pv}^1, \alpha_{pv}^1)} T_{\text{G}}^{\ell} \, \text{LEN}_\ell, \\ \left| L_p(\alpha_{pv}^2, v_{pv}^2) \right| \times T_{\text{P}} + \sum_{\ell \in L_p(\alpha_{pv}^2, v_{pv}^2)} T_{\text{G}}^{\ell} \, \text{LEN}_\ell \}$$

and T_{G}^{pv} represents the propagation time of the recovered traffic along Np-cycles upon the failure of segmentation node v of working path p. The formula for T_{G}^{pv} computation is next present.

$$T_{\text{G}}^{pv} = \sum_{c \in C} \sum_{\ell \in L} T_{\text{G}}^{\ell} \, \text{LEN}_\ell \, a_{pv\ell}^c \, z_c$$

With respect to segment Np-Cycles, the network-wide *average recovery time* is then calculated as follows.

$$\frac{\sum_{s \in S} (\sum_{\ell \in L_s} RT_s^\ell + \sum_{v \in V_s^*} RT_s^v) + \sum_{p \in P} \sum_{v \in V_p^*} RT_p^v}{\sum_{s \in S} (\left| L_s \right| + \left| V_s^* \right|) \times D_s + \sum_{p \in P} \sum_{v \in V_p^*} \left| V_p^* \right| \times D_p} \tag{5.65}$$

5.8 Numerical Results with Minimum Bandwidth Usage Design

In this section, the numerical results are obtained with the minimum bandwidth usage design model proposed in Section 5.4 for protection against any single link/node failures. Based on these results, we evaluate the performances of the proposed the segment Np-cycles protection scheme. We compare it with the segment p-cycle scheme and the path p-cycles (PpCycle) with respect to: the capacity redundancy, the dual link failure restoration ratio (R_2), the number of distinct cycles vs. the total number of one unit p-cycle occurrences and the average number of links per cycle. Segment p-cycle, as a benchmark of the spare capacity usage, is designed with the model proposed in Section 3.3 such that the spare capacity is minimized with 100% guaranteed survivability against any single link failure. Path p-cycle is designed using the model in Section 4.5 for full link and node protection.

Data Instances

Four different topologies have been used in our experiments and their main characteristics (number of nodes, number of links, and average node degree) are described in Table 5.2. For the traffic, as explained in Section 2.4, we first generated a set of requests with different granularities (OC-1, OC-3, OC-12 and OC-48) such that for each pair of nodes, the number of requests is a random number in $\{1, 2, 3, 4, 5\}$ for each granularity. Next, we use the algorithm of [Bou05, BJH11] to generate lightpaths with a set of working segments of granularity either OC-48 (reference unit in our experiments) or OC-192 ($4 \times$ the reference unit). The overall number of requests, as well as the overall number of working segments are given in the last two columns of Table 5.2. The average number of demands per working segment varies between 5.6 and 6.8 depending on the data instance with a range of values between 4 and 20.

Table 5.2: Network instances

Networks	# nodes	# links	Avg. node degree	# requests	# working segments
NSF [HBB+04]	14	21	3.0	91	68
GERMANY [HBB+04]	17	26	3.1	136	102
BELLCORE [SG03]	15	28	3.7	105	76
EON2004 [BHJ06]	20	39	3.9	190	126

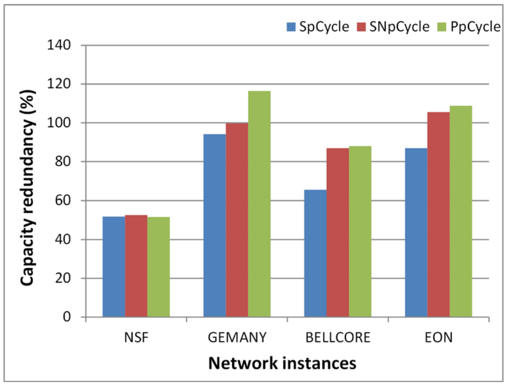

(a) Capacity redundancy

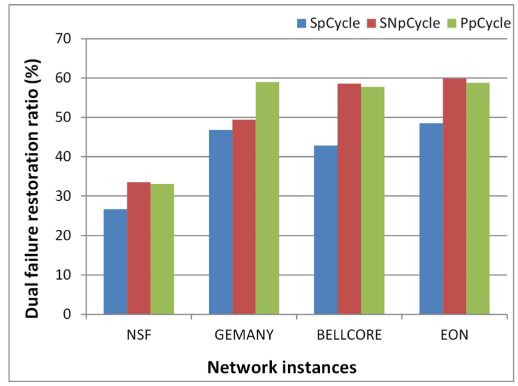

(b) Restoration ratio of dual failures

Figure 5.10: Comparisons of the solution performances

Capacity Redundancy

Figure 5.10(a) presents the comparisons for the capacity redundancy of the three protection schemes: segment p-cycles (SpCycle), segment Np-cycles (NSpCycle) and path p-cycles (PpCycle) over four network and traffic instances. Overall, segment Np-cycles require more spare capacity than segment p-cycles for the protection of segment endpoints. The differences for the capacity redundancy vary between ∼0.65% to ∼18.63%. Segment Np-cycles require less spare capacity than path p-cycles for the GERMANY instance, a similar amount for the BELLCORE and EON2004 instances, and less for the NSF instance. In other words, it varies from one instance to the next. In general, segment p-cycles are more capacity efficient than path p-cycles except for NSF. As expected, segment Np-cycles require more spare capacity than segment p-cycles, again the difference varies quite a lot from one instance to the next.

Dual Link Failure Restoration Ratio

In Figure 5.10(b), we compute the dual link failure restoration ratio (R_2), i.e., the percentage of double failures against which the network is protected, using the segment/path

p-cycles build for protection against single link/node failures. In general, segment Np-cycles offer higher R_2 value than segment p-cycles. R_2 differences range from ~0.98% to ~13.53%. Segment Np-cycles also outperform path p-cycles in terms of the R_2 value except for GERMANY instance.

Number of Distinct and Overall Copies of Cycles

In Table 5.3, we compare the number of distinct cycles and overall number of copies of p-cycles for four network instances. We observe that, whatever the protection scheme is employed, the number of distinct cycles is small in comparison of the overall number of copies, meaning an easy management of the p-cycles (several copies only differ by their wavelength assignment). Except for the GERMANY instance, segment Np-cycles have the largest number of cycle occurrences, larger than for the segment p-cycles (as expected) and slightly more than path p-cycles.

Table 5.3: Number of distinct/overall number of copies of cycles

Networks	segment p-cycles	segment Np-cycles	path p-cycles
NSF	23 (153)	25 (171)	23 (166)
GEMANY	22 (389)	21 (390)	30 (472)
BELLCORE	28 (210)	44 (435)	41 (279)
EON2004	44 (398)	50 (494)	72 (481)

Size of the p-Cycles

In Table 5.8, we present the average number of links in the cycles required by the different p-cycle schemes, for four networks. Those are the numbers obtained without setting any limit on the length of the cycles. The average cycle size of segment Np-cycles is never the largest one, and it is twice (50% of the cases) the smallest one. More investigation are needed in order to clearly identify the parameters that influence the length of the p-cycles (such as, e.g., the connectivity of the graphs or the traffic density).

Networks	Segment p-Cycles	Segment Np-Cycles	Path p-Cycles
NSF	10.1	8.8	8.7
GERMANY	12.2	11.8	11.9
BELLCORE	10.5	9.8	9.8
EON2004	10.4	10.2	10.1

5.9 Numerical Results with Minimum CAPEX Design

In this section, we present the numerical results respectively with the minimum CAPEX design models proposed in Sections 5.5.1 and 5.5.2. Specifically, in Section 5.9.1, we evaluate the efficiency of the proposed CAPEX minimization model in Section 5.5.1. Also, we evaluate the performances of the efficiency of Np-cycles from the CAPEX point of view by comparison of it with segment p-cycles. In Section 5.9.2, we evaluate the performances of the new proposed segment Np-cycles based on the CG model present in Section 5.5.2. There, we compare Np-cycles with segment p-cycles and path p-cycles designed by the models proposed in Section 5.6.

The integer solutions of the master problem have been obtained with the *accuracy* (calculated with the formula (3.35)) smaller than 10% for both the CG model I and II.

Data Instances

Four different network topologies have been used in our experiments. For the traffic carried on each network, with the algorithm of [Bou05, BJH11], the set of working segments was obtained with a normalized line rate (OC-192, 10Gb/s) to match the equipment bit rate in [HGMS08]. For each node pair, we generated a random number (between 1 and 50) of requests for each granularity in {OC-1, OC-3, OC-12 and OC-48}. For the working segment set obtained for each network, we present in Table 5.4 the distinct number of segments, the overall number of segments, and the maximal segment length (km). We also present in the table the distinct (resp. overall) number of the demands with the line rate OC-192.

We made use of the cost parameters in [HGMS08] for the p-cycle installation CAPEX, and assumed that each fiber link carries 80 wavelength channels.

Table 5.4: Network instances

	ATLANTA [OPTW07]	GERMANY [HBB+04]	BELLCORE [SG03]	NJLATA [YAK03]
# distinct segments	70	88	77	48
# overall segments	1250	1221	734	628
Maximal seg. len.	446.4	712	587.7	1,580
# distinct w-paths	105	136	105	55
# overall w-paths	832	808	553	567

5.9.1 Numerical Results of Column Generation model I

We compare the CG model I with the heuristic (Np-cycles-BWD), where the CAPEX is calculated a posteriori, using the solutions of the design of segment Np-cycles in Section 5.4. Therein, again, the objective is to minimize the spare capacity usage. With segment Np-Cycles-BWD, we set the network-wide equipment reach to the least one such that there always exists a feasible and less costly solutions. Note that the heuristic Np-cycles-BWD follows the CAPEX computation method of [GGC+09] for p-cycles.

Moreover, we evaluate the extra CAPEX required by the segment Np-cycles (with full node protection) in comparison with the CAPEX of the classical segment p-cycles (no guaranteed node protection for the intermediate segment endpoints). Both protection schemes are also compared with respect to their capacity redundancy and their average cycle lengths. In addition, we also present the transponder optical reach distribution in the solutions of segment Np-cycles.

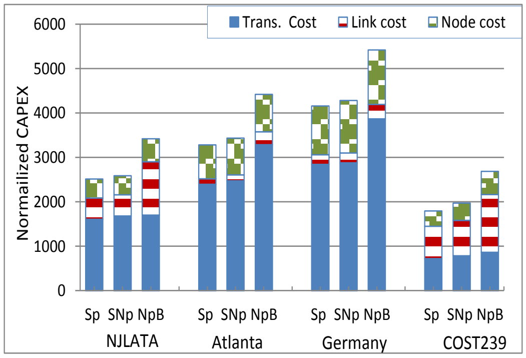

(a) CAPEX cost

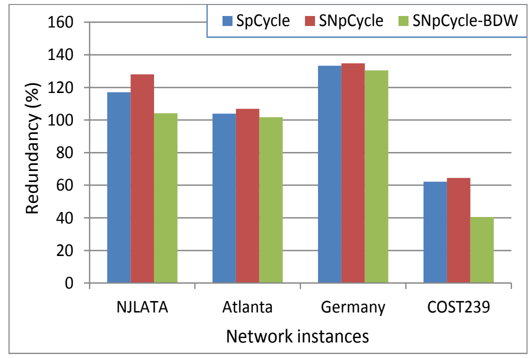

(b) Redundancy

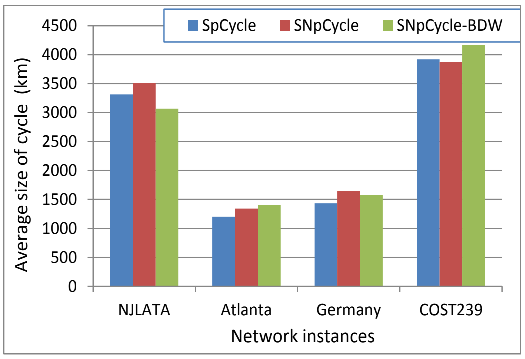

(c) Average cycle size

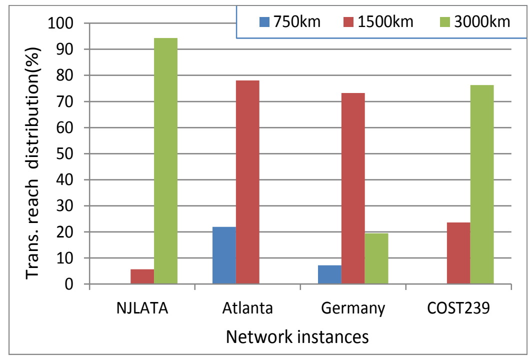

(d) Reach distribution

Figure 5.11: Comparative Performances

CAPEX cost

Figure 5.11(a) describes for the four networks the CAPEX of the solutions from the three different segment protection schemes. For each network, the three columns represent in turn the CAPEX from the designs segment p-Cycles (Sp), segment Np-Cycles (SNp) and segment Np-Cycles-BWD (NpB). Each column contains three parts: the transmission cost, the link cost and the node cost.

Overall, the segment Np-Cycle design outperforms the segment Np-Cycle-BWD in terms of the CAPEX. The cost savings of segment Np-Cycle over segment Np-Cycle-BWD vary from ∼30% to ∼37%. They mainly come from the increased sharing of the transponders and the selection of transponders with an adapted optical reach (shown in Figure 5.11(d)) in the segment Np-Cycle design. On the other hand, segment Np-cycles only require a very marginal extra CAPEX (from ∼3% to ∼10%) for full node protection in comparison with segment p-cycles for link protection. In addition, Figure 5.11(a) shows that the transmission cost is the dominating component of the CAPEX for each network excluding COST239.

Capacity redundancy

From the capacity redundancy point of view, Figure 5.11(b) presents the comparisons of the solutions from segment p-Cycle, segmentNp-Cycle and segment Np-Cycle-BWD, respectively, over four network instances. We can observe that, for each network instance, segment Np-Cycle-BWD is the most capacity efficient among these three designs, which in accordance with the objective of the segment Np-Cycles-BWD. The redundancy differences between the solutions of segment Np-Cycles and segment Np-Cycles-BWD range from ∼4% to ∼24%. In contrast with segment p-cycles, except for NJ LATA,segment Np-cycles with no more than 3% extra redundant spare capacity can provide full node protection.

Length of cycles

Figure 5.11(c) provides the average length of cycles in the designs of segment p-cycles, Np-cycles and Np-cycles-BWD, respectively. The average length of the segment Np-Cycles is longer than the one of segment Np-Cycles-BWD for NJLATA and GERMANY, while it is shorter for Atlanta and COST239. In contrast with segment p-Cycles, the average length of the segment Np-Cycles is longer except for COST239.

Reach distribution

Figure 5.11(d) shows the optical reach distribution of the transponders in the solutions of the design of segment Np-Cycles for the four network instances. For the networks NJLATA and COST239, where the maximal length of working segments is larger than 1,500km, there is no transponder with LH (750km) optical reach, and the vast majority of transponders is with ULH reach due to the transponder sharing among segments. For the other two networks Atlanta and GERMANY, where the maximal length of segments is less than 750km, the transponders with the MTD 1,500km are the most numerous. There is no transponder in Atlanta with ULH reach. In GERMANY, ∼7% transponders are with LH reach while ∼20% are with ULH reach.

5.9.2 Numerical Results of Column Generation model II

In this section, we evaluate the performances of the new proposed segment Np-cycles based on the CG model present in Section 5.5.2. we compare segment Np-cycles (with full node protection) with the classical segment p-cycles (no guaranteed protection for the intermediate segment endpoints) and path p-cycles (with full node protection). Segment p-cycles and path p-cycles are respectively designed by the models proposed in Section 5.6.

The performance metrics considered consist of the failure recovery time, the CAPEX cost, the capacity redundancy and the average cycle length. With these metrics, In addition, we also examine the optical reach distribution of transponders in the solutions of segment Np-cycle design. The network-wide maximal recovery time and the average recovery time were calculated using the formulas present in Section 5.7. The calculation of the recovery time is based on the respective solutions of the optimization models for designs of segment p-cycles, Np-cycles and path p-cycles.

Recovery time

Figure 5.12(a) (5.12(b)) presents the comparisons of the maximum recovery time (the average recovery time) among segment p-cycles, Np-cycles and path p-cycles over the four network instances.

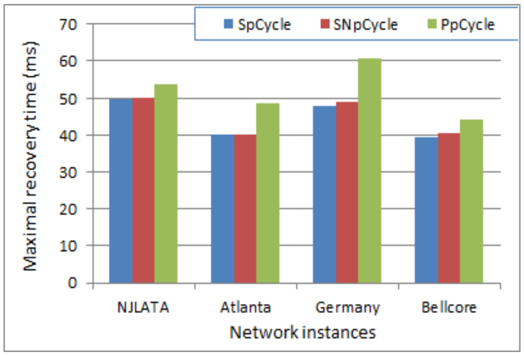

(a) Maximum recovery time

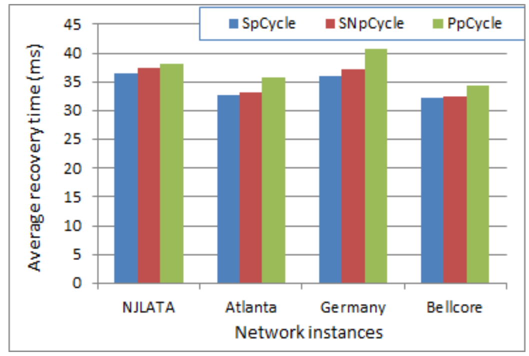

(b) Average recovery time

Figure 5.12: Recovery time comparisons

It is shown clearly that, for each data instance, segment Np-cycles and p-cycles require the shorter maximal recovery time and the average recovery time than path p-cycles. Therefore Np-cycles have faster recovery speed than path p-cycles. Segment Np-cycles reduce the maximum recovery time by 8% (NJLATA) to 25% (GERMANY) as shown in Figure 5.12(a), and the average recovery time by 2% (NJLATA) to 10 % (GERMANY) as shown in Figure 5.12(b). The recovery time reduction of segment Np-cycles is mainly due to the following two facts. The first one is that segment Np-cycle (p-cycle) protection approach requires the shorter failure notification time (see Section 5.7 for the definition) than path p-cycle approach. This is, in turn, because the working segment length is shorter than or equal to the associated working path length. The second one is that, as shown in Figure 5.13(c), the average size of segment p-cycles and Np-cycles are smaller than that of path p-cycles except for NJLATA. This translates to the shorter propagation delay along segment p-cycles (Np-cycles) than path p-cycles for traffic recovery against a single failure.

In comparison with segment p-cycles, segment Np-cycles involve very marginal extra recovery time for full link and node protection. This suggests that, Np-cycles hold the recovery speed comparable with segment p-cycles. For protection a set of segments against a single link or node failure, segment Np-cycles and p-cycles have the same notification time and the similar propagation time (see Figure 5.13(c)). The marginal extra recovery time comes from that for recovery from segmentation node failures in segment Np-cycles.

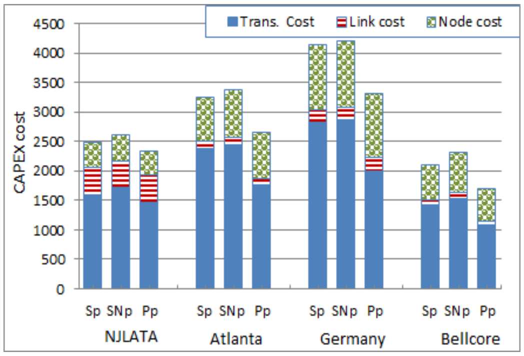

(a) CAPEX cost

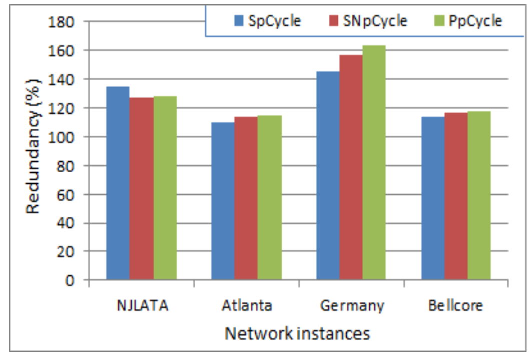

(b) Redundancy

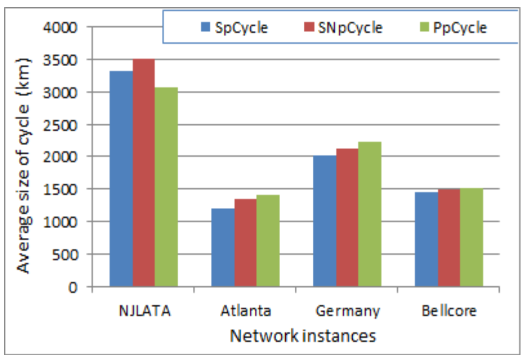

(c) Average cycle size

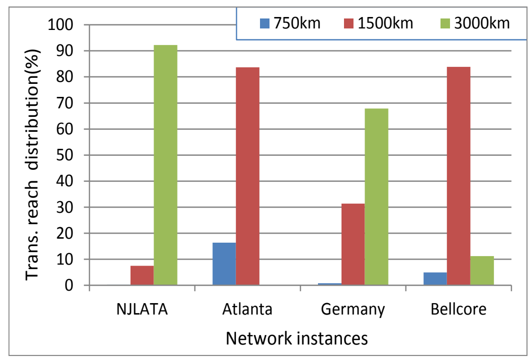

(d) Reach distribution

Figure 5.13: Comparative Performances

CAPEX cost

Figure 5.13(a) describes, over the four networks, the CAPEX comparisons of the solutions based on the three different p-cycle-based protection schemes. For each network, the three columns represent in turn the CAPEX of segment p-cycles (Sp), segment Np-cycles (SNp) and path p-cycles (Pp). Each column is made up of three components: the transmission cost, the link cost and the node cost. Among these components, the transmission cost is the dominant one in the p-cycle CAPEX.

We can observe that, for each network, segment Np-cycles only require a very marginal extra CAPEX (from ∼2% to ∼10%) for full node protection in comparison with segment

p-cycles (no protection guaranteed for segmentation nodes). This result keeps in line with what has been illustrated in Section 5.3. The reason is as follows. With segment Np-cycles, the transponders (e.g., the transponder on node v_{A} in Figure 5.4(b)) can be shared for access to Np-cycles between the related working segments ($v_{\text{A}} - v_{\text{C}} - v_{\text{D}}$) and segmentation nodes (v_{D}). Then, the transmission cost of segment Np-cycles is comparable to segment p-cycles.

On the other hand, path p-cycles are less costly than segment p-cycles (Np-cycles). The cost differences between path p-cycles and Np-cycles range from 12% to 35%. The main reason is that path p-cycles cut the transmission cost in constrast with segment Np-cycles for protection against a single link/node failure. The transmission cost savings of path p-cycles come from the fact that the less number of transponders is required for access to path p-cycles than that for access to Np-cycles. Specifically, based on path p-cycles, for each unit n-hop working path (consisting of n working segments), only two transponders are required by its two end nodes. However, with Np-cycles, at least $n+1$ transponders are required by the switching nodes (end nodes or segmentation nodes) on such n-hop path.

In addition, Figure 5.13(a) shows that, besides the transmission cost, for each protection scheme, the node (OADM/OXC) cost is the second CAPEX dominant component.

Capacity redundancy

From the capacity redundancy point of view, Figure 5.13(b) presents the comparisons of the respective solutions based on segment p-cycles, segment Np-cycles and path p-cycles, over four network instances. We can state that, for each network instance, except for NJLATA, segment p-cycles is the most capacity efficient among these three protection approaches. In comparisons with segment p-cycles, except for GERMANY, segment Np-Cycles requires no more than 3.2% extra redundant spare capacity for full node protection. On the other hand, segment Np-cycles outperform path p-cycles in terms of capacity efficiency in sparse networks.

Length of cycles

Figure 5.13(c) provides, over the four networks, the average cycle length from the respective solutions based on segment p-cycles, Np-cycles and path p-cycles. We can notice that, the average cycle length based on the segment Np-cycle solution is longer than that of segment p-cycles, while it is shorter than or equal to that of path p-cycles except for NJLATA.

Reach distribution

Figure 5.13(d) presents the optical reach distribution of the transponders in the solutions based on segment Np-cycles for the four network instances. In NJLATA and GERMANY, the transponders with long-haul (LH, 750 km) optical reach take no more than one percentage of the overall required transponders. The vast majority of transponders is with ultra-long-hual (ULH) optical reach. This is mainly because of the transponder sharing among segments and segmentation nodes. Also, this comes from the fact that, as shown in Table 4.1, the maximal length of the working segments is larger than 1,500 km (712 km) in NJLATA (GERMANY). For ATLANTA, where the maximal length of segments is less than 446 km, ∼84% transponders are with extra-long-haul (ELH) optical reach, no ULH transponder is required. For BELLCORE, ∼84% transponders are with ELH optical reach while ∼5% (resp. ∼11%) transponders are with LH (ULH) optical reach, where the maximum length of the working segments is 587.7 km.

5.10 Conclusion

In this chapter, we propose a new segment protection scheme based on p-cycles, called segment Np-cycles, which guarantee 100% protection against a single failure, whether it is a node or a link failure. From the viewpoint of minimization of bandwidth usage, although segment Np-cycles require more bandwidth than the regular segment p-cycles, the difference is not much in exchange of the additional protection for all nodes, including segment endpoints. In addition, depending on the network and traffic instances, they are sometimes more bandwidth efficient than path p-cycles.

We also developed a new CAPEX optimization model for the design of segment Np-cycles. It differs from the previous model for CAPEX minimum design of p-cycles by that the CAPEX minimization is embedded in the optimization model. The new CAPEX optimization model significantly outperforms a minimum bandwidth design with an a posteriori CAPEX calculation.

More importantly, with very marginal extra CAPEX and extra redundant spare capacity, segment Np-cycles can provide full node protection in comparison with segment p-cycles for link protection. Segment Np-cycles hold faster recovery speed than path p-cycles, although segment Np-cycles are more costly than path p-cycles.

Segment Np-cycles are therefore worth of interest within the context of multi-layer network design in order to address more failure recovery at the WDM layer.

Chapter 6

The Shortcut *p*-Cycle Scheme

6.1 Introduction

Although p-cycles represent an attractive protection approach, they have some limitations. One is related to the length of the recovery paths provided by the p-cycles even if, as found in [GS98], large p-cycles may be preferred in order to achieve a high capacity efficiency. Another is the presence of loop backs, which makes the recovery paths unnecessarily large. Long recovery paths lead to slower recovery speeds, and cause optical signal degradation en route. Moreover, the probability of survival from dual link failures is reduced as well.

In this chapter, we propose the shortcut Np-cycle protection scheme, which not only eliminates the loop backs in p-cycles, but identifies possible shortcuts in the protection paths while offering 100% guaranteed protection against any single link/node failures. As in p-cycle based schemes, shortcut Np-cycles define a pre-configured protection approach. Consider a working path and a related shortcut Np-cycle (i.e., a working path of which some links are protected by the shortcut Np-cycle). In the event of a single link/node failure, only the intersecting nodes of this path and the shortcut Np-cycle which are nearest to the the end nodes of the working path, perform real-time switching. Therefore, shortcut Np-cycles retain ring-like recovery speed. Shortcut Np-cycles can protect on-cycle and straddling intersecting segments of working paths. See Section 6.3 for the details.

Shortcut Np-cycles differ from FIPP p-cycles in that, for a given working path, they do not necessarily go through its two end nodes. Thereby, shortcut Np-cycles are more flexible than FIPP p-cycles for providing protection against single link/node failures. Moreover, with shortcut Np-cycles, the affected traffic is switched at the nodes nearest to the end nodes of working paths, thus, the recovery speed of shortcut Np-cycles is faster than the one of FIPP p-cycles. To design shortcut Np-cycles, we develop a scalable optimization model based on a large optimization tool, namely, column generation (CG) techniques, without requiring any offline candidate enumeration. Extensive experiments have been carried out in order to evaluate the performance of shortcut Np-cycles.

The rest part of this chapter is organized as follows. In Section 6.2, we illustrate the limitations of p-cycle schemes and then review the studies on the elimination of loop backs. In Section 6.3, we present our novel shortcut Np-cycle protection scheme. The optimization model for the shortcut Np-cycle design is presented in Section 6.4. Experimental results are discussed in Section 7.2 and conclusions are drawn in Section 6.6.

6.2 Shortcomings of p-Cycle Based Schemes

In this section, we first briefly illustrate the shortcomings of node p-cycles and FIPP p-cycles, followed by the literature review.

If no restriction is imposed on the length of the cycles, p-cycles tend to be quite long, which result in a high capacity efficiency. The restored paths are usually much longer than the primary paths. As a result, some links and nodes may be revisited, which give rise to

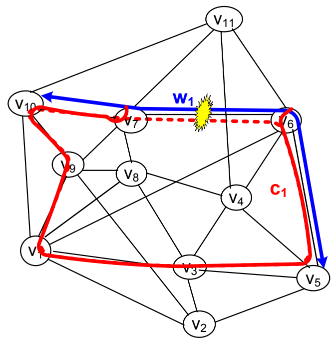

(a) A loop back

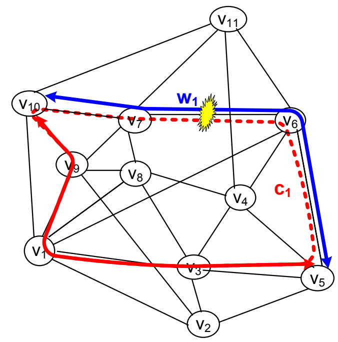

(b) Shortcut p-cycle

Figure 6.1: Illustration of a loop back and shortcut switching

loop backs in the recovery paths [AS08]. Figure 1(a) illustrates a loop back formed in a recovery path. Upon link $v_6 - v_7$ failure, the affected traffic is rerouted on the backup path along p-cycle c_1. Then, in the recovery path $v_5 - v_6 - v_5 - v_3 - v_1 - v_9 - v_{10} - v_7 - v_{10}$, besides the end nodes of the failed link $v_6 - v_7$, links $v_5 - v_6$ and $v_7 - v_{10}$, and nodes v_5 and v_{10} are visited twice. This leads to the formation of loop backs.

FIPP p-cycles are known to be more capacity efficient than link p-cycles in the context of protection against a single link failure [RJ08]. However, p-cycles have shorter recovery time. With respect to single node failures, it has been shown [JLR12] that depending on the network topology, FIPP p-cycles may be sometimes more capacity efficient, sometimes less capacity efficient than node p-cycles. In the sequel, we will shorten the term FIPP p-cycles to path p-cycles (there will be no confusion as we only consider failure independent mechanisms for path protection in this paper).

Path p-cycles are known to be more capacity efficient than link p-cycles in the context of protection against a single link failure [RJ08]. However, p-cycles have shorter recovery times. With respect to single node failures, however, it is shown in Chapter 4 that, depending on the network topology, path p-cycles may be sometimes more capacity efficient, sometimes less capacity efficient than node p-cycles, depending on the network topology.

Literature review

Grover and Scheffel [GS07] investigate whether loop backs in link-based protection schemes entail a significant capacity penalty. They develop an ILP model to design survivable networks based on link protection without worrying about loop backs. The resulting solutions of the ILP model are then analyzed, and some spare capacity is released by eliminating the loop backs. It is then shown that, loop backs lead to very small spare capacity penalty.

However, other authors [AS08, AS07] reached a different conclusion. Asthana and Singh [AS08, AS07] examine the removal of loop backs in p-cycle networks, i.e., networks where protection is ensured by p-cycles. Then, the loop backs in the resulting ILP solution are removed using a reconfiguration phase for the recovery paths. The experimental results show that considerable amount of spare capacity can be released and that the recovery path length can be also greatly reduced, a conclusion that is the opposite of [GS07].

All the above studies investigate the impact of the loop backs on the spare capacity using a 2-step solution scheme, in a context of single link failures. The present study explores the same question in a one step solution scheme for both single link and single node failures. More, some shortcuts are identified in the p-cycles in addition to the elimination of the loop backs.

6.3 Shortcut Np-Cycles: p-Cycles with No Loop Backs

As mentioned in Section 6.2, there may exist loop backs in the recovery paths based on link p-cycles. To remove such loop backs, and thus reduce the length of the recovery paths and decrease the signal attenuation, we propose the following shortcut Np-cycle protection scheme.

As p-cycles, shortcut Np-cycles define a fully pre-configured protection scheme. In a

p-cycle, for any given protected link, the two nodes where protection switching occurs are the endpoints of the protected link. In a shortcut Np-cycle, this is no more necessarily the case. Indeed, for a shortcut Np-cycle, and a subset of protected links belonging to a given working path, the two protection switching nodes are the common nodes of the working path and the p-cycle, which are nearest to the end nodes of the working path. Thereby, the links and nodes along the working path between these two switching nodes can be protected by the shortcut Np-cycle. As protection switching is performed in such nodes rather than in the end nodes of the failed link, accordingly, the entities of this protection scheme are called shortcut Np-cycles. The resulting protection scheme encompasses p-cycles in which loop backs have been removed.

With shortcut p-cycles as illustrated in Figure 1(b), upon link $v_6 - v_7$ failure, the protection switching nodes v_5 and v_{10} re-route the disrupted traffic on p-cycle c_1, and the recovery path, $v_5 - v_3 - v_1 - v_9 - v_{10}$, is free of any loop back. Indeed, the proposed shortcut p-cycles encompass p-cycles beyond the elimination of loopbacks, consider the example of Figure 2(b), where now link $v_8 - v_9$ can be protected.

Shortcut Np-cycles can protect on-cycle segments, straddling segments as well as hybrid segments of working paths. A segment is the consecutive link set along a working path. For a shortcut Np-cycle, a straddling segment is a working segment along a working path which has no common links and nodes with the p-cycle except for its two end nodes; while a hybrid segment is a segment which share some but not all links/nodes with the p-cycle. A one unit shortcut Np-cycle provides one protection flow unit for each on-cycle or hybrid working segment, while it offers two units of protection flows for each straddling segment.

Figure 6.2 illustrates a shortcut Np-cycle which protects a hybrid segment and a straddling segment with respect to a working path. Figure 2(a) shows that the working segment

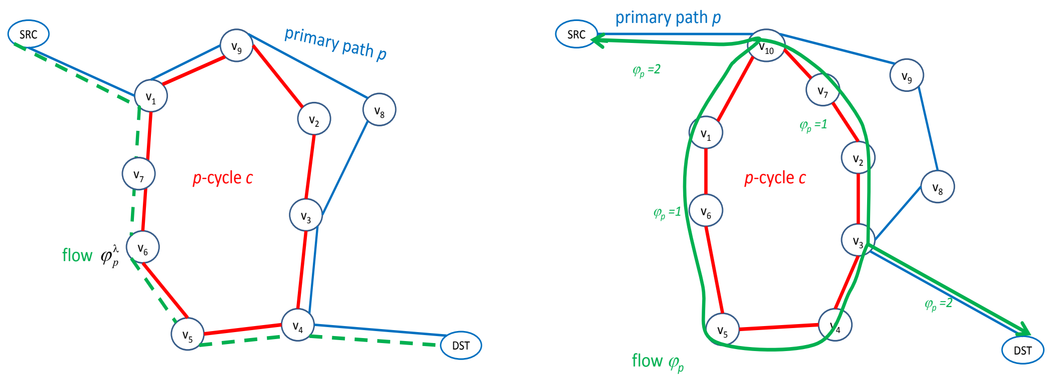

(a) A p-cycle with an enlarged protection (b) Case with a flow of 2 units

Figure 6.2: General shortcut p-cycles

$v_{10} - v_4$ along the primary path p, as a hybrid segment can be protected by p-cycle c. The primary path p drawn in blue line intersects p-cycle c at nodes v_{10}, v_3 and v_4. Then, the protection switching nodes are v_{10} and v_4 as they are nearest to the end nodes of the working path. Thereby, the working segment of path p between nodes v_{10} and v_4 can be protected by shortcut p-cycle c. Upon a link (resp. node), say, $v_3 - v_8$ (resp. v_8) failure, nodes v_{10} and v_4 switch the affected segment on p-cycle c, and the recovered path is thus rerouted on φ_p, SRC$-v_{10} - v_1 - v_6 - v_5 - v_4-$ DST.

A straddling working segment of a shortcut Np-cycle is illustrated in Figure 2(b). The working segment $v_3 - v_{10}$ of path p is a straddling segment for p-cycle c, which has two end nodes v_3 and v_{10} sitting on p-cycle c but shares no link with it. Shortcut Np-cycle c can offer segment $v_3 - v_{10}$ two units of protection flows. Upon a node, say, v_9 failure, shortcut Np-cycle c can offer two units of protection flows $v_{10} - v_1 - v_6 - v_5 - v_4 - v_3$ and $v_{10} - v_7 - v_2 - v_3$ to recover the affected traffic on the working segment $v_3 - v_{10}$.

6.3.1 Shortcut p-Cycles vs. Path p-Cycles vs. Node p-Cycles

In order to further understand the differences of shortcut Np-cycles with node p-cycles and path p-cycles, we consider an example using the BELLCORE network with three one unit demand requests, see Figure 3(a). Therein, the number on each link is the link geographical length [MK98], expressed in thousands of kilometers.

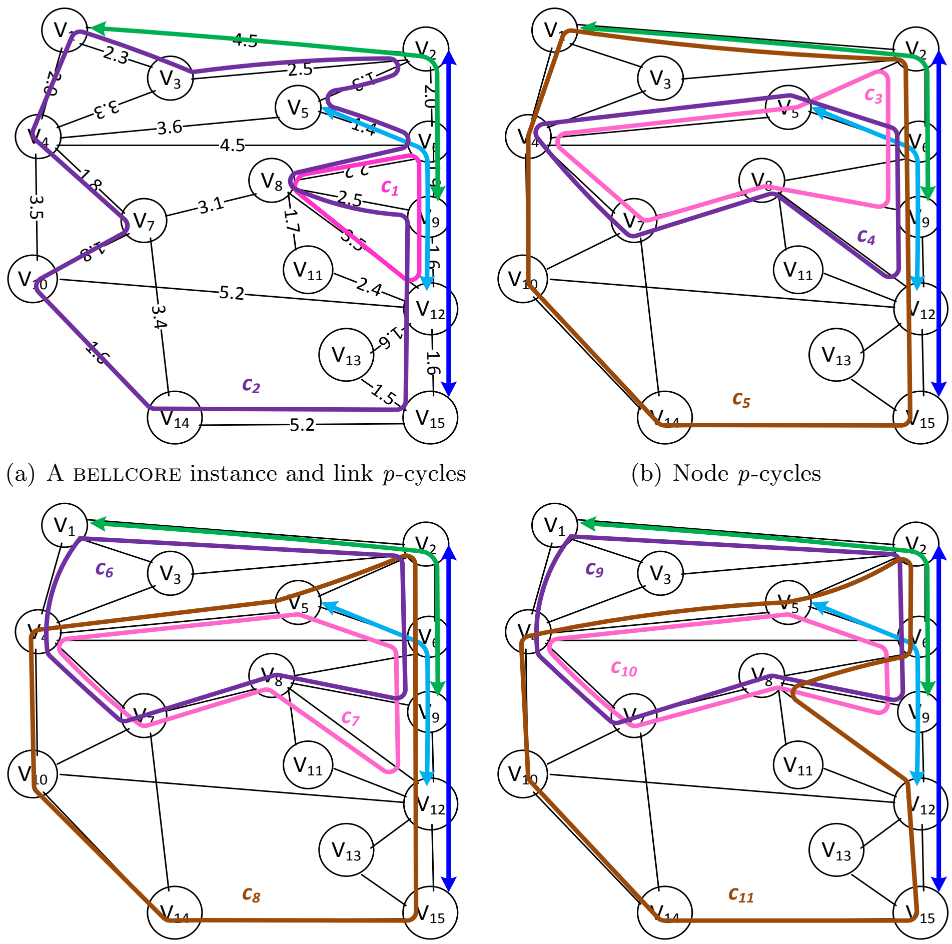

(a) A BELLCORE instance and link p-cycles (b) Node p-cycles

(c) FIPP p-cycles (d) Shortcut p-cycles

Figure 6.3: Illustration of different p-cycle-based protection schemes

Four protection schemes are illustrated in Figure 6.3: link p-cycles in Figure 3(a), i.e., the original p-cycle protection scheme against any single link failures, node p-cycle in Figure 3(b), path p-cycle in Figure 3(c), i.e., FIPP p-cycle with the required adaptations in order to guarantee node protection, and the new proposed shortcut Np-cycle in Figure 3(d).

To protect traffic against any single link failure, two link p-cycles, c_1 and c_2 as shown in Figure 3(a) are required, with a spare capacity requirement of 37. To protect against any single link/node failures, we need three node p-cycles, c_3, c_4 and c_5, different from c_1 and c_2, as depicted in Figure 3(b). The overall spare capacity cost is equal to 57. Regarding path p-cycles, three p-cycles c_6, c_7 and c_8 are also used, as shown in Figure 3(c), with a spare capacity equal to 57. These three path p-cycles differ from the node p-cycles although they are with the same capacity cost as the node p-cycles in this small example. If shortcut Np-cycles are used for protection, again, three p-cycles c_9, c_{10} and c_{11}, which differ from the previous p-cycles, are required with a space capacity cost of 56.6.

This example shows that, in comparison with link p-cycles, only designed for link protection, shortcut Np-cycles may require more spare capacity for node protection. However, with respect to node protection, shortcut Np-cycles require less spare capacity than node p-cycles and path p-cycles. This is due to the fact that shortcut Np-cycles can protect more failure scenarios than node p-cycles, and are more flexible for providing protection than path p-cycles. As will be explained in the sequel, shortcut Np-cycles are always more bandwidth efficient than node and path p-cycles. However, in comparison with link p-cycles, depending on the network topologies, shortcut Np-cycles may require more or less spare capacity in order to ensure full node protection.

6.4 A Column Generation Model

For a given working path $p \in P$ with two end nodes v_p^1 and v_p^2, let L_p be the set of links along path p.

6.4.1 Optimization Model: the Master Problem

The objective of the optimization model (the master problem) is to minimize the spare capacity usage of shortcut Np-cycles such that 100% survivability can be guaranteed against any single link/node failure. Note that, with respect to a working path, only its intermediate nodes are considered for protection against any single node failure.

The optimization model relies on a decomposition where the master problem (i.e., the model below) selects the potential shortcut Np-cycles together with the links/nodes they can protect, as generated by the pricing problem (see Section 6.4.2 for the details). A configuration (Shortcut Np-cycle) c contains a one unit cycle, and its set of protected links and nodes with respect to working paths. Formally, a configuration c is represented by:

vector $(a^c_\ell)_{\ell \in L}$	with $a^c_\ell = 1$ if link ℓ is on cycle c, 0 otherwise.
matrix $(a^c_{p\ell})_{p \in P, \ell \in L}$	with $a^c_{p\ell} = 1$ (resp. 2) if configuration c can recover one (resp. two) traffic unit(s) upon the failure of link ℓ of working path p, 0 otherwise.
matrix $(a^c_{pv})_{p \in P, v \in V}$	where $a^c_{pv} = 1$ (resp. 2) if configuration c provides one (resp. two) backup flow for protection of working path p against node v failure.

Let COST_c be the spare cost of configuration c, which is calculated as the overall spare capacity cost of the on-cycle links, i.e., $\text{COST}_c = \sum_{\ell \in L} \text{COST}_\ell a^c_\ell$.

The mathematical model is formulated as follows.

$$\min \quad \sum_{c \in C} \text{COST}_c \, z_c$$

subject to:

$$\sum_{c \in C} a^c_{p\ell}\, z_c \geq d_p \qquad p \in P,\, \ell \in L_p \tag{6.1}$$

$$\sum_{c \in C} a^c_{pv}\, z_c \geq d_p \qquad p \in P,\, v \in V^*_p \tag{6.2}$$

$$z_c \in \mathbb{Z}^+ \qquad c \in C \tag{6.3}$$

Constraints (6.1) ensure that all links on each working path are protected against any single link failure. Constraints (6.2) ensure that all demands are protected against any single node failure, i.e., intermediate node v on working path p, for all intermediate nodes on all working paths. Constraints (6.3) define the domain of the variables.

6.4.2 Solution Method and the Pricing Problem

In order to efficiently solve the model presented in Section 6.4.1, we use a column generation (CG) algorithm in order to solve the linear relaxation of the model, and then, the CPLEX ILP solver in order to obtain an integer solution (The reader can refer to, e.g., Chvatal [Chv83] for more information about column generation techniques).

Based on the CG algorithm, the shortcut Np-cycle design problem is decomposed into the master problem (i.e., the optimization model of the previous section) and the pricing problem. The master problem handles the selection of shortcut Np-cycles from the candidate set, and the pricing problem generates candidate shortcut Np-cycles. The detailed CG-based algorithm and integer solution method are as described in Section 3.7.

The pricing problem corresponds to the optimization problem for generating a configuration, i.e., defining a shortcut Np-cycle and identifying its protected set of links/nodes with respect to working paths. Its objective is to minimize the so-called reduced cost.

We introduce next the basic idea about how to generate a configuration (i.e., a candidate shortcut Np-cycle) before presenting the pricing problem model.

How to build shortcut p-cycles

In order to generate a shortcut Np-cycle (i.e., a configuration in the optimization model), we first build a simple cycle, and then identify the working segments of working paths which can be protected by this cycle. In order to identify such protection relationship, for a working path p which intersects with the cycle (with either on-cycle or straddling links), we search for a protection flow φ_p which will be, for some links of the working path, a recovery path in case of a single link/node failure. Such a protection flow φ_p therefore should have the following three properties:

1. Flow φ_p has the same end nodes as path p.
2. Flow φ_p traverses some links that are either on path p or on the current cycle under construction, but not on both. Thereby, flow φ_p can be the recovery path of path p using the cycle under construction in case of a single failure of its link or node.
3. In order to provide protection using the current cycle c, flow φ_p must share at least one link with the cycle.

After obtaining cycle c and flow φ_p for path p, we need to identify the links and nodes which are protected as well as the number of protected traffic units. Let nodes v_1 and v_2 be the intersecting nodes between flow φ_p and cycle c which are nearest to the end nodes of path p: these two nodes are the protection switching nodes of path p. Thus, flow φ_p along the current cycle between v_1 and v_2 can be used to carry the affected traffic on working path p in case of a single link/node failure between v_1 and v_2 on the working path p.

Depending on the number of traffic units carried on flow φ_p, the links/nodes of the working path between v_1 and v_2 can be protected either as an on-cycle/hybrid segment or as a straddling segment, as in segment protection, see, e.g., [GS03, JL11b]. If flow φ_p carries one unit traffic on each link en route, the associated working segment is an on-cycle/hybrid segment with respect to the current cycle under construction. The associated working segment is a straddling segment, and two unit traffic on it can be protected by the current cycle if flow φ_p carries two unit traffic on the links of path p, and splits/merges at the switching nodes with respect to the current cycle, and carries one unit traffic on each on-cycle link.

Figure 6.2(a) illustrates the identification of a hybrid working segment. Given the primary path p in blue line and a shortcut p-cycle c in red line, the protection flow φ_p represented by the green line holds the above three properties. Also, on each link en route, flow φ_p carries one unit traffic. The switching protection nodes are v_{10} and v_4. Upon a link (resp. node), say, $v_{10} - v_8$ (resp. v_8) failure, nodes v_{10} and v_4 switch the affected traffic on the protection flow $v_{10} - v_1 - v_6 - v_5 - v_4$ along p-cycle c. Thereby, with respect to path p, the working segment $v_1 - v_4$ consisting of the contiguous on-path links and nodes between v_{10} and v_4 can be protected as an hybrid segment by p-cycle c using the overlapping part of φ_p and p-cycle c.

The identification of straddling segments is illustrated in Figure 6.2(b). With respect to path p and p-cycle c, flow φ_p carries two unit traffic on the links, e.g., SRC-v_{10} of path p. When meeting with p-cycle c, flow φ_p splits / merges at nodes v_3 and v_{10}, and travels on paths $v_{10} - v_7 - v_2 - v_3$ and $v_{10} - v_1 - v_6 - v_5 - v_4 - v_3$ along cycle c. On each on-cycle link, e.g., $v_1 - v_6$, flow φ_p carries one unit traffic. As a result, working segment $v_3 - v_{10}$ of path p is a straddling segment, and two units of traffic can be protected.

Optimization Model

The objective function of the pricing problem is written as follows.

$$\min \qquad \text{COST}_c - \sum_{p \in P} \sum_{\ell \in L_p} u_{p\ell}\, a^c_{p\ell} - \sum_{p \in P} \sum_{v \in V^*_p} u_{pv}\, a^c_{pv}$$

where $u_{p\ell}$ and u_{pv} are the dual variables associated with constraints (6.1) and (6.2) respectively.

Before giving the mathematical expression of the constraints of the pricing problem, we need to introduce the following notations:

Parameters

p_ℓ $= 1$ if link ℓ belongs to p, 0 otherwise

p_v $= 1$ if node v is an intermediate node of p, 0 otherwise

Variables

$\varphi_{p\ell}$ $=$ 2 (resp. 1) if link ℓ of flow φ_p carries two (resp. one) unit traffic on path p, 0 otherwise.

$y_{p\ell}$ $=$ 2 (resp. 1) if two (resp. one) traffic units on link ℓ with respect to path p is protected by the current cycle, 0 otherwise.

x_{pv} $=$ 2 (resp. 1) if two (resp. one) traffic units on path p across node v is protected by the current cycle, 0 otherwise.

α_{pv} $=$ 2 (resp. 1) if flow φ_p across node v carries two (resp. one) traffic units on path p, 0 otherwise.

With these notations, the objective function of the pricing problem can be rewritten as follows:

$$\min \overbrace{\sum_{\ell \in L} \text{COST}_\ell x_\ell}^{\text{COST}_c} - \sum_{p \in P} \sum_{\ell \in L_p} u_{p\ell} \overbrace{y_{p\ell}}^{a^c_{p\ell}} - \sum_{p \in P} \sum_{v \in V^*_p} u_{pv} \overbrace{x_{pv}}^{a^c_{pv}}$$

The pricing problem model is subject to the following three blocks of constraints. The first block of constraints is present next to build a simple cycle, which consists of constraints (3.9) - (3.11).

Based on the basic idea described above for building a shortcut Np-cycle, the second block of constraints identifies the protection flow φ_p which holds the three properties mentioned there.

$$\sum_{\ell \in \omega(v^1_p)} \varphi_{p\ell} = \sum_{\ell \in \omega(v^2_p)} \varphi_{p\ell} \leq 2 \qquad p \in P \tag{6.4}$$

$$\sum_{\ell \in \omega(v)} \varphi_{p\ell} = 2\, \alpha_{pv} \qquad p \in P, v \in V \setminus \{v^1_p, v^2_p\} \tag{6.5}$$

$$\sum_{\ell \in \omega(v) \setminus \{\ell'\}} \varphi_{p\ell} \geq \varphi_{p\ell'} \qquad p \in P, \ell' \in \omega(v), v \in V \setminus \{v^1_p, v^2_p\} \tag{6.6}$$

$$\varphi_{p\ell} \leq (1 - p_\ell)\, x_\ell + 2\,(1 - x_\ell)\, p_\ell \qquad \ell \in L, p \in P \tag{6.7}$$

$$\sum_{\ell \in L} (\,1 \,-\, p_\ell\,)\, \varphi_{p\ell} \,\geq \sum_{\ell \in \omega(v^1_p)} \varphi_{p\ell} \qquad p \in P \tag{6.8}$$

$$\sum_{p \in P_v} (\,1 \,-\, p_\ell\,)\, \varphi_{p\ell} \,\leq\, x_\ell \qquad \ell \in L,\ v \in V \tag{6.9}$$

Constraints (6.4) - (6.6) are flow conservation constraints for finding protection flow φ_p which hold the first property with respect to working path p. Constraints (6.4) say that, for each path p, flow φ_p must end at its two end nodes, and the sum of the protection flow φ_p must be equal at these two end nodes. Also, these constraints ensure that flow φ_p can carry at most two unit traffic. Constraints (6.5) say that, for each node except the end nodes of path p, flow φ_p must cross this node if this node is on φ_p. In other words, the overall links of flow φ_p incident on this node must carry an even (0, 2, or 4) number of traffic units. Constraints (6.6) ensure that, for node v which is not an end node of path p, flow φ_p cannot be carried only on a single link incident on node v. Constraints (6.7) ensure that, with respect to path p, flow φ_p must also hold the second property (i.e., flow φ_p must be carried on links that are either on path p or on the current cycle under construction, but not on both). Constraints (6.8) ensure that flow φ_p must also hold the third property with respect to path p (i.e., the protection flow φ_p cannot follow a route identical to the route of this path if such flow exists). As a result, flow φ_p must have at least one common link with the current cycle under construction. Constraints (6.9) say, for pairwise node non-disjoint working paths, the associated protection flows cannot share any link on the current cycle under construction. Note that constraints (6.9) allow that, with respect to two paths sharing the intermediate node v, if the associated protection flows along the current cycle are disjoint, the failure of node v can be recovered by the current cycle under construction. For the flow φ_p carrying two units of traffic, along the current shortcut Np-cycle, it splits at the protection switching nodes, and then are carried on two disjoint paths along the current cycle under construction. Therefore, it is allowed by this set of constraints.

With the above two blocks of constraints, we can achieve a simple cycle and the protection flow φ_p for path p. The last block constraints is next formulated for identification of the protected nodes and links as well as the number of protected traffic units by the current cycle according to the shortcut Np-cycle construction described Section 6.4.2.

$$y_{p\ell} \leq \sum_{\ell' \in \omega(v_p^1)} \varphi_{p\ell'} - \varphi_{p\ell} \qquad p \in P,\ \ell \in L_p \tag{6.10}$$

$$x_{pv} \leq \sum_{\ell \in \omega(v_p^1)} \varphi_{p\ell} - \alpha_{pv} \qquad p \in P,\ v \in V_p \tag{6.11}$$

$$x_{pv} \leq \sum_{\ell \in \omega(v)} p_\ell \, y_{p\ell} \qquad p \in P,\ v \in V_p \tag{6.12}$$

$$x_\ell \in \{0,1\},\ \alpha_{pv} \in \{0,1,2\} \qquad \ell \in L,\ v \in V \tag{6.13}$$

$$\varphi_{p\ell},\ y_{p\ell},\ x_{pv} \in \{0,1,2\} \qquad \ell \in L,\ p \in P,\ v \in V_p \tag{6.14}$$

Constraints (6.10) say that link ℓ of path p can be protected if flow φ_p exists and does not traverse link ℓ. Also, these constraints say that, at most two units of traffic can be re-routed on flow φ_p against the failure of link ℓ. Constraints (6.11) say that flow φ_p can protect the intermediate node v of path p if flow φ_p exists and does not cross node v. Also, it is ensured that no more than two units of traffic across node v can be re-routed on flow φ_p in case of the failure of node v. Constraints (6.12) ensure that, with respect to a working path p, an intermediate node can be protected only if one of its adjacent on-path links is also protected by the current cycle under construction.

6.5 Computational Results

We now evaluate the shortcut Np-cycle performances for full node protection. We compare shortcut Np-cycles with three other p-cycle based schemes:

(i) original link p-cycles as a benchmark without any concern about node protection, for which we use the column generation model of [RJ08];

(ii) node p-cycles for full node protection, for which we use the optimization model of Section 4.3;

(iii) path p-cycles for full node protection, which is designed using the CG model of Section 4.5.

For the performance evaluation and comparison, we use the following three metrics.

- Capacity redundancy - $R^{\mathrm{p/w}}$, i.e., the ratio of spare capacity cost over working capacity cost. Here, the working (resp. spare) capacity cost is calculated as the sum of the geographical distances of the link channels along the working (resp. protection) paths, assuming the cost to be proportional to this parameter.

- Dual link failure recovery ratio - R_2 (as formula (8.3), in p. 510 of Grover [Gro04a]) defined by Equation 4.47.

- Number of topologically distinct p-cycles which need to be configured upon the deployment of a p-cycle scheme, an approximate measure of the complexity of the protection management overhead.

Data Instances

Five diverse network instances have been used, which are described in Table 6.1. For each network instance, we provide the number of nodes, the number of edges, the average nodal degree as an indicator of the regularity of the network connectivity. Also, We calculate the network diameter, i.e., the length of the longest path among the shortest paths for any node pair in the network.

Traffic instances are described by their number of distinct demand requests and working capacity cost (i.e., the overall geographical distances of link channels which are required for the primary paths), in the last two columns of Table 6.1. For each network, the number of demand units between a given node pair is randomly generated (uniform distribution) in the interval [1..20]. Working paths are computed in such a way as to guarantee that they are of minimum length subject to the condition that there exists at least one potential protection path that is link and node disjoint with the working path.

Table 6.1: Data instances

Networks	Nodes	Edges	Node Degree	Network Diameter	Number Demands	Working Cost
NSF [HBB+04]	14	21	3.0	5,316	91	2,801,534
GERMANY [HBB+04]	17	26	3.1	951	136	578,512
BELLCORE [SG03]	15	28	3.7	1,160	105	743,738
ATLANTA [OPTW07]	15	22	2.9	708	105	284,762
COST239 [BDH+99]	11	26	4.7	1,660	55	503,661

6.5.1 Capacity Redundancy

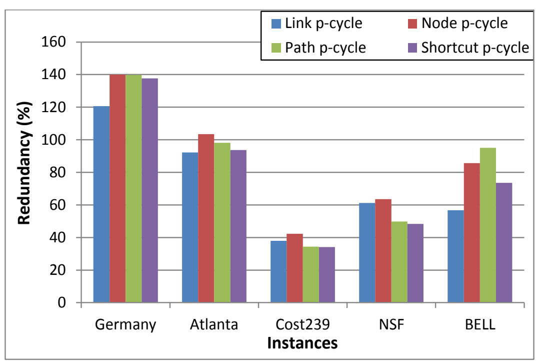

Figure 6.4: Capacity redundancy

We first evaluate shortcut Np-cycles from the capacity efficiency perspective. Under the requirement for full node protection, we compare shortcut Np-cycles with the two other protection schemes, node p-cycles and path p-cycles. Also, we compare shortcut Np-cycles with classical link p-cycles as a benchmark of capacity efficiency. Results are summarized in Figures 6.4 over five network instances.

Shortcut Np-cycles are more capacity efficient than node p-cycles and path p-cycles for all network instances, keeping in line with the example presented in Section 6.3.1. The redundancy differences between shortcut Np-cycles and path p-cycles (resp. node p-cycles) vary from ∼1% to 22% (resp. from 3% to 15%). In contrast with path p-cycles, shortcut Np-cycles do not require that the two end nodes of the working paths must sit on the same p-cycles. Therefore, shortcut Np-cycles are more flexible, and thus more capacity efficient for providing protection against single link and node failures. In comparison with node p-cycles, shortcut Np-cycles are more capacity efficient due to the fact that shortcut Np-cycles can protect against more failure scenarios rather than just straddling link failures, as illustrated in Figure 2(b).

Depending on the network topology, extra spare capacity may still be required by shortcut Np-cycles for node protection in contrast with link p-cycles only for link protection. Specifically, in GERMANY, ATLANTA and BELLCORE, shortcut Np-cycles require from 1.5% to 17% more bandwidth than link p-cycles, while providing 100% protection against single link and node failures. However, for NSF and COST239, shortcut Np-cycles with full node protection is more capacity efficient than link p-cycles, just as path p-cycles. This is mainly due to the fact that, in these two networks, there are more chances to find shortcut Np-cycles such that links and nodes can be protected using straddling segments.

6.5.2 Number of the Cycles

Provided that no any length limit on p-cycles, in Figure 6.5, we present the number of the distinct cycles and of the overall number of cycle occurrences in the optimal solutions of link p-cycles, node p-cycles, path p-cycles and shortcut Np-cycles. As mentioned in Section 6.1, the excessive p-cycle length usually leads to negative impacts on the recovered traffic, such as increased propagation delay and signal degradation. We will study, in Section 6.5.4, the impact of curtailing p-cycles on the performance metrics.

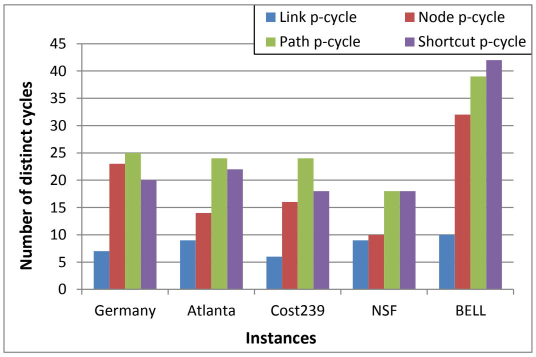

(a) Number of the distinct cycles

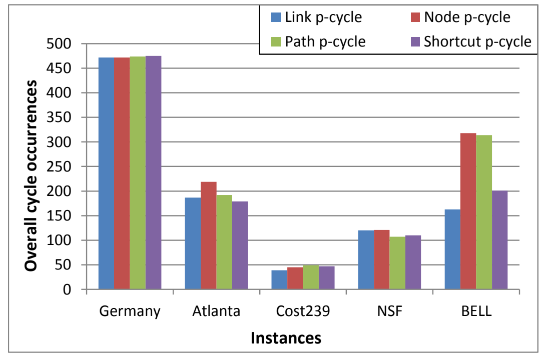

(b) Number of overall p-cycle occurrences

Figure 6.5: Number of cycles

Overall, we can observe from Figure 6.5(a) that, the link p-cycle scheme requires the smallest number of distinct cycles among the four protection schemes for all instances (independently of the topologies). Regarding shortcut Np-cycles versus path p-cycles, shortcut Np-cycles ask for the smallest number of distinct cycles for all instances except for BELLCORE. Therefore, shortcut Np-cycles hold a possible advantage for the cycle management over path p-cycles. However, in contrast with the node p-cycle scheme, shortcut Np-cycles require more distinct cycles in all instances except GERMANY.

Figure 6.5(b) presents the overall number of cycle occurrences in the optimal solutions of the four protection schemes over five instances. The ranking of these four schemes depends on the network topology. Among the three schemes ensuring full node protection, in ATLANTA and BELLCORE, shortcut Np-cycles need the smallest overall number of occurrences of p-cycles while, in the other three instances, the differences of these three schemes are very small.

6.5.3 Average Cycle Length and Protection against Dual Link Failures

From the viewpoint of the average length of the p-cycles, Figure 6.6(a) shows that, the ranking of these four protection scheme also depends on the network topology. In order to ensure node protection, shortcut Np-cycles are smaller in GERMANY and NSF, while larger in ATLANTA and BELLCORE than the other two protection schemes (node p-cycles and path p-cycles). In comparison with link p-cycles, the average length of shortcut Np-cycles is smaller in NSF and COST239 while larger in the other three instances.

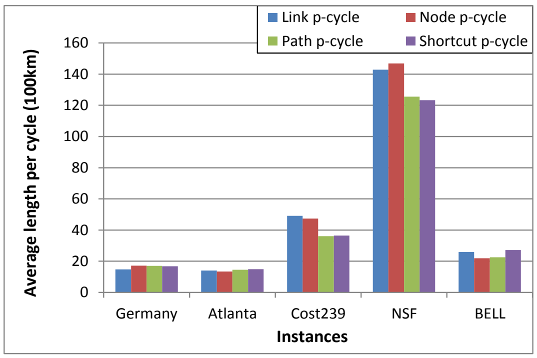

(a) Average size of cycle length

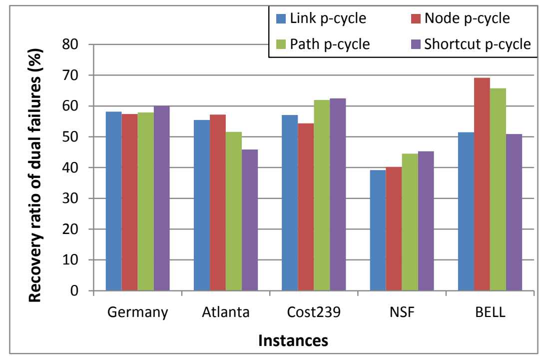

(b) Dual failure recovery ratio

Figure 6.6: Solution structure and dual link failure recovery ratio

With respect to the dual link failure restoration ratio (R_2), Figure 6.6(b) summarizes the results for the four protection schemes over the five network instances. Note that here the protection against dual link failures comes for free from the solutions of these four schemes.

Shortcut Np-cycles offer the largest R_2 for GERMANY, COST239 and NSF among these four protection schemes. This comes from the fact that the average length of the cycles in the solutions with shortcut Np-cycles is (very close to) the smallest possible one in these three instances, as shown in Figure 6.6(a). For these three instances, shortcut Np-cycles provide the R_2 3% to 8% higher than node p-cycles, while similar to path p-cycles. For these three instances, shortcut Np-cycles provide the R_2 3% to 8% higher than for node p-cycles, while similar to path p-cycles. For the other two instances, i.e., (BELLCORE and ATLANTA), shortcut Np-cycles provide the smallest R_2 as the average cycle length of shortcut Np-cycles is the largest one among these protection schemes.

6.5.4 Impacts of Cycle Length Limitation on Performance Metrics

The numerical results presented above have been calculated without concerns about the p-cycle length, as in most of the p-cycle studies in the literature. However, the length limitation may need to be considered in the design, if the delay of a connection is limited, especially if we assume that wavelength conversion is available at each node (the assumption of this study). Also, the signal transmission quality may not be guaranteed if the related protection paths along p-cycles become too long. To this end, we next study further, under the restrictions on the length of the p-cycles, the performance of shortcut Np-cycles through comparisons with the other two schemes for full node protection (node p-cycles and path p-cycles). Accordingly, we added the following constraint in the pricing problems of the associated designs:

$$\sum_{\ell \in L} \text{LENGTH}_\ell \, x_\ell \leq \overline{\text{LENGTH}}, \tag{6.15}$$

where $\overline{\text{LENGTH}}$ is the length limit on the p-cycles.

Experiments are carried out on the COST239 instance, and the numerical results are shown in Figure 6.7. $\overline{\text{LENGTH}}$ value ranges between 3,000 km and 6,000km, and no limit on the length of the p-cycles). Those values have been selected in order to guarantee that solutions exist for Shortcut Np-cycles with 100% node protection. Note that for values slightly smaller, COST239 cannot be fully protected by any of these three protection schemes.

Figure 6.7(a) shows the decrease of the redundancy ratio as the length of the p-cycles increases. Note that there is no path p-cycle protection ensuring full link/node protection earlier than shortcut Np-cycles and node p-cycle as the length limit of p-cycles decreases. The reason is as follows.

For path p-cycles, the length limit on the cycle should be at least twice as much as the

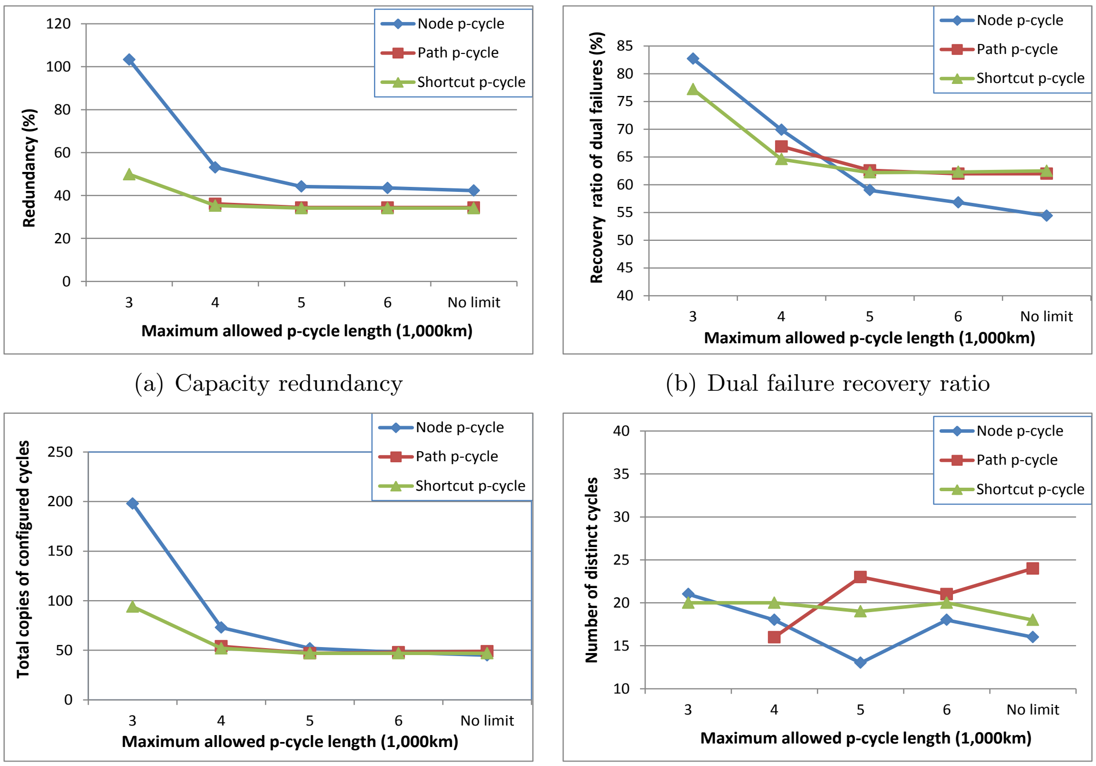

(a) Capacity redundancy

(b) Dual failure recovery ratio

(c) Overall copies of p-cycles

(d) Number of distinct cycles

Figure 6.7: Solution performance of protection approaches

network diameter (1,660km for COST239, as shown in Table 4.1) to ensure 100% guaranteed link and node protection for all demands. For shortcut Np-cycle and node p-cycle, however, there is no such restriction, and the length limit on cycles only needs to be larger than the size of any cycle ensuring 100% link protection. Moreover, with the cycle length no more than 3000km, Shortcut Np-cycle is much more capacity efficient than node p-cycle, the difference of the capacity redundancy is up to 53%. This implies that, Shortcut Np-cycle is a promising scheme for link and node protection in the context of the existence of very restricted length limit.

For COST239, there is a length threshold (4,000km), beyond which the redundancy of these three protection schemes does not decrease significantly.

Figure 6.7(b) shows that, with short p-cycles, these three protection schemes, especially the shortcut Np-cycle one, have advantages for dual link failure recovery, say, 77% with only 45% capacity redundancy, when $\overline{\text{LENGTH}} = 3,000$. Note that such R_2 comes for free from the solutions of protection against a single node/link failure. This suggests that, with shortcut Np-cycles, it is quite possible to achieve the aimed R_2 while ensuring protection against a single link/node failure without requirement of extra bandwidth.

For the overall number of p-cycles, there is a sharp increase of their number as the length limit decreases, especially behind the threshold value (i.e., 4000km) for shortcut Np-cycles and node p-cycles, as shown in Figure 6.7(c). However, as shown in Figure 6.7(d), the number of distinct cycles (with respect to the links they use) remains relatively stable. This suggests that the length limit has a minor impact on the management overhead.

6.6 Summary and Conclusion

In this chapter, we proposed a novel protection scheme, called shortcut Np-cycles, in WDM networks to protect against any single link/node failures. Shortcut Np-cycles offer a fully pre-cross connected shared protection approach. Upon a single link/node failure, with respect to a working path, the common nodes with a shortcut Np-cycle nearest to the end nodes of the working path switch automatically the affected traffic along the shortcut Np-cycle. Thereby, in contrast with classical link p-cycles, shortcut Np-cycles can remove all possible loop-backs. In comparison with path p-cycles, shortcut Np-cycles can provide more flexible protection for link and node protection by no requirement that two end nodes of working paths must sit on the same cycles. Numerical results reveal that shortcut Np-cycles outperform node p-cycles and path p-cycles in terms of capacity efficiency. Also, in the context of restricted length cycles, shortcut Np-cycle solutions exist for much smaller cycles than path p-cycles for full link and node protection, and more capacity efficient than node p-cycles. The above observations suggest that shortcut Np-cycles with node protection is a promising alternative of path p-cycles and node p-cycles for full link and node protection.

Chapter 7

Exhaustive Numerical Comparison of p-Cycle Based Schemes

7.1 Introduction

Regarding the design of the classical p-cycle based schemes, most studies deal with single link failures. However, a node may also fail due to disasters, e.g., fires or flooding destroying the node, which leads to devastating consequences.

To ensure full (intermediate) node protection, node p-cycles are proposed in Chapter 4, as an extension of original link-protecting p-cycles. Segment p-cycles can provide node protection, however, they cannot protect the end node of a segment. Segment Np-cycles have been proposed in Chapter 5 for full node protection with segment p-cycles. Path p-cycles provide full node protection, assuming that only node-disjoint paths can share protection paths along path p-cycles. These three schemes for full node protection will be collectively named as enhanced p-cycle based schemes in the sequel in order to distinguish them from the classical schemes.

To evaluate the performances of these p-cycle based schemes, comparative studies have been conducted in [HS07, GGC+07, WYH08, RJ08] under the single link failure scenario. In [HS07], p-cycles are compared with SBPP and pre-cross-connected trails (PXT) [CCF04]. Therein, the results reveal that they are comparable in the dense networks. In [GGC+07], link p-cycles are compared with path p-cycles, PXT, demand-wise shared protection [KZJH05] and p-tree [SHY04]. In all these comparative studies, the ILP models selects off-line enumerated candidates. The authors in [RJ08] revisit link-protecting / path p-cycles versus shared link/path protection. Therein, the scalable design and solution methods are proposed and the comparison is conducted based on the exact solution for each protection scheme.

In this chapter, we present the first exhaustive quantitative comparisons of p-cycle based schemes and its enhancements. We compare the performances of these schemes using the designs with two different objectives, spare capacity minimization and CAPEX minimization. Also, two failure scenarios are considered, single link failures and single link/node failures.

7.2 Numerical Results

In this section, we compare the solution performances of the classical p-cycle based schemes for protection against single link failures, which include link p-cycles (LpCycle), segment p-cycles (SpCycle) and path p-cycles (PpCycle). Also, we compare the enhanced schemes for protection against single link/node failures, which consist of node p-cycles (LNpCycle), segment Np-cycles (SNpCycle) and path p-cycles (PNpCycle).

As far as the spare capacity usage is concerned, the classical p-cycle based schemes are designed using the following models for protection against single link failures.

- Link p-cycles (LpCycle) are designed using the model in [RJ08].

- Segment p-cycles (SpCycle) are designed using the model in Section 3.3.
- Path p-cycles (PpCycle) are designed using the model in [RJ12].

The enhanced p-cycle schemes are designed using the following models in order to protect against single link/node failures such that the spare capacity cost is minimized.

- Node p-cycles (LNpCycle) are designed using the model presented in Section 4.3.
- Segment Np-cycles (SNpCycle) are designed using the model presented in Section 5.4.
- Path p-cycles (PNpCycle) are designed using the model presented in Section 4.5.

With respect to the spare CAPEX, the classical and enhanced p-cycle schemes are designed using the optimization models proposed in Section 5.5 and Section 5.6. Note that, for the designs of link p-cycles and node p-cycles, the associated CAPEX optimization model can be easily derived from the models presented in Section 5.6 and 5.5. The model in Section 5.6 (resp. 5.5) can be used for link (resp. node) p-cycle CAPEX optimization design if we feed the models with, along each work path, the link set in place of the segment set.

Data Instances

Four network instances are exploited for comparisons with diverse topology characteristics. For each network, we generate connection demands between each node pair. These demands are carried respectively with line rate OC-1, OC-3, OC-12 and OC-48. For each node pair, the number of the connection demands with the line rate OC-1 (resp. OC-3, OC-12 and OC-48) is a random number uniformly distributed on the interval [48, 64] (resp. [24, 32], [24, 32] and [4, 8]). For each network, using the algorithm of [Bou05, BJH11], we obtain the set of working paths and the set of working segments at OC-192 line rate (10Gb/s) to match the equipment bit rate in [HGMS08]. The total number of working paths and of segments are present in Table 7.1 for each network instance.

Table 7.1: Network Instances

Networks	Num. nodes	Num. links	Avg. node degree	Num. Demands	Num. segments
COST239 [BDH+99]	11	26	4.7	196	215
ATLANTA [OPTW07]	15	22	2.9	373	494
BELLCORE [SG03]	15	28	3.7	377	450
GERMANY [HBB+04]	17	26	3.1	485	704

7.2.1 Optimal Spare Capacity Design

In this section, the solutions for comparisons are obtained from the designs with the objective of minimizing the spare capacity usage. We compare the solution performances of classical (resp. enhanced) p-cycle based schemes for protection against any single link failure (resp. any single link or single node failure). Two metrics are utilized for comparison: one is the capacity redundancy, and the other is the average cycle length in each solution. Also, we investigate how the capacity redundancy of each scheme varies with the cycle length limit.

Capacity redundancy

Fig 7.1(a) (resp. 7.1(b)) exhibits, over four network instances, the comparison of the capacity redundancy of classical p-cycle based schemes: LpCycle, SpCycle and PpCycle (resp. enhanced schemes: LNpCycle, SNpCycle and PNpCycle).

We can observe from Figure 7.1(a) that, LpCycle is the most costly for each instance except GERMANY, while SpCycle is the most economical one for recovery from any single link failure. The differences of the capacity redundancy between SpCycle and LpCycle (resp. between SpCycle and PpCycle) range from ∼1% to ∼9% (resp. from ∼1% to ∼5%). These

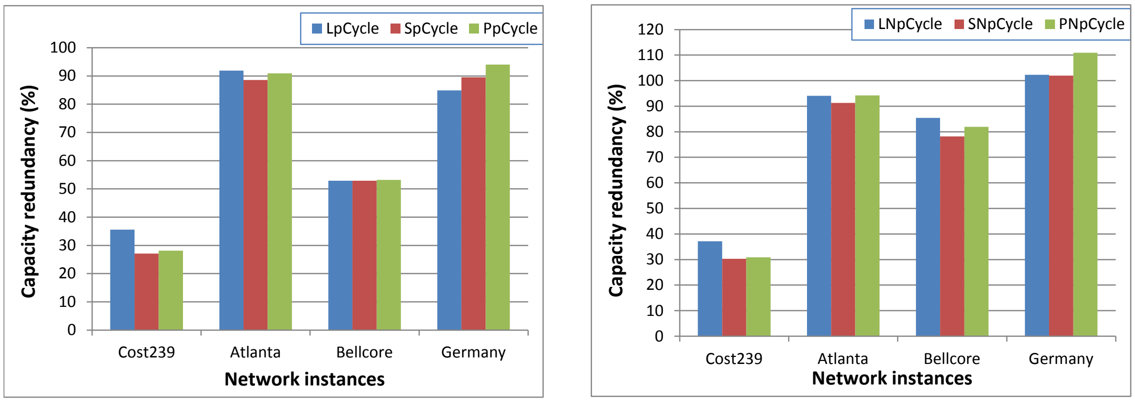

(a) Link protection (b) Node protection

Figure 7.1: Capacity redundancy: bandwidth minimization

mainly come from the fact that, among three classical p-cycle schemes, in general, SpCycle can protect more failure scenarios than LpCycle, and is a more flexible protection scheme for spare bandwidth sharing than PpCycle.

Figure 7.1(b) shows that, for each instances, SNpCycle is the most economical one among three enhance schemes for protection against any single link or single node failure. The differences between SNpCycle and LNpCycle (resp. between SNpCycle and PNpCycle) range from ∼1% to ∼7% (resp. ∼1% to ∼9%). Regarding LNpCycle versus PNpCycle, PNpCycle outperforms LNpCycle in COST239 and BELLCORE while are inferior to LNpCycle in another two instances. This suggests that the network topology has a big impact on the capacity efficiency of these two schemes.

Average Cycle Size

Figure 7.2(a) (resp. 7.2(b)) presents, over four network instances, the average length per cycle in the solutions of the three classical (resp. enhanced) p-cycle based schemes.

Figure 7.2(a) shows that, for recovery from single link failures, the average cycle length using the PpCycle scheme is the longest among the three classical schemes in all instances except COST239. In comparison of LpCycle with SpCycle, the average cycle length with

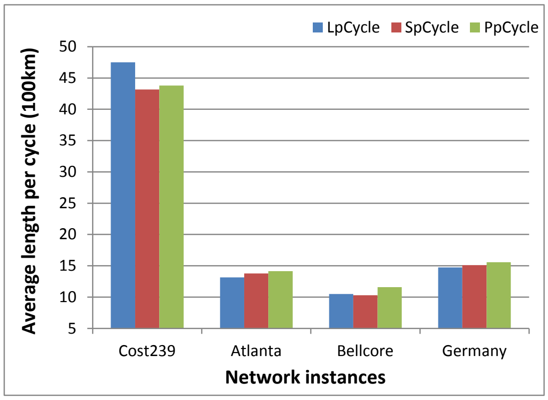

(a) Link protection

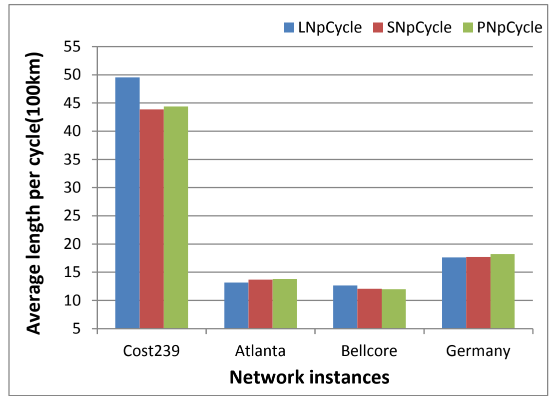

(b) Node protection

Figure 7.2: Average cycle size: bandwidth minimization

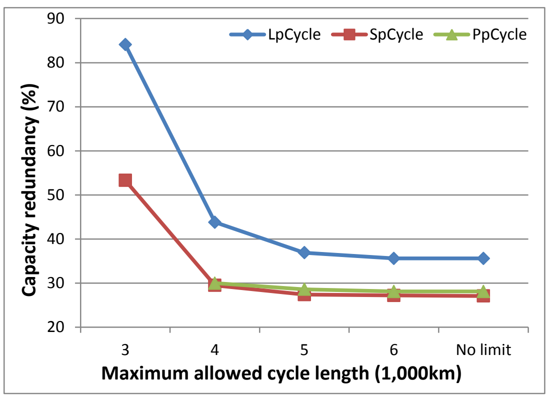

(a) Link protection

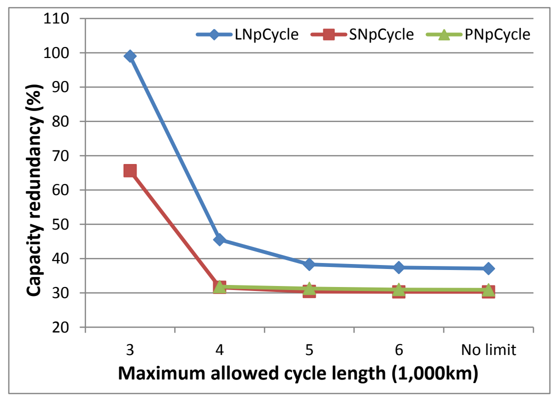

(b) Node protection

Figure 7.3: Redundancy vs. cycle size: COST239

LpCycle is longer in COST239 and BELLCORE while shorter in the other two data instances.

Figure 7.2(b) shows that, among three enhanced schemes for protection against single node / link failures, the average cycle length with LNpCycle is longest in COST239 and BELLCORE while shortest in the other two instances. The average cycle length with PNpCycle is longer than SNpCycle in all instances except BELLCORE.

Capacity Redundancy versus Cycle Length Limit

It has been criticized that protection path length along *p*-cycles is too long [CJ07, SG03]. In order to understand how the cycle length limit impacts the solution performances of classical and enhanced *p*-cycle based schemes, we conduct the experiments on COST239. The cycle length limit starts from the value where the LpCycle or LNpCycle design has feasible solution.

Figure 7.3(a) (resp. 7.3(b)) shows the capacity redundancy of the solutions with classical (resp. enhanced) *p*-cycle based schemes varies with the maximum allowed cycle length.

From Figure 7.3, we can observe that, for each scheme, the capacity redundancy decreases with the cycle length increase. Also, after the length reaches to 5,000 km, the increase on the length has less impact on the redundancy for each scheme. PpCycle (resp. PNpCycle) design has no feasible solution earlier than LpCycle and SpCycle (resp. LNpCycle and SNpCycle) when the cycle length limit decreases. SpCycle (resp. SNpCycle) hold capacity efficiency close to PpCycle, while is more efficiency LpCycle (resp. LNpCycle).

7.2.2 Minimum CAPEX Cost Design

The solutions shown in Figure 7.4 - Figure 7.6 are obtained from the designs with the objective of minimizing CAPEX of classical and enhanced *p*-cycle based schemes. Three metrics are used for comparisons, which include the CAPEX cost, the capacity redundancy and the average cycle length.

CAPEX Cost

Figure 7.4(a) (resp. 7.4(b)) depicts, over the four instances, the CAPEX cost of the solutions with the classical (resp. enhanced) *p*-cycle based schemes. In Figure 7.4(a) (resp. 7.4(b)), for each instance, the three columns represent in turn the CAPEX using LpCycle (Lp), SpCycle (Sp) and PpCycle (Pp) (resp. LNpCycle (LNp), SNpCycle (SNp) and PNpCycle (PNp)). Each column contains three parts: the transmission cost, the link cost and the node cost. For each protection scheme, it is shown clearly, that the transmission cost (i.e.,

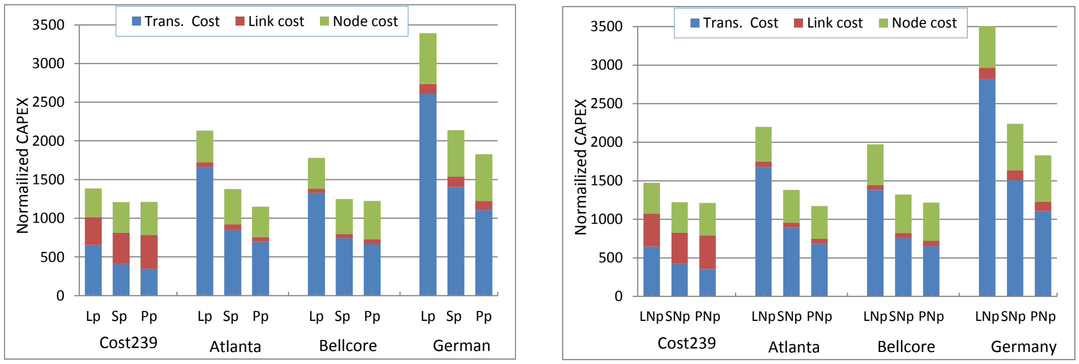

(a) Link protection (b) Node protection

Figure 7.4: CAPEX cost: CAPEX minimization

the transponder cost) is the dominant component cost of the CAPEX.

Overall, for each network instance, among the classical schemes (resp. the enhanced schemes), the solutions using PpCycle (resp. PNpCycle) are the most economical ones while the solutions using LpCycle (resp. LNpCycle) are the most costly ones, and SpCycle (resp. SNpCycle) sits in between. With the classical (resp. enhanced) p-cycle based schemes, the CAPEX differences between SpCycle and LpCycle (resp. SNpCycle and LNpCycle) ranges from 15% to 59% (resp. from 21% to 62%), while the differences between SpCycle and PpCycle (resp. SNpCycle and PNpCycle) vary from 1% to 20% (resp. 1% to 22%). The reason is due to the fact that with LpCycle (resp. LNpCycle), each end node of each unit link requires a transponder for access to one unit p-cycle, while with PpCycle (resp. PNpCycle), only end node of each unit lightpath asks for a transponder for access to one unit p-cycle.

Capacity Redundancy

From the perspective of the capacity redundancy, Figure 7.5(a) (resp. 7.5(b)) presents the solution comparisons based on the classical (resp. enhanced) p-cycle based schemes over four network instances. We can observe that, the solution with LpCycle (resp. LNpCycle) is the most bandwidth costly one among the classical (resp. enhanced) p-cycle based schemes in

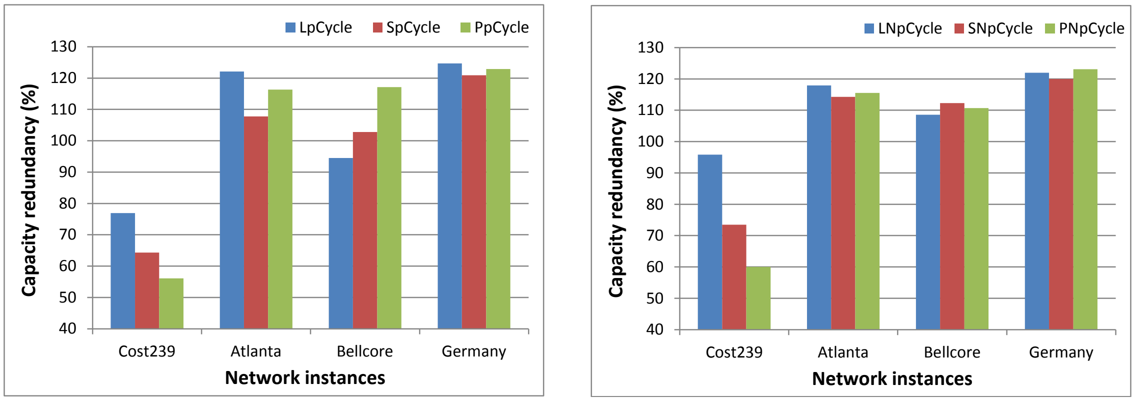

(a) Link protection (b) Node protection

Figure 7.5: Capacity redundancy: CAPEX minimization

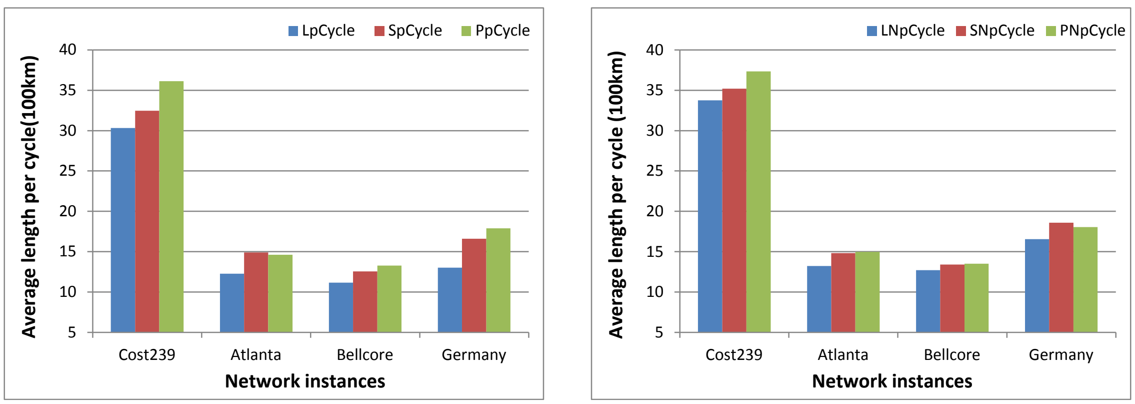

(a) Capacity redundancy (b) Average cycle size

Figure 7.6: Average cycle size: CAPEX minimization

each network instance except BELLCORE. In comparisons of SpCycle (resp. SNpCycle) with PpCycle (resp.PNpCycle), SpCycle (resp. SNpCycle) outperforms PpCycle (resp.PNpCycle) in each network instance except COST239 (resp. COST239 and BELLCORE).

Average Cycle Size

Figure 7.6(a) (resp. 7.6(b)) presents the average length per cycle in the solutions with three classical (resp. enhanced) p-cycle based schemes over four network instances. Among the classical (resp. enhanced) p-cycle based schemes, in all instances except ATLANTA (resp. GERMANY), the average length per cycle with PpCycle (resp. PNpCycle) is longest, while is shortest with LpCycle (resp. LNpCycle).

7.3 Summary

In this chapter, we conducted exhaustive numerical comparisons of the classical p-cycle based schemes and their enhancements. We compared the performances of these schemes with respect to CAPEX, capacity redundancy and average cycle length. Under the design of minimization of spare bandwidth usage, segment p-cycle (resp. segment Np-cycle) outperforms the other schemes for recovery from link (resp. link/node) failure. As far as the CAPEX cost is concerned, path p-cycle have an advantage over the others. The performance of these schemes relies on the network topology characteristic.

Chapter 8

Conclusions and Future Work

8.1 Conclusions

Survivability is a paramount requirement in the design of WDM optical networks. This thesis has studied a whole sequence of protection schemes from link p-cycles to path p-cycles in survivable WDM mesh networks against a single failure. p-Cycle based schemes are attractive protection approaches for WDM networks. However, toward the design of p-cycle based survivable networks, several issues still need to be addressed.

(i) There exists a scalability issue in the optimization models for the design of p-cycles.

(ii) Another issue exists in the choice of the optimization criterion, i.e., objective of the optimization model. Most related studies have sought to minimize the spare capacity usage. However, once optical fibers have been deployed, the CAPEX cost of network elements becomes significant for deployment of p-cycle structures.

(iii) Besides, most p-cycle designs cope with a single link failure without any concern about node failures. However, a single node failure may occur and the consequence could be catastrophic.

(iv) Furthermore, some loop backs may exist in the recovery paths using link or node p-cycles, which unnecessarily enlarge the recovered path length and in turn decrease the recovery speed.

We proposed a multi-granularity segment p-cycle scheme for efficiently protecting working segments with different granularities (e.g., OC-48, OC-192 or OC-768). To design such p-cycles, we develop a scalable CG model, with the study of the objectives of minimizing the nodal cost and of minimizing the spare capacity cost respectively. Numerical results show clearly that the optimization design of spare node equipment outperforms the classical optimization design of link spare capacity in terms of the node cost and management. This node-cost optimization model then can assist network operators effectively deploy multi-granularity segment p-cycles.

In order to ensure 100% guarantee protection against a single node failure, we proposed node p-cycles and developed a scalable CG-based optimization model. It is shown that node p-cycles offering node and link protection only require slightly more spare capacity than link p-cycles. Numerical results also reveal that, depending on the network topology, node p-cycles hold comparable capacity efficiency as path p-cycles, or are even more capacity efficient than path p-cycles. Regarding restricted length cycles, node p-cycle solutions have much smaller cycles than in path p-cycle solutions for full link and node protection. The above observations suggest that node p-cycle is a promising alternative to path p-cycles for full link and node protection, especially in large networks.

Moreover, we proposed an efficient protection approach based on segment p-cycles, called segment Np-cycles, which ensure 100% protection against any single failure, either link or node (endpoints of requests are excluded). We developed two scalable optimization models based on the CG techniques for the design of segment Np-cycles with the objective of minimizing spare capacity cost and of minimizing CAPEX cost respectively. Also, we developed the formulas for estimation of the recovery time respectively for segment p-cycles, Np-cycles and path p-cycles. Numerical results demonstrate that, in order to ensure 100% node protection, Np-cycles only require a marginal extra cost (spare capacity or CAPEX cost) than the regular segment p-cycles. In comparisons with path p-cycles, Segment Np-cycles offer faster recovery speed, and more capacity efficient in some networks depending on the network topology although they may require more CAPEX. Segment Np-cycles are therefore worth of interest within the context of multi-layer network design in order to address more failure recovery at the WDM layer.

We proposed the shortcut p-cycle scheme for 100% guaranteed protection of links and nodes against any single failures in WDM mesh networks. Based on link p-cycles, shortcut Np-cycles offer the recovered paths free of loop backs. Shortcut p-cycles differ from path p-cycles by reducing the recovery time, as the switching nodes are not necessarily the two end nodes of the protected working paths. In order to design shortcut p-cycles, we developed a scalable optimization model based on CG techniques. Numerical results show that shortcut Np-cycles are more capacity efficient that node p-cycles and path p-cycles for full node protection. Also, in the context of restricted length cycles, shortcut Np-cycle solutions exist for much smaller cycles than path p-cycle for full link and node protection. These observations suggest that shortcut Np-cycles are a promising alternative of path p-cycles and node p-cycles for full link and node protection. The performance advantage is achieved at the price of higher calculation complexity.

It is no doubts that p-cycles define a promising protection approach for survivable WDM mesh networks, although the last decades have not seen the deployment of p-cycles in the read world. Currently, SONET rings and other protection approaches still well meet the requirement for carrying the survivable traffic. On the other hand, it will be very costly to upgrade the legacy telecommunication infrastructures to survivable WDM mesh networks based on p-cycles. Nevertheless, as the unique characteristic of p-cycles holds, high capacity efficiency and fast recovery speed, and the ever-increasing traffic volume, the future will see p-cycles implemented in the real world. Specifically, for a survivable WDM mesh network, which is constructed from the beginning, the proposed segment Np-cycles is a promising option for full link and node protection as it well balances the capacity efficiency and the recovery speed. In the context of the very strict cycle length limitation, the proposed node p-cycles and shortcut p-cycles are attractive protection approaches against any single failure of a link or a node. Shortcut p-cycles are superior to node p-cycles in terms of capacity efficiency but inferior to them in terms of signaling. In this respect, this thesis makes contributions to the increase of the knowledge of p-cycle networking, and assists network operators in well deploying p-cycles.

8.2 Future Directions

WDM mesh optical networks may carry traffic with different granularities, say, OC-48, OC-192 and OC-768. The price of network elements varies with the granularities. Thus, it will be interesting that the design of p-cycle based schemes with differentiated granularities such that the CAPEX is minimized with 100% guaranteed survivability against any single link/node failure. The CG-based model should be developed in order to deal with the scalability issue. Moreover, due to the high complexity of this combinatorial optimization problem, an efficient heuristic would also be prefered for design of real-world large survivable networks.

It will save some p-cycle CAPEX if the recovery signals are kept in the optical domain along protection paths. However, for large WDM networks, it may be the case that the protection path length is longer than the maximum optical reach of available transponders at its end nodes. To this end, re-generators are required en route to maintain the signal transmission quality. Then, it will be interesting to jointly design of p-cycles together with the location of regenerators such that the spare CAPEX is minimized.

In Chapter 3 and Chapter 5, the input to the design methods, i.e., the working segment set, comes from the GRWA (short for grooming routing and wavelength assignment) heuristic in [BJH11, Bou05] given traffic defined by a set of requests of various granularities. It is left open that joint optimization of survivable GRWA based on segment p-cycles such that the overall cost of working segments and p-cycles is minimized.

For the issues addressed in this thesis, as in most studies on p-cycle design, we assume that the networks carry symmetrical traffic, and each node in a network holds the wavelength conversion capability. In practice, this assumptions could be invalid. It is possible that only some nodes are with the limited wavelength conversion capability, and some nodes, e.g., Google servers results in traffic asymmetrical in WDM networks. In this context, it could be practical and interesting that investigate the design of p-cycle based schemes and their enhancements under the wavelength continuity constraints to protect asymmetrical traffic against any single link/node failure in WDM networks [HJ11a].

Bibliography

[AD09] J. Akpuh and J. Doucette. Enhanced failure-specific p-cycle network dual-failure restorability design and optimization. Journal of Optical Networking, 8:1–13, 2009.

[AR08] A. Atamtürk and D. Rajan. Partition inequalities for capacitated survivable network design based on directed p-cycles. Discrete Optimization, 5:415–433, 2008.

[AS07] R. Asthana and Y.N. Singh. Second phase reconfiguration of restored path for removal of loop back in p-cycle protection. IEEE Communications Letters, 11(2):201 –203, 2007.

[AS08] R. Asthana and Y.N. Singh. Distributed protocol for removal of loop backs and optimum allocation of p-cycles to minimize the restored path lengths. IEEE Journal of Lightwave Technology, 26(5):616 –627, 2008.

[BDH+99] P. Batchelor, B. Daino, P. Heinzmann, D.R. Hjelme, R. Inkret, H.A. Jäger, M. Joindot, A. Kuchar, E. Le Coquil, P. Leuthold, G. de Marchis, F. Matera, B. Mikac, H.-P. Nolting, J. Späth, F. Tillerot, B. Van Caenegem, N. Wauters, and C. Weinert. Ultra high-capacity optical transmission networks: Final report of action COST 239. Technical report, Faculty of Electrical Engineering and Computing, University of Zagreb, 1999.

[BGK08] D. Baloukov, W.D. Grover, and A. Kodian. Toward jointly optimized design of failure-independent path-protecting p-cycle networks. Journal of Optical Networking, 7(1):62–79, 2008.

[BHJ06] A. Bouffard, A.C. Houle, and B. Jaumard. GRWA provisionning and segment protection in WDM optical networks. In Canadian Conference on Electrical and Computer Engineering - CCECE, pages 999–1002, 2006.

[BJH11] A. Bouffard, B. Jaumard, and A. Houle. GRWA provisionning and segment protection in WDM optical networks. submitted for publication, 2011.

[BJN+98] C. Barnhart, E.L. Johnson, G.L. Nemhauser, M.W.P. Savelsbergh, and P.H. Vance. Branch-and-price: Column generation for solving huge integer programs. Operations Research, 46(3):316–329, May-June 1998.

[Bou05] A. Bouffard. Dimensionnement GRWA et protection par segment dans les réseaux optiques WDM. Master's thesis, Université de Montréal, Canada, 2005.

[CCF04] T. Chow, F. Chudak, and A. Ffrench. Fast optical layer mesh protection using pre-cross-connected trails. IEEE/ACM Transactions on Networking, 12(3):539–548, 2004.

[CG02] M. Clouqueur and W. D. Grover. Mesh-restorable networks with complete dual failure restorability and with selectively enhanced dual-failure restorability properties. In Optical Networking and Communications - OptiComm, volume 4874, pages 1–12, 2002.

[CG05a] M. Clouqueur and W.D. Grover. Availability analysis and enhanced availability design in p-cycle-based networks. Photonic Network Communications, 10(1):55–71, 2005.

[CG05b] M. Clouqueur and W.D. Grover. Mesh-restorable networks with enhanced dual-failure restorability properties. Photonic Network Communications, 9(1):7–18, 2005.

[Chv83] V. Chvatal. Linear Programming. Freeman, 1983.

[CJ07] P. Cholda and A. Jajszczyk. Reliability assessment of optical p-cycles. IEEE/ACM Transactions on Networking, 15(6):1579–1592, 2007.

[DHGY03] J. Doucette, D. He, W.D. Grover, and O. Yang. Algorithmic approaches for efficient enumeration of candidate p-cycles and capacitated p-cycle network design. In Proceedings of IEEE/VDE Workshop on Design of Reliable Communication Networks - DRCN, pages 212–220, October 2003.

[DLZ07] J. Doucette, W. Li, and M. Zuo. Failure-specific p-cycle network dual-failure restorability design. In Proceedings of IEEE/VDE Workshop on Design of Reliable Communication Networks - DRCN, pages 1–9, October 2007.

[ELS12] M. Eiger, H. Luss, and D. Shallcross. Network restoration under dual failures using path-protecting preconfigured cycles. Telecommunication Systems, 49:271–286, 2012.

[EM09] A.E. Eshoul and H.T. Mouftah. Survivability approaches using p-cycles in WDM mesh networks under static traffic. IEEE/ACM Transactions on Networking (TON), 17(2):671–683, 2009.

[Fre02] R.L. Freeman. Fiber-Optic Systems for Telecommunications. Wiley, New York, 2002. ch. 6 and 10.

[GBSZ07] C. Ge, N. Bai, X. Sun, and M. Zhang. Iterative joint design approach for failure-independent path-protecting p-cycle networks. Journal of Optical Networking, 6(12):1329–1339, 2007.

[GD02] W. D. Grover and J. Doucette. Advances in optical network design with p-cycles: Joint optimization and pre-selection of candidate p-cycles. In Proc. IEEE LEOS Summer Topical Meetings, pages 49–50, July 2002.

[GGC+07] A. Grue, W.D. Grover, M. Clouqueur, D.A. Schupke, J.Doucette, B. Forst, D. Onguetou, and D. Baloukov. Comparative study of fully pre-cross-connected protection architectures for transparent optical networks. In Workshop on Design of Reliable Communication Networks - DRCN, pages 1–8, 2007.

[GGC+09] A. Grue, W.D. Grover, M. Clouqueur, D.A. Schupke, D. Baloukov, D. Onguetou, and B. Forst. CAPEX costs of lightly loaded restorable networks under a consistent WDM layer cost model. In IEEE International Conference on Communications - ICC, pages 1 – 6, June 2009.

[GLW+06] M. Gunkel, R. Leppla, M. Wade, A. Lord, D. Schupke, G. Lehmann, C. Furst, S. Bodamer, B. Bollenz, H. Haunstein, H. Nakajima, and J. Martensson. A cost model for the WDM layer. In International Conference on Photonics in Switching (PS), Herakleion (Crete), Greece, October 2006.

[GO09] W.D. Grover and D.P. Onguetou. A new approach to node-failure protection with span-protecting p-cycles. In 11th International Conference on Transparent Optical Networks (ICTON), pages 1–5, July 2009.

[GR00] O. Gerstel and R. Ramaswami. Optical layer survivability: a services perspective. IEEE Communications Magazine, 38:108–113, March 2000.

[Gro04a] W.D. Grover. Mesh-Based Survivable Networks. Prentice-Hall, 2004.

[Gro04b] W.D. Grover. The protected working capacity envelope concept: an alternate paradigm for automated service provisioning. IEEE Communications Magazine, 42(1):62 – 69, 2004.

[Gro07] W. Grover. Globally optimal distributed synchronous batch reconfiguration for efficient hazard-free dynamic provisioning: How an entire network can " think globally and act locally"? In Proceedings of IEEE/VDE Workshop on Design of Reliable Communication Networks - DRCN, pages 1–8, October 2007.

[Gru03] C.G. Gruber. Resilient networks with non-simple p-cycles. In 10th International Conference on Telecommunications - (ICT), pages 1027–1032, 2003.

[GS98] W. D. Grover and D. Stamatelakis. Cycle-oriented distributed preconfiguration: Ring-like speed with mesh-like capacity for self-planning network restoration. In IEEE International Conference on Communications - ICC, pages 537–543, June 1998.

[GS00] W.D. Grover and D. Stamatelakis. Bridging the ring-mesh dichotomy with p-cycles. In Proceedings of IEEE/VDE Workshop on Design of Reliable Communication Networks - DRCN, pages 92–104, Munich, Germany, April 2000.

[GS02] C. G. Gruber and D. A. Schupke. Capacity-efficient planning of resilient networks with p-cycles. In International Telecommunications Network Strategy and Planning Symposium (NETWORKS), volume 10, 2002.

[GS03] W.D. Grover and G. Shen. Extending the p-cycle concept to path-segment protection. In IEEE International Conference on Communications - ICC, volume 2, pages 1314 – 1319, May 2003.

[GS07] W.D. Grover and M. Scheffel. Resolving a question about span restoration: Do loopbacks involve a capacity penalty? In Proceedings of IEEE/VDE Workshop on Design of Reliable Communication Networks - DRCN, pages 1–6, Oct. 2007.

[HBB+04] R. Hulsermann, S. Bodamer, M. Barry, A. Betker, C. Gauger, M. Jager, M. Kohn, and J. Spath. A set of typical transport network scenarios for network modeling. Technical report, ITG Fachtagung Photonische Netze, Leipzig, 2004.

[HCM07] R. He, K. C. Chua, and G. Mohan. Protected working lightpath envelope: a new paradigm for dynamic survivable routing. In International Conference on Computer Communications and Networks - ICCCN, pages 291 –296, August 2007.

[HCM08] R. He, K. C. Chua, and G. Mohan. Lightpath-protecting p-cycle selection for protected working lightpath envelope. In IEEE Global Telecommunications Conference - GLOBECOM, pages 1 –5, December 2008.

[HFS05] W. He, J. Fang, and A.K. Somani. A p-cycle based survivable design for dynamic traffic in WDM networks. In IEEE Global Telecommunications Conference - GLOBECOM, pages 1869–1873, 2005.

[HGMS08] R. Hulsermann, M. Gunkel, C. Meusburger, and D. A. Schupke. Cost modeling and evaluation of capital expenditures in optical multilayer networks. Journal of Optical Networking, 7(9):814–833, Sep 2008.

[HJ11a] H. A. Hoang and B. Jaumard. Design of p-cycles under a wavelength continuity assumption. In IEEE International Conference on Communications - ICC, pages 1 –5, June 2011.

[HJ11b] H. A. Hoang and B. Jaumard. A new flow formulation for FIPP p-cycle protection subject to multiple link failures. In IEEE RNDM, pages 1 –7, October 2011.

[HP99] B. Hafuer and J. Pultz. Network failures: Be afraid, be very afraid. Technical Report NoteSPA.09.12851, GartnerGroup, September 1999.

[HS07] W. He and A. Somani. Comparison of protection mechanisms: Capacity efficiency and recovery time. In IEEE International Conference on Communications - ICC, pages 2218–2223, 2007.

[IBM11] IBM. IBM ILOG CPLEX 11.0 Optimization Studio, 2011.

[JHD12] B. Jaumard, H. A. Hoang, and D.T.Kien. Robust FIPP p-cycles against dual link failures. to appear in Telecommunication Systems, 2012.

[JL11a] B. Jaumard and H. Li. Design of p-cycles for full node protection in WDM mesh networks. In IEEE International Conference on Communications - ICC, pages 1–6, May 2011.

[JL11b] B. Jaumard and H. Li. Segment p-cycle design with full node protection in WDM mesh networks. In 18th IEEE Workshop on Local Metropolitan Area Networks (LANMAN), pages 1 – 6, October 2011.

[JL12] B. Jaumard and H. Li. Minimum CAPEX design of segment p-cycles with full node protection. In IEEE International Conference on Optical Network Design and Management - ONDM, pages 1–6, April 2012.

[JLR12] B. Jaumard, H. Li, and C. Rocha. Design of efficient node p-Cycles in WDM mesh networks. 2012. submitted for publication.

[JLS10] B. Jaumard, H. Li, and S. Sebbah. Design of path-segment-protecting p-cycles in survivable WDM mesh networks. In 14th International Telecommunications Network Strategy and Planning Symposium (NETWORKS), pages 1–6, September 2010.

[JM10] B. Jaumard and A. Metnani. Stability of p-cycles under dynamic traffic. In IEEE Global Telecommunications Conference - GLOBECOM, pages 1–5, December 2010.

[JRBG07] B. Jaumard, C. Rocha, D. Baloukov, and W. D. Grover. A column generation approach for design of networks using path-protecting p-cycles. In Proceedings of IEEE/VDE Workshop on Design of Reliable Communication Networks - DRCN, October 2007.

[KAJ09] M.S. Kiaei, C. Assi, and B. Jaumard. A survey on the p-cycle protection method. Communications Surveys Tutorials, IEEE, 11(3):53 –70, 2009.

[KG05] A. Kodian and W.D. Grover. Failure-independent path-protecting p-cycles efficient and simple fully preconnected optical-path protection. Journal of Lightwave Technology, 23(10):3241–3259, 2005.

[KGD05] A. Kodian, W.D. Grover, and J. Doucette. A disjoint route sets approach to design of failure-independent path-protection p-cycle networks. In Proceedings of IEEE/VDE Workshop on Design of Reliable Communication Networks - DRCN, October 2005. 8pp.

[KRJA09] M.S. Kiaei, A. Ranjbar, B. Jaumard, and C. Assi. An improved analysis for availability-aware provisioning in p -cycle-based mesh networks. Journal of Lightwave Technology, 27(20):4424 –4434, 2009.

[KSG05] A. Kodian, A. Sack, and W.D. Grover. The threshold hop-limit effect in p-cycles: Comparing hop- and circumference-limited design. Optical Switching and Networking, 2:72–85, 2005.

[KZJH05] A. Koster, A. Zymolka, M. Jger, and R. Hulsermann. Demand-wise shared protection for meshed optical networks. Journal of Network and Systems Management, 13(1):35–55, 2005.

[LDZ07] W. Li, J. Doucette, and M. Zuo. p-cycle network design for specified minimum dual-failure restorability. In IEEE International Conference on Communications - ICC, pages 2204 –2210, June 2007.

[Lem] S. Lemon. Earthquake disrupts Internet access in Asia. `http://www.computerworld.com/s/article/9006819/Earthquake_disrupts_Internet_access_in_Asia?intsrc=news_ts_head`. Last visit on October 2012.

[LHP$^+$06] K. Lo, D. Habibi, Q.V. Phung, A. Rassau, and H.N. Nguyen. Efficient p-cycles design by heuristic p-cycle selection and refinement for survivable WDM mesh networks. In IEEE Global Telecommunications Conference - GLOBECOM, pages 1–5, Nov. 27 - Dec. 1 2006.

[LR06a] C. Liu and L. Ruan. Dynamic provisioning of survivable services using path-segment protecting p-cycles in WDM networks. In International Conference on Computer Communications and Networks - ICCCN, pages 275–280, October 2006.

[LR06b] C. Liu and L. Ruan. p-Cycle design in survivable WDM networks with shared risk link groups (SRLGs). Photonic Network Communications, 11(3):301–311, 2006.

[LT04] H. Liu and F. Tobagi. A novel efficient technique for traffic grooming in WDOM SONET with multiple line speeds. In International Conference on Communications - ICC, volume 3, pages 1494–1698, 2004.

[LW06] T.J. Li and B. Wang. On optimal p-cycle-based protection in WDM optical networks with sparse-partial wavelength conversion. IEEE Transactions on Reliability, 55:496–506, 2006.

[MAA06] D. S. Mukherjee, C. Assi, and A. Agarwal. An alternative approach for enhanced availability analysis and design methods in p-cycle-based networks. IEEE Journal on Selected Areas in Communications, 24:23–34, 2006.

[Mau03] C. Mauz. p-Cycle protection in wavelength routed networks. In IEEE International Conference on Optical Network Design and Management - ONDM, Budapest, Hungary, February 2003.

[MJ09] A. Metnani and B. Jaumard. Directed *p*-cycle protection in dynamic WDM networks. In IEEE International Workshop on Reliable Networks Design and Modeling - RNDM, pages 1–6, St Petersburg, Russia, October 2009.

[MJ11a] A. Metnani and B. Jaumard. Dynamic protection provisioning with FIPP *p*-cycles in WDM networks. In IEEE International Conference on Optical Network Design and Management - ONDM, pages 1–6, Bologna, Italy, February 2011.

[MJ11b] A. Metnani and B. Jaumard. Dynamic provisioning and stability of *p*-cycles in WDM networks. Journal of Optical Communications and Networking, 3:713 – 724, 2011.

[MK98] K. Murakami and H. Kim. Optimal capacity and flow assignment for self-healing ATM networks based on line and end-to-end restoration. IEEE/ACM Transactions on Networking, 6(2):207 221, 1998.

[NHP+06] H.N. Nguyen, D. Habibi, V.Q. Phung, S. Lachowicz, K. Lo, and B. Kang. Joint optimization in capacity design of networks with *p*-cycle using the fundamental cycle set. In IEEE Global Telecommunications Conference - GLOBECOM, 2006.

[NHP10] H. Nguyen, D. Habibi, and Q. Phung. Efficient optimization of network protection design with *p*-cycles. Photonic Network Communications, 19:22–31, 2010.

[OBG09] D.P. Onguetou, D. Baloukov, and W.D. Grover. Near-optimal FIPP *p*-cycle network designs using general path-protecting *p*-cycles and combined GA-ILP methods. In Proceedings of IEEE/VDE Workshop on Design of Reliable Communication Networks - DRCN, pages 243 –250, October 2009.

[OG08a] D. P. Onguetou and W. D. Grover. Approaches to p-cycle network design with controlled optical path lengths in the restored network state. Journal of Optical Networking, 7(7):673–691, 2008.

[OG08b] D.P. Onguetou and W.D. Grover. A new insight and approach to node failure protection with ordinary p-cycles. In IEEE International Conference on Communications - ICC, pages 5145 –5149, May 2008.

[OG11] D.P. Onguetou and W.D. Grover. p-Cycle protection at the glass fiber level. Computer Communications, 34:1399 – 1409, 2011.

[OPTW07] S. Orlowski, M. Pióro, A. Tomaszewski, and R. Wessäly. SNDlib 1.0–Survivable Network Design Library. In Proceedings of the 3rd International Network Optimization Conference (INOC 2007), Spa, Belgium, April 2007.

[RA02] D. Rajan and A. Atamturk. Survivable network design: routing of flows and slacks. In G. Anandalingam and S. Raghavan, editors, Telecommunications Network Design and Management, chapter 4, pages 65–82. Kluwer, 2002.

[RA09] A. Ranjbar and C. Assi. Availability-aware design in mesh networks with failure-independent path-protecting p -cycles. Reliability, IEEE Transactions on, 58(2):348 –363, 2009.

[Ram08] S. Ramasubramanian. Supporting multiple protection strategies in optical networks. Networking, IEEE/ACM Transactions on, 16(6):1352 –1365, Dec. 2008.

[RJ08] C. Rocha and B. Jaumard. Revisiting p-cycles / FIPP p-cycles vs. shared link / path protection. In International Conference on Computer Communications and Networks - ICCCN, pages 1–6, 2008.

[RJ12] C. Rocha and B. Jaumard. Efficient computation of FIPP p-cycles. to appear in Telecommunication Systems, 2012.

[RJB09] C. Rocha, B. Jaumard, and P.-E. Bougué. Directed vs. undirected p-cycles and FIPP p-cycles. In International Network Optimization Conference (INOC), pages 1–9, 2009.

[RM99] S. Ramamurthy and B. Mukherjee. Survivable wdm mesh networks. ii. restoration. In IEEE International Conference on Communications - ICC, volume 3, pages 2023 –2030, 1999.

[RSM03] S. Ramamurthy, L. Sahasrabuddhe, and B. Mukherjee. Survivable WDM mesh networks. Journal of Lightwave Technology, 21(4):870–883, 2003.

[RSS09] R. Ramaswami, K.N. Sivarajan, and G.H. Sasaki. Optical Networks - A Practical Perspective. Morgan Kaufmann, 3nd edition edition, 2009. ch. 1 and 9.

[RT05] L. Ruan and F. Tang. Dynamic establishment of restorable connections using p-cycle protection in WDM networks. In International Conference on Broadband Networks, volume 1, pages 137 – 144, October 2005.

[RTL06] L. Ruan, F. Tang, and C. Liu. Dynamic establishment of restorable connections using p-cycle protection in WDM networks. Optical Switching and Networking, 3:191–201, 2006.

[Sch03a] D.A. Schupke. Multiple failure survivability in WDM networks with p-cycles. In International Symposium on Circuits and Systems - ISCAS, volume 3, pages III–866 – III–869 vol.3, May 2003.

[Sch03b] D.A. Schupke. The tradeoff between the number of deployed p-cycles and the survivability to dual fiber duct failures. In IEEE International Conference on Communications - ICC, volume 2, pages 1428 – 1432, May 2003.

[Sch04] D.A. Schupke. An ILP for optimal p-cycle selection without cycle enumeration. In Proceedings of the 8th Working Conference on Optical Network Design and Modelling (ONDM), Ghent, Belgium, February 2004.

[Sch05a] D. Schupke. Comparison of p-cycle configuration methods for dynamic networks. In Ken-Ichi Kitayama, Francesco Masetti-Placci, and Giancarlo Prati, editors, Optical Networks and Technologies, volume 164 of IFIP International Federation for Information Processing, pages 153–159. Springer Boston, 2005.

[Sch05b] D.A. Schupke. Automatic protection switching for p-cycless in WDM networks. Optical Switching and Networking, 2(1):35 – 48, 2005.

[SD09] C.-C. Sue and J.-Y. Du. Capacity-efficient strategy for 100% dual-failure restorability in optical mesh networks utilising reconfigurable p-cycles and a forcer filling concept. IET Communications, 3:198 – 208, 2009.

[SG00a] D. Stamatelakis and W. D. Grover. Theoretical underpinnings for the efficiency of restorable networks using pre-configured cycles. IEEE Transactions on Communications,, 48(8):1262–1265, 2000.

[SG00b] D. Stamatelakis and W.D. Grover. IP layer restoration and network planning based on virtual protection cycles. IEEE Journal on Selected Areas in Communications, 18:1938– 1949, 2000.

[SG03] G. Shen and W.D. Grover. Extending the *p*-cycle concept to path segment protection for span and node failure recovery. IEEE Journal on Selected Areas in Communications, 21(8):1306–1319, 2003.

[SG05] G. Shen and W. D. Grover. Design and performance of protected working capacity envelopes based on *p*-cycles for dynamic provisioning of survivable services. Journal of Optical Networking, 4:361–390, July 2005.

[SGA02] D.A. Schupke, C.G. Gruber, and A. Autenrieth. Optimal configuration of *p*-cycles in WDM networks. In IEEE International Conference on Communications - ICC, volume 5, pages 2761 – 2765, 2002.

[SGC04] D.A. Schupke, W.D. Grover, and M. Clouqueur. Strategies for enhanced dual failure restorability with static or reconfigurable *p*-cycle networks. In IEEE International Conference on Communications - ICC, volume 3, pages 1628–1633, June 2004.

[SHY04] S. Shah-Heydari and O. Yang. Hierarchical protection tree scheme for failure recovery in mesh networks. Photonic Network Communications, 7(2):145–149, 2004.

[SJ08a] S. Sebbah and B. Jaumard. Efficient and scalable design of protected working capacity envelope. In 13th International Telecommunications Network Strategy and Planning Symposium - Networks, pages 1 – 21, 2008.

[SJ08b] S. Sebbah and B. Jaumard. Efficient and scalable design of protected working capacity envelope. In 13th International Telecommunications Network Strategy and Planning Symposium, Networks, pages 1–21, 2008.

[SJ08c] S. Sebbah and B. Jaumard. Survivable WDM networks design with non-simple p-cycle-based PWCE. In IEEE Global Telecommunications Conference - GLOBECOM, pages 1–6, 2008.

[SJ09] S. Sebbah and B. Jaumard. Dual failure recovery in WDM networks based on p-cycles. In International Conference on Optical Networking Design and Modeling - ONDM, pages 1–6, Braunschweig, Germany, 2009.

[SJ11] S. Sebbah and B. Jaumard. Differentiated quality-of-recovery in survivable optical mesh networks using p -structures. IEEE/ACM Transactions on Networking, pages 798 – 810, 2011.

[SS12] A.A.M. Saleh and J.M. Simmons. All-optical networking - evolution, benefits, challenges, and future vision. Proceedings of the IEEE, 100(5):1105 –1117, 2012.

[SSG03] D. A. Schupke, M. C. Scheffel, and W. D. Grover. Configuration of p-cycles in WDM networks with partial wavelength conversion. Photonic Network Communications, 6:239–252, 2003.

[ST05] T. Stidsen and T. Thomadsen. Joint routing and protection using p-cycles. Technical report, Technical Univ. of Denmark, DTU, 2005.

[THV+08] J. Tapolcai, P.-H. Ho, D. Verchere, T. Cinkler, and A. Haque. A new shared segment protection method for survivable networks with guaranteed recovery time. IEEE Transactions on Reliability, 57:272–282, June 2008.

[WM05] H. Wang and H.T. Mouftah. p-Cycles in multi-failure network survivability. In 7th International Conference on Transparent Optical Networks (ICTON), volume 1, pages 381 – 384 Vol. 1, July 2005.

[WYH08] B. Wu, K.L. Yeung, and P.-H. Ho. A comparative study of fast protection schemes in WDM mesh networks. In IEEE International Conference on Communications - ICC, pages 5160 – 5164, 2008.

[WYH10a] B. Wu, K.L. Yeung, and P. Ho. ILP formulations for *p*-cycle design without candidate cycle enumeration. IEEE/ACM Transactions on Networking, 18(1):284 –295, 2010.

[WYH10b] B. Wu, K.L. Yeung, and P.-H. Ho. ILP formulations for non-simple *p*-cycle and *p*-trail design in WDM mesh networks. Computer Networks, 54(5):716–725, 2010.

[Xin] Xinhuanet. Damage to undersea cables disrupts int'l telecom services. `http://news.xinhuanet.com/english/2009-08/18/content_11904208.htm`. Last visit on September 2012.

[XXQ03] D. Xu, Y. Xiong, and C. Qiao. Novel algorithms for shared segment protection. IEEE Journal of Selected Areas in Communications, 21(8):1320–1331, October 2003.

[YAK03] Y. Yoo, S. Ahn, and C.S. Kim. Supporting multiple classes of traffic in IP over WDM networks. IEEE Journal on Selected Areas in Communications, 21:1263 – 1273, 2003.

[ZJM00] H. Zang, J. P. Jue, and B. Mukherjee. A review of routing and wavelength assignment approaches for wavelength-routed optical WDM networks. Optical Networks Magazine, pages 47–60, January 2000.

[ZM04] J. Zhang and B. Mukheriee. A review of fault management in wdm mesh networks: basic concepts and research challenges. IEEE Network,, 18(2):41–48, 2004.

[ZS00] D. Zhou and S. Subramaniam. Survivability in optical networks. IEEE Network,, 14(6):16 – 23, Nov/Dec 2000.

[ZY02] H. Zhang and O. Yang. Finding protection cycles in DWDM networks. In IEEE International Conference on Communications - ICC, volume 5, pages 2756 – 2760 vol.5, 2002.

[ZYL04] Y. Zhang, O. Yang, and H. Liu. A Lagrangean relaxation and subgradient framework for the routing and wavelength assignment problem in WDM networks. IEEE Journal on Selected Areas in Communications, 22:1752 – 1765, November 2004.

[ZZ05] W.D. Zhong and Z. Zhang. *p*-Cycles-based dynamic protection provisioning in optical WDM networks. IEICE Transactions on Communications, 88(5):1921–1926, 2005.

[ZZ06] F. Zhang and W.-D. Zhong. A novel path-protecting *p*-cycle heuristic algorithm. In Proceeding of the International Conference on Transparent Optical Networks (ICTON), volume 3, pages 203–206, Nottingham, UK, June 2006.

[ZZB05] Z. Zhang, W. Zhong, and S.K. Bose. Dynamically survivable WDM network design with *p*-cycle-based PWCE. IEEE Communications Letters, 9(8):756 – 758, 2005.